PROCEEDINGS OF THE 2023 GEORGIA WATER RESOURCES CONFERENCE

GEORGIA WATER RESOURCES CONFERENCE

30 AND 31 MARCH, 2023

GEORGIA CENTER FOR CONTINUING EDUCATION, ATHENS, GA

The Georgia Water Resources Conference is funded by the Georgia Water Resources Institute and other sponsors, organized by the UGA River Basin Center, and fueled by the innovation of its participants.

Georgia Water Resources Institute

UNIVERSITY OF GEORGIA River Basin Center

Revised October 16, 2023

WADEABLE STREAM HABITAT RESURVEYS AT CHATTAHOOCHEE RIVER NATIONAL RECREATION AREA

Rachel Bell[1], Jacob M. Bateman McDonald[1], Christopher S. Cooper[2]
[1]University of North Georgia, [2]National Park Service

REFERENCE: *Proceedings of the 2023 Georgia Water Resources Conference*, held March 30–31, 2023, at the University of Georgia.

Abstract. The Southeast Coast Network (SECN) is one of 32 networks of the National Park Service's (NPS) Inventory and Monitoring Division (IMD). The SECN is tasked with collecting long-term monitoring data with an expressed purpose of helping NPS personnel identify and manage threats to vital natural resources. One of the long-term monitoring protocols implemented by the SECN is the Wadeable Stream Habitat Monitoring Protocol. During late spring (early May) 2021, thirteen monitored 1st through 3rd order stream reaches at Chattahoochee River National Recreation Area (CHAT) were resurveyed to identify and quantify changes since the first surveys were completed in 2017. Data collected at each stream reach included but was not limited to: identification and mapping of geomorphic channel units (i.e., run, riffle, pool), traditional survey tape and stadia rod measurements of channel widths and bank heights (channel geometry), a total station survey of three 'detailed' transects (cross-sections), and the longitudinal profile of the monitored reach. The purpose of this poster is to highlight the most interesting changes that were identified and to show examples of the primary processes of change that influence these lower order streams at CHAT. One of the biggest drivers of change was movement of large wood within and through these reaches. While the watersheds of the surveyed stream reaches range from drainage areas of 0.20 km^2 to 16.88 km^2, the processes affecting each stream reach are similar. The main difference between these reaches is the rates by which change occurs and the overall amount of change that was observed.

Introduction. The Southeast Coast Network (SECN) is one of 32 networks of the National Park Service's (NPS) Inventory and Monitoring Division (IMD). The SECN is tasked with collecting long-term monitoring data with an expressed purpose of helping NPS personnel identify and manage threats to vital natural resources. One of the long-term monitoring protocols implemented by the SECN is the Wadeable Stream Habitat Monitoring Protocol. The main objectives of this protocol are to determine: 1) how watershed characteristics may affect stream habitat; 2) the status and trends in the geomorphic dimensions of the selected stream reaches; and 3) the status of and trends in physical measures of benthic and riparian habitat.

During late spring (early May) 2021, thirteen previously monitored 1st through 3rd order stream reaches at Chattahoochee River National Recreation Area (CHAT) were resurveyed to identify and quantify changes since the first surveys were completed in 2017. This poster highlights some of the significant changes that have occurred since the 2017 surveys and provides insight into the processes that are influencing these lower order Appalachian Piedmont streams. Specifically, this poster focuses on six stream reaches (2 of each order 1st through 3rd) to provide examples of how each stream order has changed in the last four years.

Study Area. The Chattahoochee River National Recreation Area (CHAT) buffers 48 miles of the Chattahoochee River and consists of 16 non-contiguous management units. CHAT stretches from Buford Dam to north Atlanta, GA covering 6,800 acres of mixed pine/hardwood forests and wetlands. The Chattahoochee River is utilized for recreation, power generation, as a water supply, and for wastewater assimilation for the greater metropolitan Atlanta area. This section of the Chattahoochee River is highly regulated by flows from Buford Dam.

Thirteen streams are currently being monitored at CHAT. A fourteenth was surveyed during the 2017 (initial) surveys but for safety reasons this site was dropped from the protocol. Five of the streams are 1st order, six are 2nd order, and the remaining two are 3rd order. The 1st order streams have rather steep watersheds and range from mostly forested to heavily developed. The 2nd order stream watersheds all have average watershed slope and relief and were mostly covered by development though one stream (CHAT005 – "Egg Creek") was mostly forested. The two 3rd order stream watersheds have average watershed slope and relief and are mostly developed.

The 1st order streams picked for this poster include CHAT002 – "Undercut Creek" and CHAT006 – "Three Mind Creek". In 2017, CHAT002's instream habitat was classified as "good" due to its variety of instream habitat, coarse bedload, and high volume of large woody debris (LWD). On the other hand, CHAT006's instream habitat was classified as "poor" in 2017, due to a lack of instream habitat diversity (low energy runs and pools), fine bed sediment, and low volume of LWD. The geomorphic processes that were seen affecting CHAT002 included bank slumping and a flood chute bisecting its floodplain on river left. The most interesting geomorphic process observed at CHAT006 was a significant knickpoint that had headcut into the reach.

The 2nd order streams chosen for this presentation include CHAT005 – "Egg Creek" and CHAT014 – Whitewater Creek. In 2017, CHAT005's instream habitat was classified as "fair" because, though it had a mixture of instream habitat and a high volume of LWD, it had relatively fine bed sediment. CHAT014's instream habitat was classified as "poor" in 2017 due to the low energy instream habitats and very fine bed sediment. The most interesting geomorphic process observed in 2017 on CHAT005 was the headward migration of a knickpoint into the middle of this reach. The geomorphic processes that were seen affecting CHAT014 included bank slumping and a flood chute affecting the out-of-channel area on river left.

Both 3rd order streams monitored by SECN are included in this poster. CHAT001 – Haw Creek's instream habitat was classified as "fair" to "good" because it had a mixture of instream habitat types, coarse bed sediment and an average amount of LWD. CHAT013 – Long Island Creek's instream habitat was also classified as "fair" to "good" because, though it had finer bed sediment, it had a greater variety of instream habitat and more LWD. The geomorphic processes that were seen affecting CHAT001 included bank slumping and significant lateral erosion creating large floodplain areas inset within the entrenched channel. The most interesting geomorphic process influencing CHAT013 was related to a large amount of large woody debris creating a step-pool sequence near the upper portions of the surveyed reach.

Methods. The data collected as part of the SECN wadeable stream monitoring protocol are divided into three scales of analysis: (1) basin-scale characteristics; (2) reach-scale measurements, along and between 11 standard transects per reach, and; (3) detailed cross-sectional measurements, at three of the 11 transects per reach. A list of standard operating procedures and an overview of the methods used to collect the surveys and process the data are available in McDonald et al. (2018). This presentation focuses on the results of the detailed cross-sectional measurements for the six selected stream reaches described in the previous section.

The detailed cross-sectional surveys are conducted on three of the eleven standard transects using a survey grade (sub-centimeter accuracy) total station. These surveys allow lateral variability along each transect to be quantified and in- and out-of-channel changes to be monitored through time. All surveys are completed from a known point (benchmark). Surveys are run perpendicular to flow and survey points are chosen to represent the local slope and to identify diagnostic geomorphic surfaces (e.g., channel-full and bankfull bank tops, thalweg locations, terraces, and in-channel bars). These data are used to calculate bankfull and channel-full characteristics (i.e., width, height, area) and are compared to previous surveys to identify areas of change (e.g., incision/aggradation, bank movement, changes in bar morphology).

Results. *CHAT002 - "Undercut Creek."* Based on the instream habitat, bed sediment, and measures of large woody debris, the habitat at CHAT002 was reclassified as "fair to good". This 'downgrade' in habitat (from 'good') is due to the loss of pool habitats (increase in run habitat) and an increase in the amount of fine sediment (decrease in minimum and d5 sediment). This classification is based on the data collected on that day and it needs to be noted that a large rain event hit this stream a few days prior and pools observed in 2017 could have been ephemerally filled in following that event.

The most significant geomorphic changes that occurred at CHAT002 were channel incision in the downstream portions of the reach, a concomitant increase in channel slope, and erosion of the upstream natural levee which had protected the entrance to the flood chute along the river left floodplain. These changes are inferred to be related as an increase in the frequency with which the flood chute is being used is reducing the length of the channel in this portion of the reach which is hypothesized to be providing the increased energy needed to cause channel incision and an increase in channel slope.

CHAT006 - "Three Mind Creek." Based on the instream habitat, bed sediment, and measures of large woody debris, the habitat at CHAT006 was again classified as 'poor'. While there was an increase in the amount of large wood observed in the reach, as well as a slight coarsening of the bed sediment, the dominant in-stream habitat changed from a mixture of riffle, run, and pool to run.

The most significant geomorphic change that occurred at CHAT006 was significant channel aggradation in the lower portion of the reach **(Figure 1)**. This aggradation event was related to a large wood jam that had developed just downstream of the surveyed reach. An estimated 3 m^2 of sediment are being stored behind the large wood jam.

CHAT005 - "Egg Creek." Water Based on the instream habitat, bed sediment, and measures of large woody debris, the habitat at CHAT005 was again classified as 'fair'. While there was an increase in the volume of large wood observed in the reach, as well as a slight coarsening of the bed sediment, the reach showed an overall infilling of the bed as pool habitats were converted into run habitat.

The most significant geomorphic change that occurred at CHAT005 was significant channel bed incision in the lower portion of the reach **(Figure 2)**. This incision was related to a large wood jam failing in the time since the 2017 survey. An estimated 6 m^2 of sediment were mobilized/eroded from the channel as a result of the large wood jam failure.

CHAT014 - "Whitewater Creek." Based on the instream habitat, bed sediment, and measures of large woody debris, the habitat at CHAT014 was again classified as 'poor'. While there was an increase in the number of pieces of large wood observed in the reach, as well as a slight coarsening of the mean size of the bed sediment, the reach showed an overall infilling of the bed as pool habitats were converted into run habitat.

The most significant geomorphic change that occurred at CHAT014 occurred outside of the channel. A large pulse of hillslope sediment (likely from upslope construction) deposited as a large amount of sandy sediment on the river right historical terrace, completely burying the benchmark on detailed transect 2.

*CHAT001 - "Haw Creek." B*ased on the instream habitat, bed sediment, and measures of large woody debris, the habitat at CHAT001 was again classified as 'fair' to 'good'. While there were changes in the variables used to classify habitat, these changes were not large enough to warrant a change in classification.

The most significant geomorphic change that occurred at CHAT001 was a large bank collapse on detailed transect 1 **(Figure 3)**. An estimated 200 m^2 of bank material was lost in this collapse. This large section of bank is hypothesized to have been lost as a cohesive unit due to the influence of subsurface flow, between the underlying bedrock and the stream bank (overburden), coupled with the highly cohesive clay-rich sediment characteristic of Appalachian Piedmont alluvial legacy sediments.

CHAT013 - "Long Island Creek." Based on the instream habitat, bed sediment, and measures of large woody debris, the habitat at CHAT013 was again classified as 'fair' to 'good'. While there were changes in the variables used to classify habitat, these changes were not large enough to warrant a change in classification.

The most significant geomorphic change that occurred at CHAT013 was a large bank collapse on detailed transect 3 **(Figure 4)**. An estimated 140 m^2 of bank material was lost in this collapse. This large section of bank collapsed as a result of a (very large) tree fall. During the survey, the tree and a large root ball that contained the majority of the lost bank (and the 2017 benchmark) were in the stream approximately 10 m from the river left bank. The large tree fall had created a large jam and the majority of Long Island Creek was diverted from river right to running along river left (further eroding the disturbed bank).

Discussion/Conclusion. Across all of the sites, a common theme was the influence temporally proximal storms (sometimes) ephemerally have on rivers and streams. It is hypothesized that the majority of the bed sediment fining and loss of habitat variability was due to a recent influx of fine sediments. The addition of large wood to the majority of the streams was seen as a positive (for habitat classifications). Habitat classifications did not improve for many of these sites because of the loss of habitat variability. It is believed that after a few smaller storm events (that do not provide extra hillslope sediments) most of these streams will regain their habitat variability and or their habitat classification will improve. Work needs to be done to determine the permanency of bed sediment in these systems to determine how variability habitat variability is during the year.

Geomorphically, these streams were seen to have been affected significantly by large wood. Large wood jams were observed to have led to channel bed aggradation (when they form) and incision (when they inevitably fail). Developing an understanding of the spatial distribution of large wood jams (exposed and buried) is vital to understanding the long-term storage and transport of bed sediment from these lower order tributaries of the Chattahoochee River. A significant volume of sediment was lost on one of the 3rd order streams as a result of tree fall (CHAT013). An additional large volume of sediment was lost on the other 3rd order stream potentially related to the interaction between groundwater, legacy sediments (overburden), and the underlying bedrock.

References:

McDonald, J. M., M. B. Gregory, J. W. Riley, and E. N. Starkey. 2018. Monitoring wadeable stream habitat conditions in Southeast Coast Network Parks: Protocol narrative. Natural Resource Report NPS/SECN/NRR—2018/1715. National Park Service, Fort Collins, Colorado. Available at: https://irma.nps.gov/DataStore/Reference/Profile/2254874 (last accessed March 6, 2023).

U.S. Geological Survey. 2010. 3m Digital Elevation Model (DEM) of the Conterminous United States, Version 1.0, Release Date: 2010-03-08. Access Information: https://data.usgs.gov/datacatalog/data/USGS:40e52270-5c4b-497d-987f-827e374becff. (last accessed May 30, 2021).

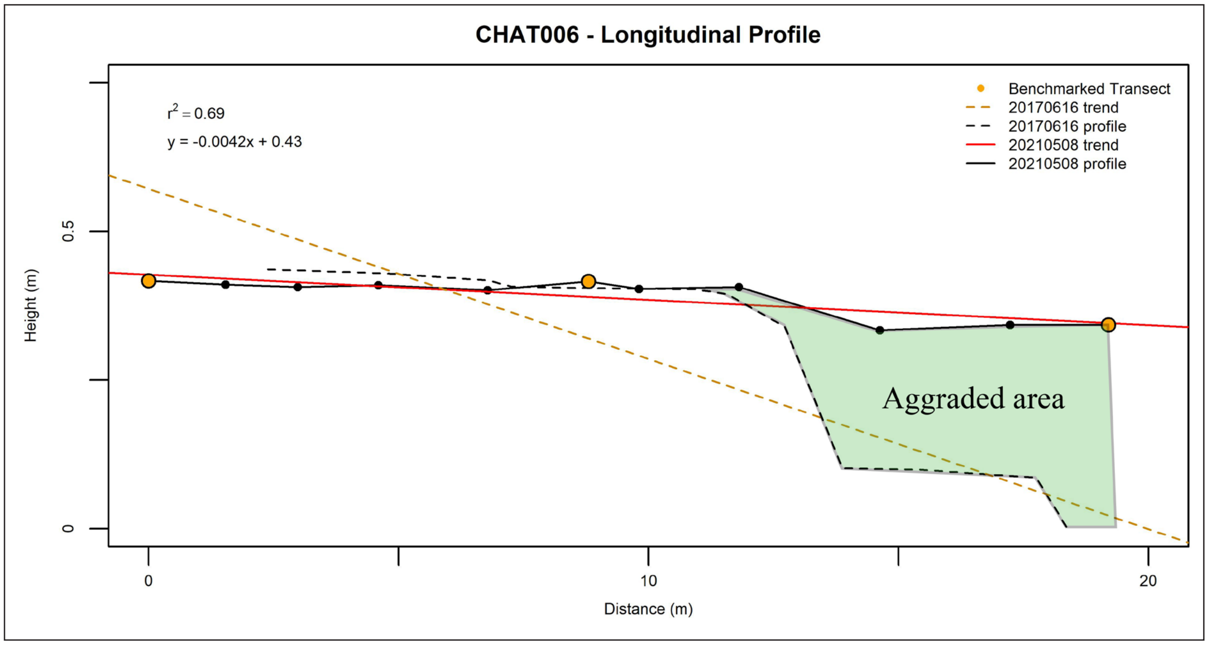

Figure 1. Longitudinal profile of CHAT006 comparing the 2017 and 2021 surveys. Aggraded area (behind a large wood jam) is shown in green.

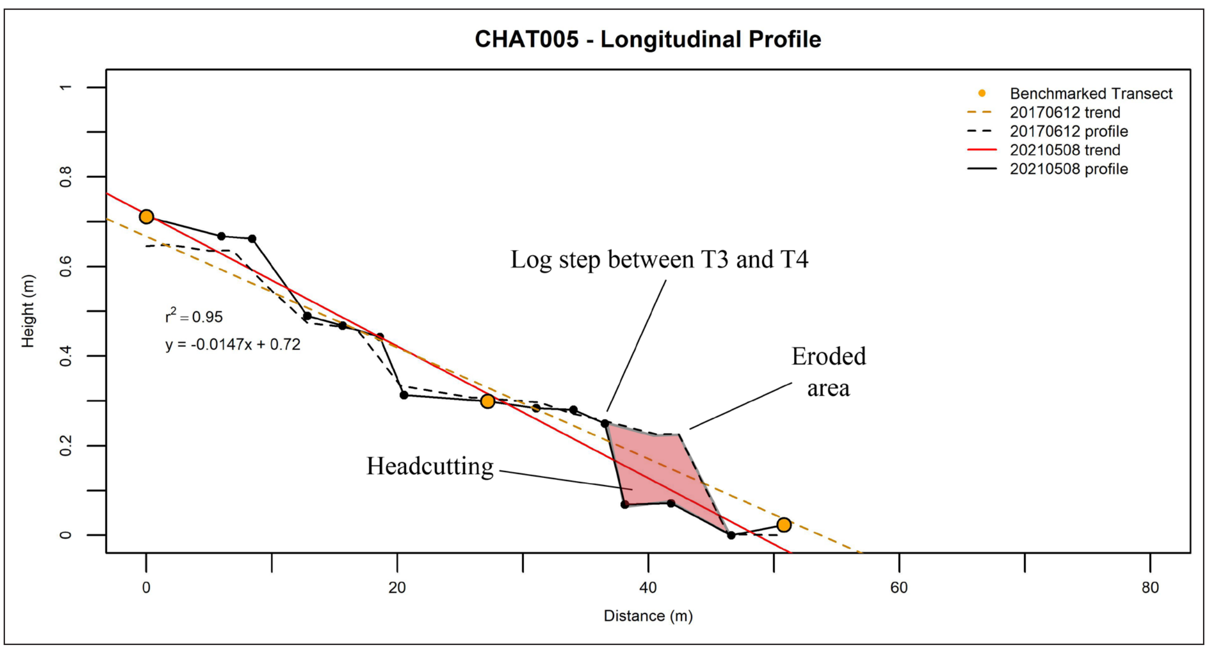

Figure 2. Longitudinal profile of CHAT005 comparing the 2017 and 2021 surveys. Incised area (sediment lost after large wood jam failure) shown in red.

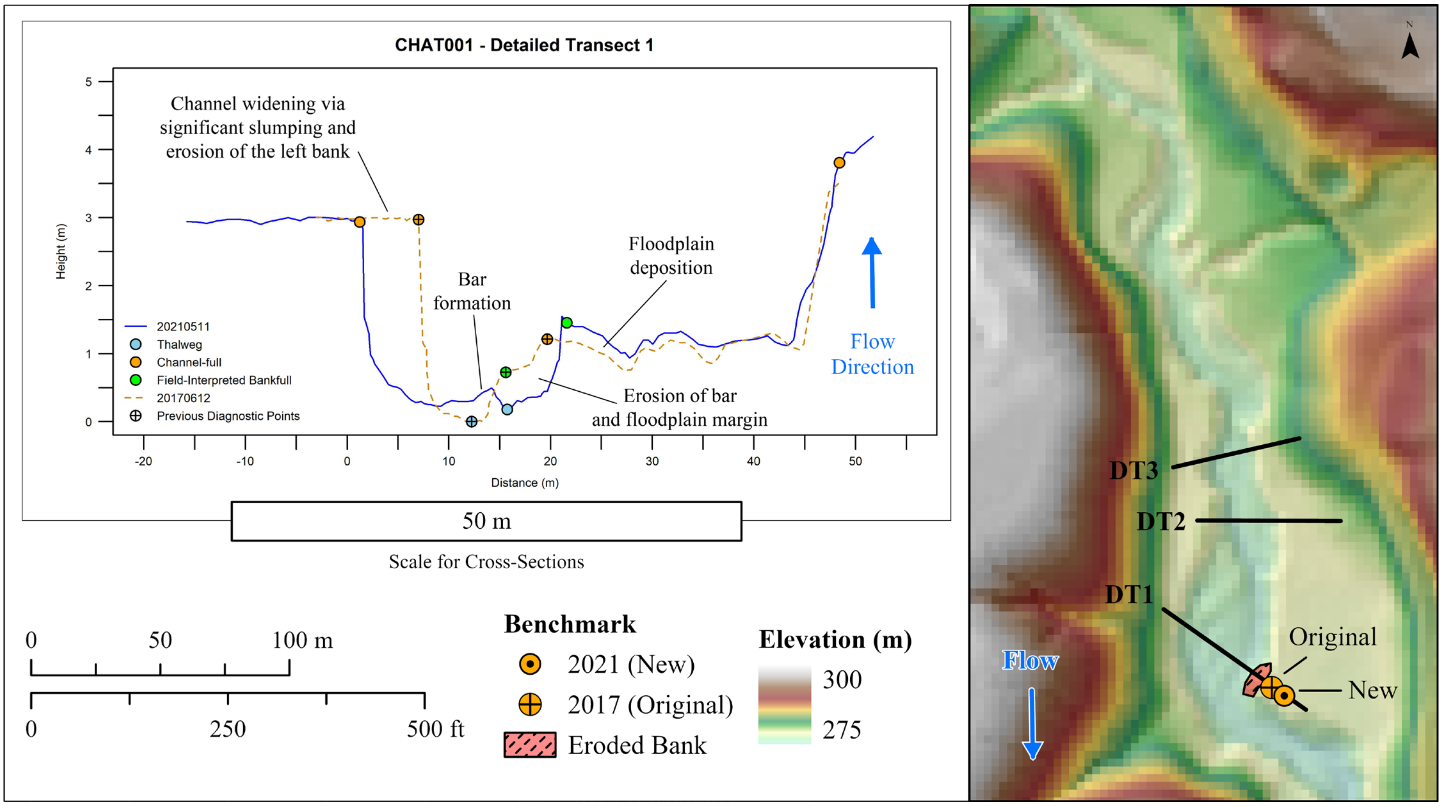

Figure 3. Cross-section compares the 2017 and 2021 surveys on detailed transect 1 (DT1) at CHAT001 - Haw Creek. Map shows the segment-scale context for the observed bank erosion. Eroded bank area was estimated from the 3 m DEM (USGS, 2010) using field notes as a guide.

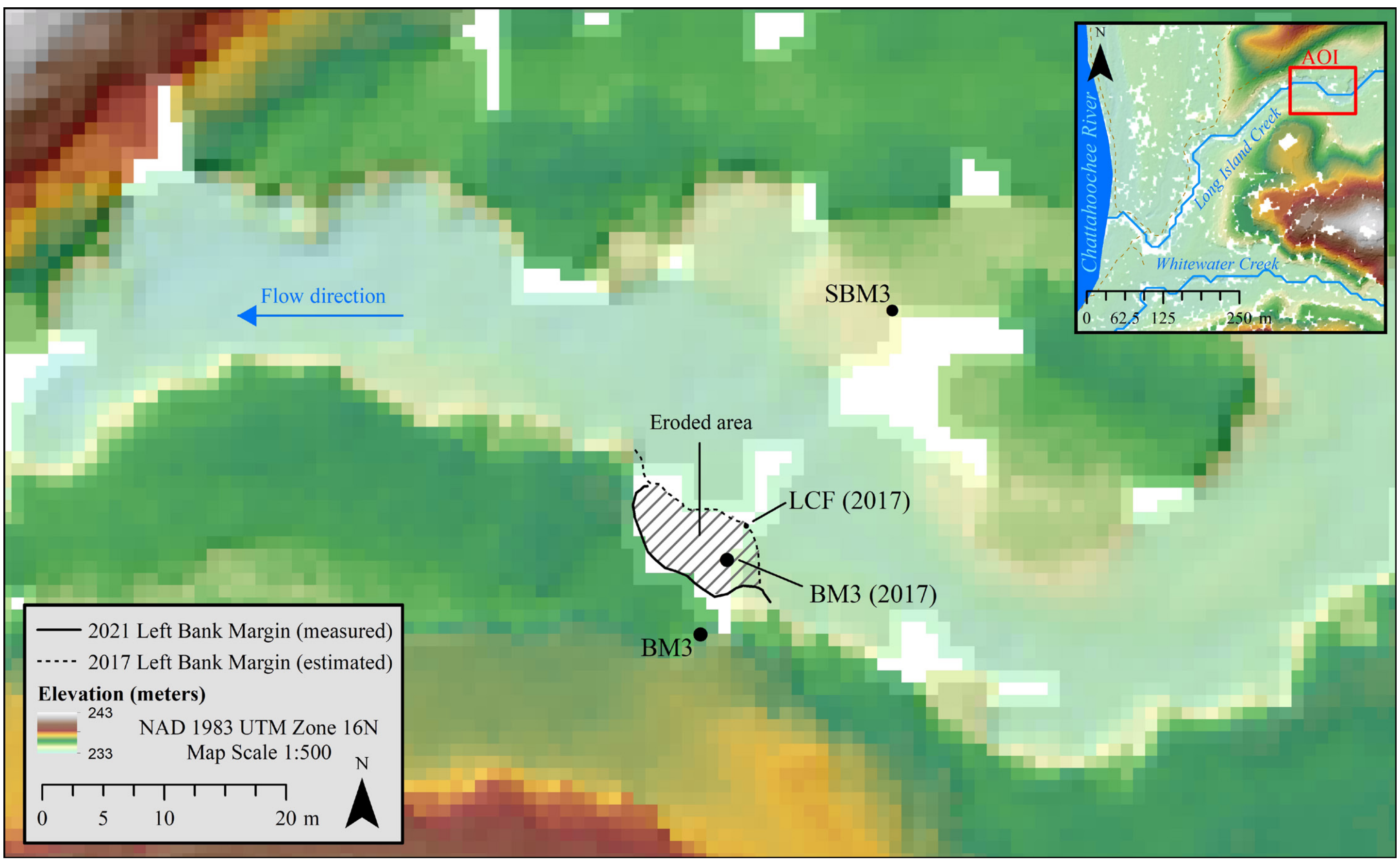

Figure 4. Map of CHAT013 showing the out-of-channel area that was lost between the 2017 and 2021 surveys on detailed transect 3. LCF is the "left channel full" point on the top of the bank from the 2017 survey.

EFFECTS OF DISSOLVED OXYGEN AND TURBIDITY ON BIODIVERSITY IN FRESHWATER POND ECOSYSTEMS

Soraya Byrdsong, Kimberly K. Takagi, Anna Palmaieri, Sa'mya Ivy
College of Coastal Georgia, Department of Natural Sciences

REFERENCE: *Proceedings of the 2023 Georgia Water Resources Conference*, held March 30–31, 2023, at the University of Georgia.

Introduction. In the United States alone, over 2 million acres of the land has been converted to golf courses. These golf courses have been found to hold many threatened species not only on the courses themselves, but in structures that have become a staple for golf courses everywhere, such as ponds, lakes, and other bodies of water. Freshwater wetland and pond ecosystems, especially those in urban, developed areas, act as a refuge for many terrestrial, transitional, and aquatic species (Liu & Lu 2021).

This study focuses on the inorganic water quality factors: dissolved oxygen (DO) and turbidity, as they can be influenced by the presence of fountains, a common structure in many ponds. DO and turbidity are often higher in areas surrounding fountains due to the increased water movement as a result of turbulence created by the fountains. At the initial survey point near the fountain in Pond 3, one pond on the study site, very few animals were observed; however, after moving away from the fountain, the biodiversity in the pond increased rapidly. This phenomenon has been observed in several studies. One such study was conducted in 2021 which determined that fountains had the lowest occurrence of alien freshwater turtles (Fiu & Fu 2021). Turbidity is often higher around ponds with fountains. Higher turbidity causes a decrease in species richness and biodiversity (Lunt and Smee 2020). Higher DO is often a limiting factor in biodiversity for several species and affects the distribution of species (Trowbridge, et. al. 2017).

In this study, data from water quality surveys and animal surveys will be compared from four total sample sites between three ponds to see how the presence of fountains affect turbidity and DO levels, and how those altered levels affect biodiversity of reptiles, amphibians, and macroinvertebrates. Our hypothesis is that ponds without fountains will have lower DO and turbidity and higher biodiversity and species richness. The objective for this study is to look at how fountain structures in ponds affect the distribution of wildlife in and around the pond, and how differing levels of DO and turbidity affect species distribution.

Methods and Materials. *Site Characterization.* The study sites were three of the eight ponds located on the former golf course at Sea Palms West on St. Simons Island in Georgia, U.S.A **(Figure 1)**. The golf course was converted to a greenspace in 2018 and most regular maintenance was discontinued. The use of insecticides ceased, but herbicides and algaecides are still applied 21 times a year (Waldron, D *pers. comm*).

Water Quality Survey. Dissolved oxygen (DO) and turbidity concentrations were measured and recorded once a week over a fourteen-week period (Aug-Nov 2022). Turbidity was measured with a LaMotte 2020i Turbidimeter. DO concentrations were measured using a LaMotte Dissolved Oxygen Kit, which used a modified Winkler Titration.

Fauna Surveys. Three different surveys were conducted to observe fauna biodiversity. A macroinvertebrate survey, a bird and turtle survey, and a night survey for reptiles and amphibians. For the macroinvertebrate survey, a dip net was used to scrape the edge of the pond and then its contents were emptied onto a tray. The net was swept a meter to the left and a meter to the right. This was done ten times for one sample. The goal was to collect and identify macroinvertebrates in five samples or identify 100 individuals. This survey was done twice at Ponds 2, 3A, and 5 and once at Pond 3B. For the bird and turtle survey, we walked twice around the parts of the ponds accessible to us. We identified each bird and turtle species as we walked the perimeter of the pond. This survey was done twice. The reptile and amphibian survey was conducted at night, using the spotlight technique. A flashlight was pointed at the animals and each organism found was identified to the lowest taxonomic level possible. This survey was only conducted once.

Data analysis. Simpson and Shannon Indices were calculated to determine the biodiversity across the sites. A different Simpson and Shannon's Index was calculated for macroinvertebrates and reptiles and amphibians at each site, for a total of eight Shannon's and eight Simpson index calculations. Excel was used to find the mean DO and turbidity for each site and Pearson Correlation Test was then calculated in Excel to determine a correlation between the levels of DO or turbidity and Shannon and Simpson's indices. A Kruskal-Wallis test was calculated in SPSS to determine if there was a statistical difference between the levels of DO at each site. Post-hoc pairwise comparisons were then used to determine which sites significantly differed from each other ($p<0.05$).

Results. *Means.* The mean turbidity and dissolved oxygen (DO) from all four sites have been compared in figure 2. The highest mean turbidity was 36.29 FNU at Pond 3B and the lowest mean turbidity was 4.22 FNU at Pond 2 **(Figure 2)**. The highest mean DO was 9.1 ppm at Pond 2, while the lowest mean DO was 1.22 ppm at Pond 5.

Biodiversity. To compare biodiversity, both Shannon and Simpson indices were run. For reptiles and amphibians, the highest Shannon and Simpson indices were 1.16 and 2.81, respectively, both of which were found at Pond 5. The lowest Shannon and Simpson indices were 0.66 and 1.88, respectively, both at Pond 2. For macroinvertebrates, the highest Shannon and Simpson indices were 2.22 and 6.26, respectively, both at Pond 5. The lowest Shannon and Simpson indices were 1.04 and 2.67, respectively, both at Pond 3A **(Table 1)**.

Statistical Differences. There was significant statistical difference for the levels of DO and turbidity between the four sites. For DO, Pond 5 was significantly different from Ponds 3A and 2. Ponds 3B and 2 were also significantly different from each other. For turbidity, Pond 5 was significantly different from Pods 3A, 3B, and 2.

Correlations. A Pearson correlation was calculated to determine if a correlation existed between biodiversity and the mean DO or turbidity levels from the sampling sites. For DO, there was a weak (< 0.7) negative correlation between mean DO and biodiversity of macroinvertebrates. However, there was a strong (> 0.7) negative correlation between mean DO and biodiversity of reptiles and amphibians **(Table 2)**.

For turbidity, there was a strong negative correlation between the mean turbidity and biodiversity of macroinvertebrates. There was a moderately strong positive correlation between turbidity means and biodiversity of reptiles and amphibians **(Table 3)**.

Discussion. *Seasonality.* Our hypothesis stated that ponds without a fountain would have a lower dissolved oxygen (DO) and turbidity and greater biodiversity. For the macroinvertebrate surveys in ponds 2 and 3A, this was partly true. Pond 2 (fountain absent) had a lower turbidity, but a lower biodiversity. Pond 3A (fountain present) had lower DO, but higher biodiversity. This could be due to the time of year this study was conducted. Some studies state that levels of DO and turbidity are significantly influenced by the season. Turbidity would be higher in the summer and DO would be higher in the winter (Yan, et al. 2019). The macroinvertebrate survey at Pond 3B was taken closer to winter, which could have influenced the low biodiversity since macroinvertebrate densities are often lower in the winter (Aristone, et al. 2022). However, this literature on this topic is conflicting, as one study suggested that macroinvertebrate community densities increase in fall and winter, so the reason for lower macroinvertebrate biodiversity at Pond 3B remains unclear (Chi, et al. 2017).

Turbulence and Flow. Due to the presence of a fountain in Pond 3, we assumed the site nearest to the fountain would have the highest DO. This assumption was proven wrong. Pond 2, the fountain actually had the highest DO levels. It was discovered that Pond 2 has a definitive inflow which likely keeps the water circulating better than the fountain could. Pond 3 had no inflow, so it was more stagnant than Pond 2. Thus, flow likely has a bigger impact of DO and turbidity than the presence of a fountain, especially for larger ponds. The lack of inflow circulating the water likely explains the low reptiles and amphibian biodiversity at Pond 2. Pond 5 contained the lowest DO levels, but the highest biodiversity for all surveyed organismal groups. This pond had a fountain, but since it was so far from the sampling site, its effects were likely negligible. Higher levels of DO have been shown to have a negative impact on some amphibian species, which is supported in our study (Saeed & Yousefkani 2021). The pond sites with higher DO also had a lower biodiversity of reptiles and amphibians. Many amphibian species are indicator species, which means that they are sensitive to changing factors in the water. Pond 2 was the only pond that contained large game fish, as all the other ponds only contained small minnow species. These fish require high DO levels to live successfully, which indicates that large, fully aquatic species need more DO than transitional aquatic species.

Further Research. Further research for this study could be conducted to look at the effects of DO and turbidity not just on biodiversity, but on the health of the organisms in those species. It could indicate more about the actual pond health than just biodiversity. More animal surveys could also be done to get a larger sample size for better indexes and analysis to be calculated. A biodiversity survey for fish could also be run. Since the time of year has been shown to affect macroinvertebrate biodiversity especially, this study could be run again in cooler temperatures to examine a possible difference in biodiversity at the same site. Further research could also quantify the flow in each pond to clarify the reason behind the extreme variations of DO within them.

Acknowledgements. Thank you to the College of Coastal Georgia for their valuable advice and access to resources. I would also like to thank Sea Palms West for letting us use their greenspace for research.

References:

Aristone, C., Mehdi, H., Hamilton, J., Bowen, K.L., Currie, W.J.S, Kidd, K.A., Balshine, S. (2022). Impacts of wastewater treatment plants on benthic macroinvertebrate communities in summer and winter. Science of the Total Environment. 820.

Chi, S., Li, S., Chen, M., Zheng, J., Hu, J. (2017). Temporal variations in macroinvertebrate communities from the tributaries in the Three Gorges Reservoir Catchment, China. Revista Chilena de Historia Natural. 90(6).

Colding, J., Lundberg, J., Lundberg, S., Anderson, S. (2009). Golf courses and wetland fauna. Ecological Applications. 19(6): 1481-1491.

Liu F., Lu, F. (2021). Ecological engineering approaches to restoring the aquatic biological community of an urban pond ecosystem and its effects on water quality - a case study of the urban Xixi National Wetland Park in China. Knowledge and Management of Aquatic Ecosystems. 0(422): 24.

Lunt, J., Smee, L. (2020). Turbidity alters estuarine biodiversity and species composition. ICES Journal of Marine Science. 77(1): 379-387.

Saeed, S., Yousefkani, H. (2021). Conservation biology of the critically endangered salamander, Paradactylodon persicus gorganensis (Clergue-Gazeau & Thorn, 1979) (Amphibia: Hynobiidae) in northeastern Iran. Animal Biology. 71(4): 349-360. doi:10.1163/15707563-bja10057.

Trowbridge, C. D., Kachmarik, K., Plowman, C.Q., Little, C., Stirling, P., McAllen, R. (2017). Biodiversity of shallow subtidal, under-rock invertebrates in Europe's first marine reserve: Effects of physical factors and scientific sampling. Estuarine Coastal & Shelf Science. (187): 43-52.

Yan, J., Sui, J., Xu, Y., Li, X., Wang, H., Zhang, B. (2019). Relationship between mild seasonal oxygen deficiency and seasonal variations of macrozoobenthic community: A case study in the Yangtze River estuary and its adjacent area, China. Marine Pollution Bulletin, (144):11-19. doi:10.1016/j.marpolbul.2019.05.00.

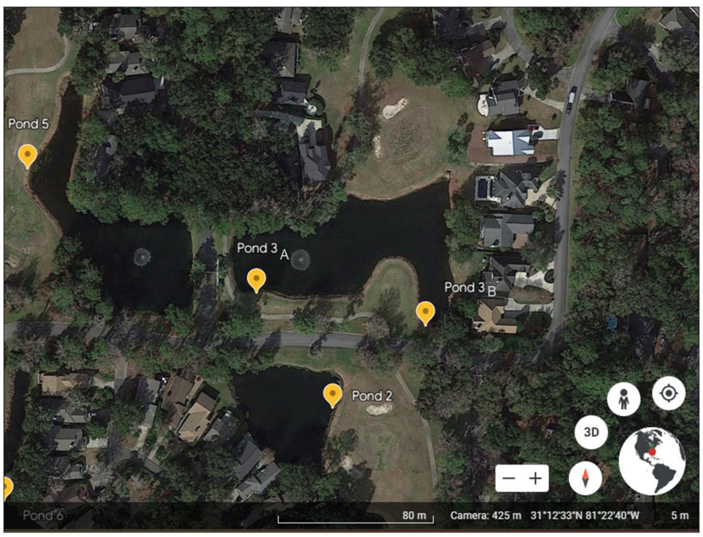

Figure 1. Sampling sites 2, 3A, 3B, and 5 at study site Sea Palms West, St. Simons, Georgia.

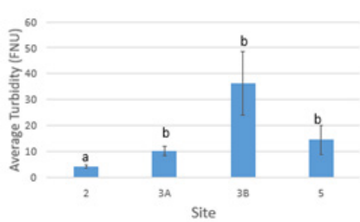

Figure 2. Average turbidity for each pond and site.

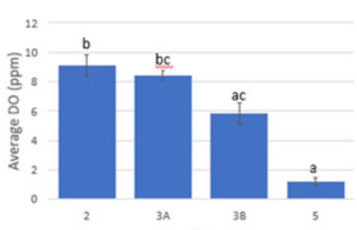

Figure 3. Average DO for each pond and site.

Table 1. Shannon's and Simpson's Indexes for macroinvertebrates and reptiles and amphibians at ponds 2, 3A, 3B, and 5.

Pond, Section	Type of organisms	Shannon (H)	Simpson (D)
Pond 2	Macroinvertebrates	1.9	5.3
Pond 3, A	Macroinvertebrates	2.06	5.71
Pond 3, B	Macroinvertebrates	1.04	2.67
Pond 5	Macroinvertebrates	2.22	6.26
Pond 2	Reptiles and amphibians	0.66	1.88
Pond 3, A	Reptiles and amphibians	0.67	1.92
Pond 3, B	Reptiles and amphibians	0.97	2.46
Pond 5	Reptiles and amphibians	1.16	2.81

Table 2. Correlation between mean DO levels at each site and biodiversity index of macroinvertebrates and reptiles and amphibians.

Index	Organism Group	Correlation Value
Shannon	Macroinvertebrates	-0.1694
Simpson	Macroinvertebrates	-0.1765
Shannon	Reptiles and Amphibians	-0.9706
Simpson	Reptiles and Amphibians	-0.9718

Table 3. Correlation between mean turbidity levels at each site and biodiversity index of macroinvertebrates and reptiles and amphibians.

Index	Organism Group	Correlation Value
Shannon	Macroinvertebrates	-0.8489
Simpson	Macroinvertebrates	-0.8505
Shannon	Reptiles and Amphibians	0.5114
Simpson	Reptiles and Amphibians	0.514

HISTORICAL CLIMATE TRENDS IN GEORGIA

Shivani Chougule, Husayn El Sharif, and Aris P. Georgakakos

REFERENCE: *Proceedings of the 2023 Georgia Water Resources Conference*, held March 30–31, 2023, at the University of Georgia.

Abstract. Climate variability and trends are important for Georgia's agriculture and the management of water resources. According to the EPA (US EPA, 2016), while Georgia has warmed less than most of the United States during the past century, over the next few decades the state is expected to become warmer and experience more severe floods and droughts. In this study, we assess the Georgia climate trends from 1980s to the present-day, using data from the Climatic Research Unit (CRU) gridded (~ 50x50 km) time series data (Harris *et al.,* 2020).

Assessments are performed for the monthly average minimum daily temperature (TMN), monthly average daily temperature (TMP), monthly average maximum daily temperature (TMX), monthly potential evapotranspiration (PET), monthly precipitation (PRE), and the difference between monthly precipitation and potential evapotranspiration (PRE - PET). This study focuses on state-wide climatic trends, and for this reason, all gridded variable data are first averaged over the entire state. Moreover, to identify trends at different time resolutions, the state-wide data are analyzed at monthly, annual, bi annual, and four-year time scales.

Figures 1, **2**, and **3** show that there has been a clear rising trend in state-wide average daily minimum, mean, and maximum temperatures over the last 10 to 15 years. Comparing the pre- and post-2010 historical periods, these temperature increases equal or exceed 1.5 °C (or 2.7 °F) for all three variables. Furthermore, the 1-, 2-, and 4-year rolling average sequences indicate that the interval (in years) during which each temperature variable *exceeds* a specific threshold has also been rising sharply. For example, prior to 2010, Georgia's 4-yr average maximum temperature *only slightly* exceeded 18 °C (64.6 °F) during 1990–1993 (3 yrs), 2001 (1 yr), and 2006–2007 (2 yrs). By contrast, post 2010, Georgia's 4-yr average maximum temperature has exceeded 18 °C *continuously* for more than 12 years. The rising temperature trends are expected to have important implications for agriculture, hydrology, water resources management, human health, and other socio-economic sectors.

A similar rising trend is observed for potential evapotranspiration (PET), which denotes the maximum water amount abstracted from the land by the atmosphere **(Figure 4)**. All moving average sequences plotted in this figure show the increasing trend indicate an increase in the duration of higher potential evapotranspiration **(Figure 4)**. In particular, the 4-yr moving average plot shows that pre-2010, the average PET was approximately 108 mm/month (~ 4.25 in/month) and attained a maximum of 113.5 mm/month (4.47 in/month). Post-2010, however, the average PET has reached 113.5 mm/month (4.47 in/month), has continuously *exceeded* the pre-2010 average (of 108 mm/month), and has attained a new maximum of 117 mm/month (4.6 in/month). Depending on precipitation changes (see below), these PET trends may have adverse impacts for Georgia's agriculture, hydrology (surface and subsurface), and water resources management, as under a no-change precipitation scenario, they imply a growing water supply deficit.

The precipitation data are shown on **Figure 5**. Precipitation is more variable (over all time scales) than temperature and PET, and its trends are more difficult to ascertain. The plots indicate that heavy (maximum) precipitation appears to be increasing, but average precipitation appears to remain stable or increase slightly. Thus, a key question is whether the precipitation trends counteract those of the PET.

The plots of (PRE-PET) in **Figure 6** is a first attempt to glean an answer to this question. The plots in this figure show that in the last decade, the difference (PRE-PET) exhibits a pattern similar to that of the 1987-1997 historical period. They also show that the period 1997-2013 was unprecedented in deficit (PRE-PET < 0) persistence and severity. Thus, the data presented here do not yet suggest a *statistically* conclusive answer to the above question. If, however, the Georgia climate in the next 10 years repeats the 1997-2013 pattern, this would suggest a clear climatic shift toward extended and deep deficits.

We also note that part of the difficulty in reaching a conclusive answer to the previous question is that the quantity PRE-PET is not a suitable metric for assessing water cycle changes. Specifically, the previous analysis focuses on *average* values of PRE and PET and ignores their distinctly different variability over finer time scales. A conclusive answer may be obtained by explicitly incorporating the underlying hydrologic processes in the water cycle and assessing the shifts in soil moisture, streamflow, and surface and subsurface water storage. Such a hydrologic assessment is currently on-going for different hydrologic basins at the Georgia Water Resources Institute (GWRI).

Lastly, the assessment presented in this article pertains to climatic averages for the *entire* state. However, Georgia's climate exhibits noteworthy differences at least over three climatic regions, including the Blue Ridge Mountain region in the north, the Piedmont plateau in the middle, and the coastal region in the south **(Figure 7)**. Another on-going effort at GWRI is to assess the observed climatic shifts in each of these regions, quantify the most likely climatic projections, and assess their water resources implications for the state's economy and environment.

Acknowledgements. This study was sponsored by the Georgia Water Resources Institute at Georgia Tech.

References:

Harris, I., Osborn, T. J., Jones, P., & Lister, D. (2020). Version 4 of the CRU TS monthly high-resolution gridded multivariate climate dataset. Scientific Data, 7(1), 109. https://doi.org/10.1038/s41597-020-0453-3

U.S. Environmental Protection Agency (EPA). (2016). What Climate Change Means for Georgia. US EPA. https://19january2017snapshot.epa.gov/sites/production/files/2016-09/documents/climate-change ga.pdf

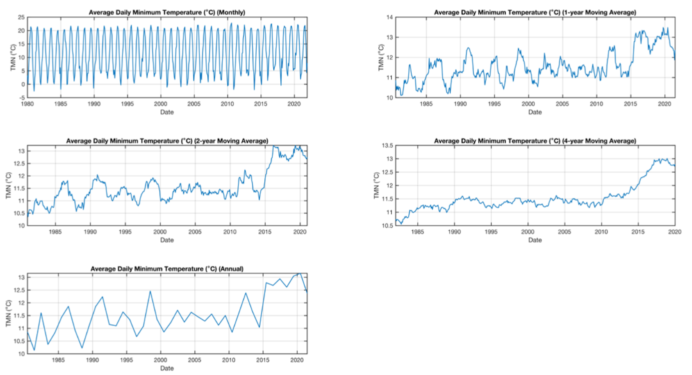

Figure 1. Average daily minimum temperature (TMN): Monthly, 1-year, 2-year, 4-year moving average sequences and annual series.

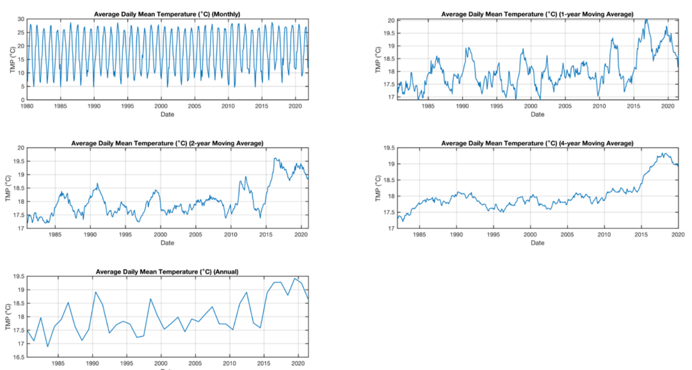

Figure 2. Average daily mean temperature (TMP): Monthly, 1-year, 2-year, 4-year moving average sequences and annual series.

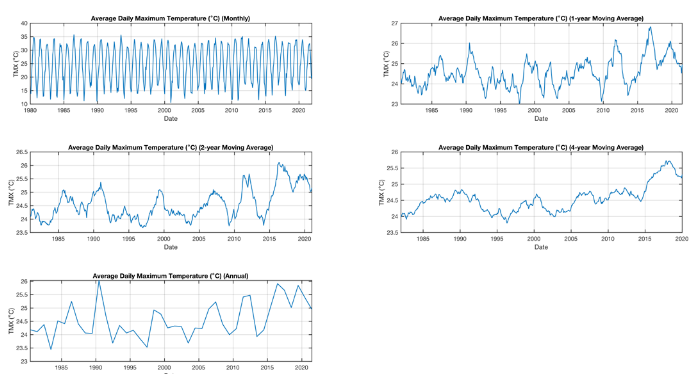

Figure 3. Average daily maximum temperature (TMX): Monthly, 1-year, 2-year, 4-year moving average sequences and annual series.

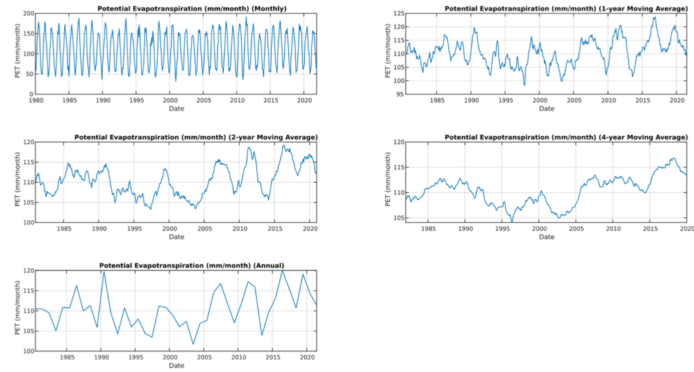

Figure 4. Potential Evapotranspiration (PET): Monthly, 1-year, 2-year, 4-year moving average sequences and annual series.

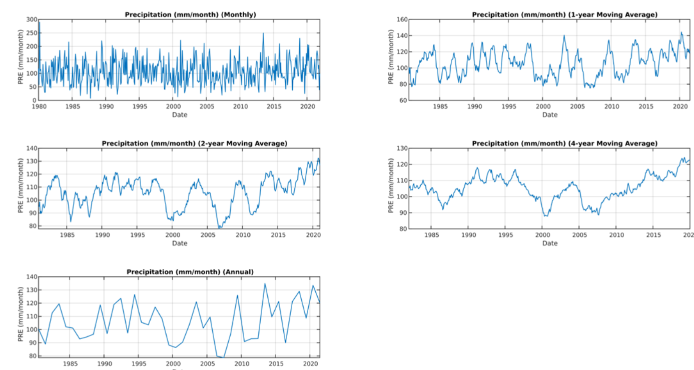

Figure 5. Precipitation (PRE): Monthly, 1-year, 2-year, 4-year moving average sequences and annual series.

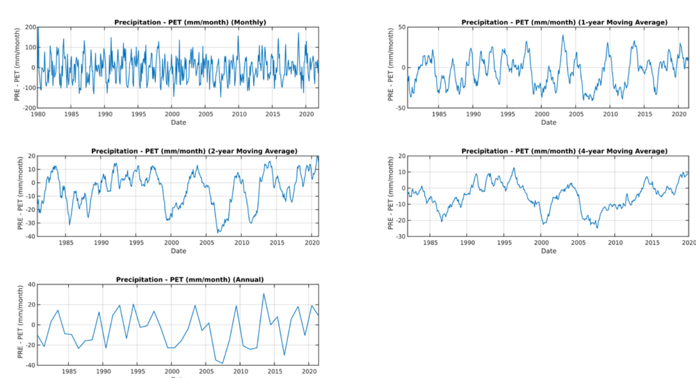

Figure 6. Difference between precipitation (PRE) and PET: Monthly, 1-year, 2-year, 4-year moving average sequences and annual series.

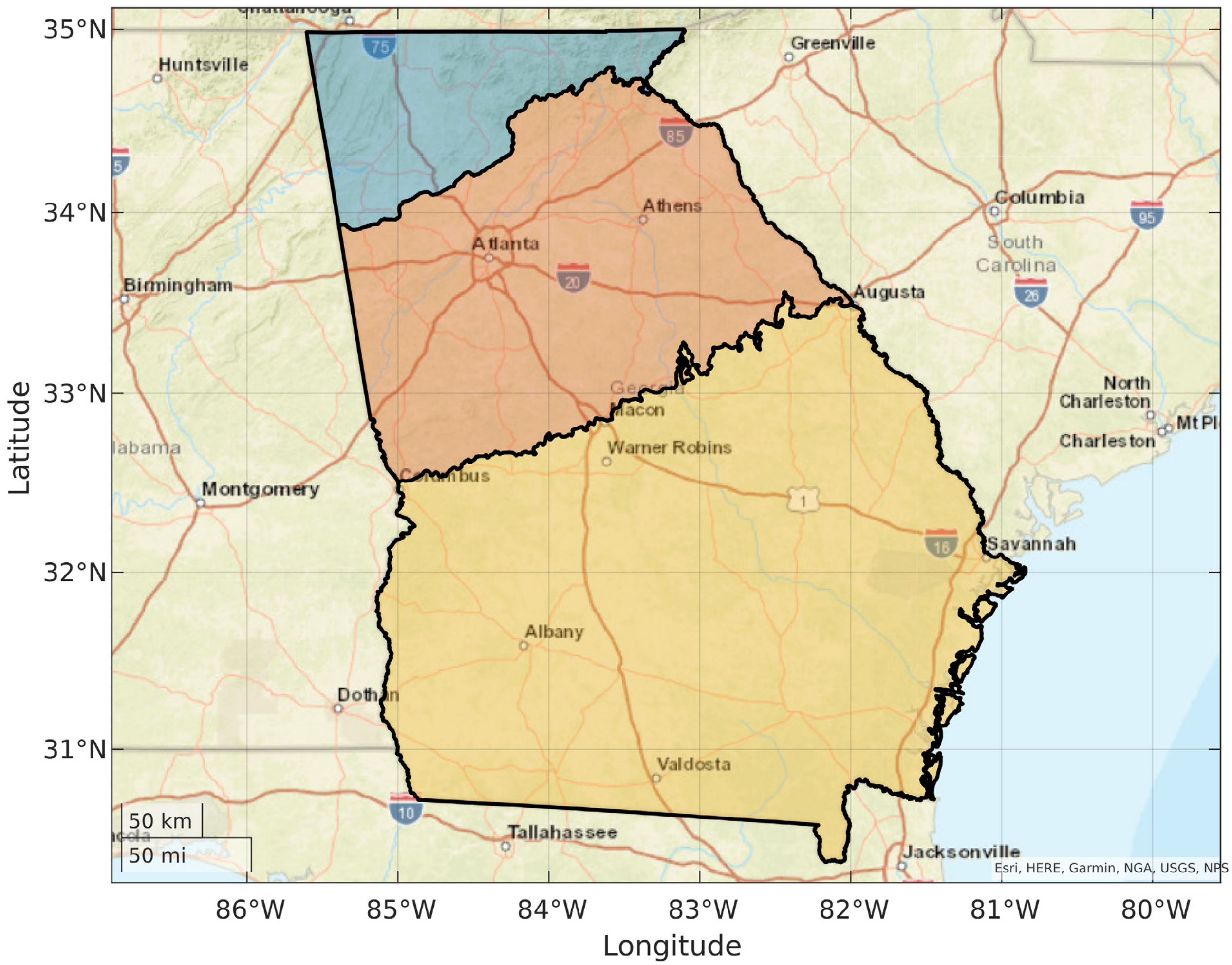

Figure 7. Three physiographic regions of Georgia: Blue Ridge Mountains (blue shading), Piedmont (orange shading), Coastal Plain (yellow shading).

WIND VELOCITY'S INFLUENCE ON ENHANCED TIDAL FLOODING OF LITTLE CUMBERLAND ISLAND, GA

Conlan Bertram, Dr. Robin McLachlan
College of Coastal Georgia, Department of Natural Science 02/28/2023

REFERENCE: *Proceedings of the 2023 Georgia Water Resources Conference*, held March 30–31, 2023, at the University of Georgia.

Introduction and Study Site. Due to sea level rise, tidal flooding has increased in frequency and magnitude in many coastal environments. Coastal communities are the first to be affected and could have to uproot their lives. Within 15 years, two-thirds of communities along the East and Gulf Coast of the United States could experience at least triple the number of high-tide flood events (Spanger-Siegfried, Fitzpatrick, & Dahl, 2014). While local sea-level rise is the primary driver of increased tidal flooding, climate change is also changing wind patterns and could potentially exacerbate flooding by wind set up where the wind velocity aligns with the direction of greatest fetch (Spanger-Siegfried, Fitzpatrick, & Dahl, 2014).

The barrier islands along the Georgia coast have dynamic geomorphological settings in which sediment transport can vary over small temporal scales due to the complex interaction between tides, waves, and local bathymetry. Little Cumberland Island (LCI) is one of the many barrier islands along the Georgia coast. LCI is privately owned and managed by a homeowner association whose covenants require that the island remain as natural as reasonably possible. This limits the options for residents when it comes to finding management solutions to the problems on the island, such as localized flooding and erosion. With no bridge connection to the mainland, a single small dock serves as the only access to the island. Additionally, all roads are constructed from local sediment, which makes many of the low-elevation roads very susceptible to tidal flooding and erosion. When tidal flooding exceeds approximately one foot above the road, the roads become inoperable resulting in the temporary stranding of the residents.

The main roads studied here are named Otter Trail, The Isthmus, and East Ridge **(Figure 1)**. East Ridge is the most susceptible to tidal flooding and coastal erosion as it is on the southeast portion of the island and is closest to the beaches that are being stripped away by the northward migration of Christmas Creek. The Isthmus connects the southern end of the island to the larger northern section, where most of the homes are located. It is primarily surrounded by marshes. Otter Trail connects the dock to all other sections of the island. Each of these roads is important to residents for different reasons, whether it be because their homes are along it or because it is their main way to get on and off the island. Residents have reported a connection between stronger wind speeds coming from the northeast and more extreme tidal flooding. This study aims to quantify the reported connection and to determine the validity of the observations.

.

Methods and Results. Twelve Water pressure was recorded using seven HOBO pressure sensors deployed throughout the island along the most flood-prone roads and at the dock **(Figure 1)**. Water pressure at each site was converted to water depth accounting for atmospheric pressure and then compared to the lowest elevation of the nearest road. Enhanced tidal flooding was calculated by differentiating the measured water level from water level predicted by NOAA (Station ID 8677832), which does not consider wind set up or local bathymetric impacts. It should be noted that the vertical datum for the measured high tide was not the same as that for predicted tidal levels; to compensate for this unknown offset, the average elevations for all predicted and all measured high tides were calculated and had the difference taken. This difference was then added to the measured tidal elevations with the assumption that the average elevation of high tide was equal throughout the region given both wind set up and draw down.

MATLAB was used to perform multivariable linear regressions and create scatter plots on polar axes. Originally, we were going to reference onshore wind data measured on the adjacent Jekyll Island due to its close proximity (15 km) to LCI; surprisingly, results indicate that wind measured by NOAA buoy 41008, which is 70 km offshore, is better correlated with enhanced tidal flooding than wind measured onshore closer to LCI. The onshore wind having a lower correlation could be due to local-scale barriers such as vegetation, buildings, and topography. Additionally, the offshore station likely accounts for storms forming offshore and other large-scale wind systems which can have a more significant effect on tidal flooding.

Preliminary results from the dock validate residents' reports that strong wind velocity, above 15 mph, particularly in the direction of greatest fetch (from the northeast) can enhance tidal flooding by tens of centimeters **(Figure 2)**. Inversely, winds from a southwest direction tend to suppress the enhancement. Site 1, however, showed weaker responses, indicating that location on the island affects these relationships. Using regression analysis, we found a highly significant influence of both wind speed ($p<.001$) and direction ($p<.001$) on tidal flooding at the dock. For site one, neither speed nor direction were significant.

Discussion. Wind set up is a crucial factor when analyzing tidal flooding and enhancement. We expect that as we analyze more sites and velocity will be a stronger influence in the more inland site. Many resources exist that allow residents to predict future flooding based on predicted tidal levels (e.g., NOAA) and expected sea-level rise (e.g., NOAA Sea

Level Rise Viewer). However, these national and global-scale resources do not account for the local interactions between wind set up and topography/bathymetry, which we have shown here to impact tidal flooding. Therefore, individual communities need more individualized attention and recommendations.

Localized studies that do exist most often focus on larger cities with larger populations; smaller communities like LCI are often not given the same attention. The two closest large cities to LCI are Jacksonville, FL and Savannah, GA. While the research focused on those cities will give insight into the effects of tidal flooding and sea level rise, the morphodynamics and landscapes are vastly different from LCI and are, therefore, often irrelevant to making local-scale management decisions. Having local examples for relatively small communities will allow us to communicate the very real effects climate change will have on small communities that often do not have the same defense systems as larger cities, such as seawalls and regular renourishment. Specifically focusing on the tidal flooding of LCI, we have predicted that the severity of the road flooding frequency will increase with time given expected rates of sea-level rise. Conclusions made here will allow island residents to predict event-scale flooding, plan their travel to and from the island, and more effectively manage their roads. They can also use these data to better understand the dynamic nature of their beaches, which are rapidly eroding.

References:

Spanger-Siegfried, E., Fitzpatrick, M. F., & Dahl, K. A. (2013). Encroaching Tides: How Sea Level Rise and Tidal Flooding Threaten U.S. East and Gulf Coast Communities over the Next 30 Years. *Union of Concerned Scientists*.

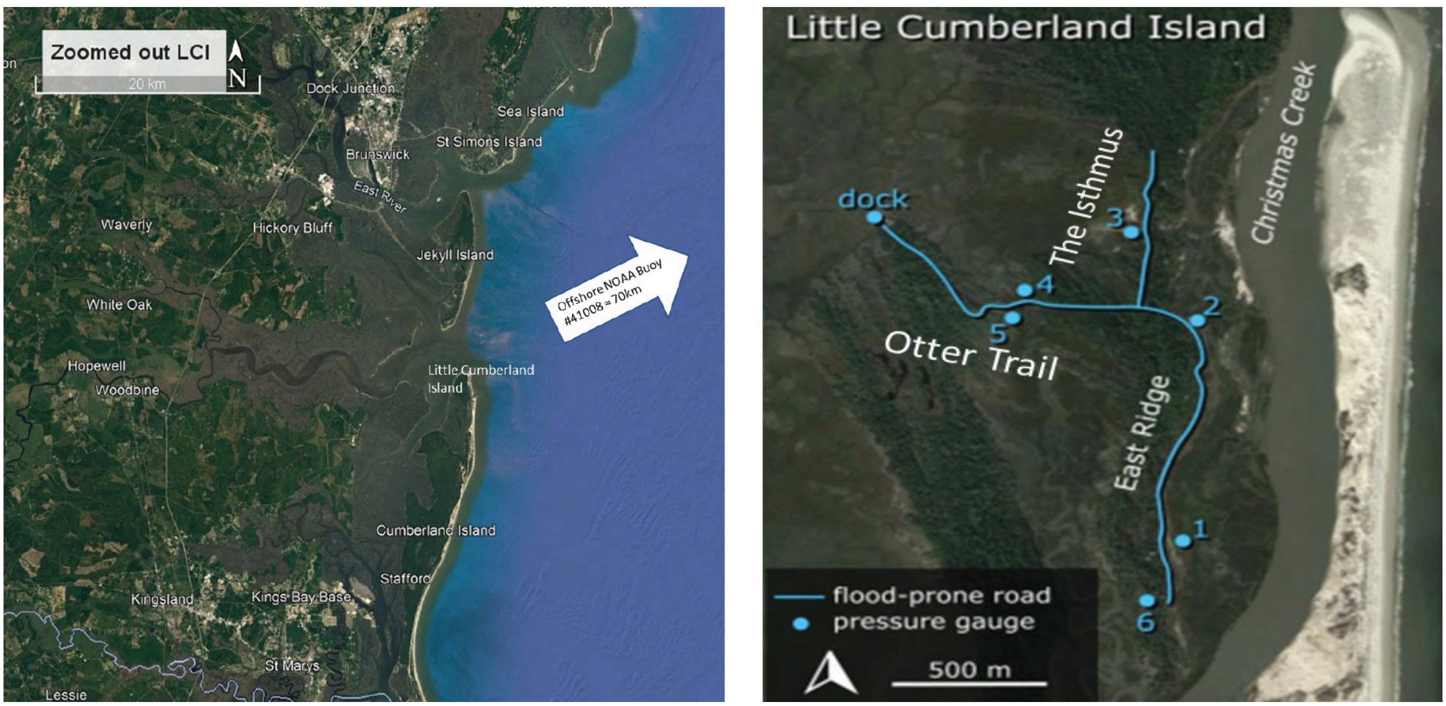

Figure 1. Site map of Little Cumberland Island showing the roads and HOBO pressure sensor sites

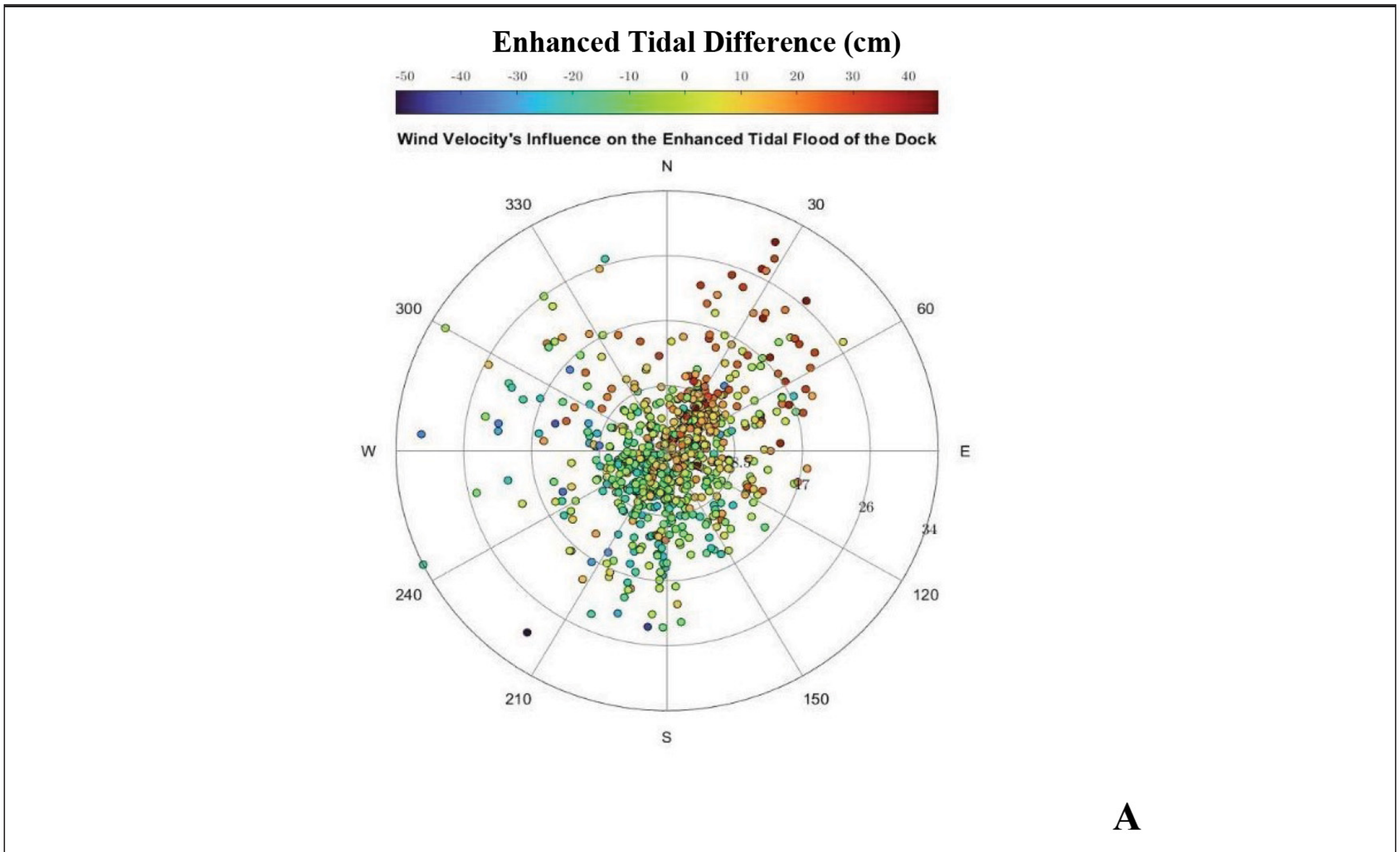

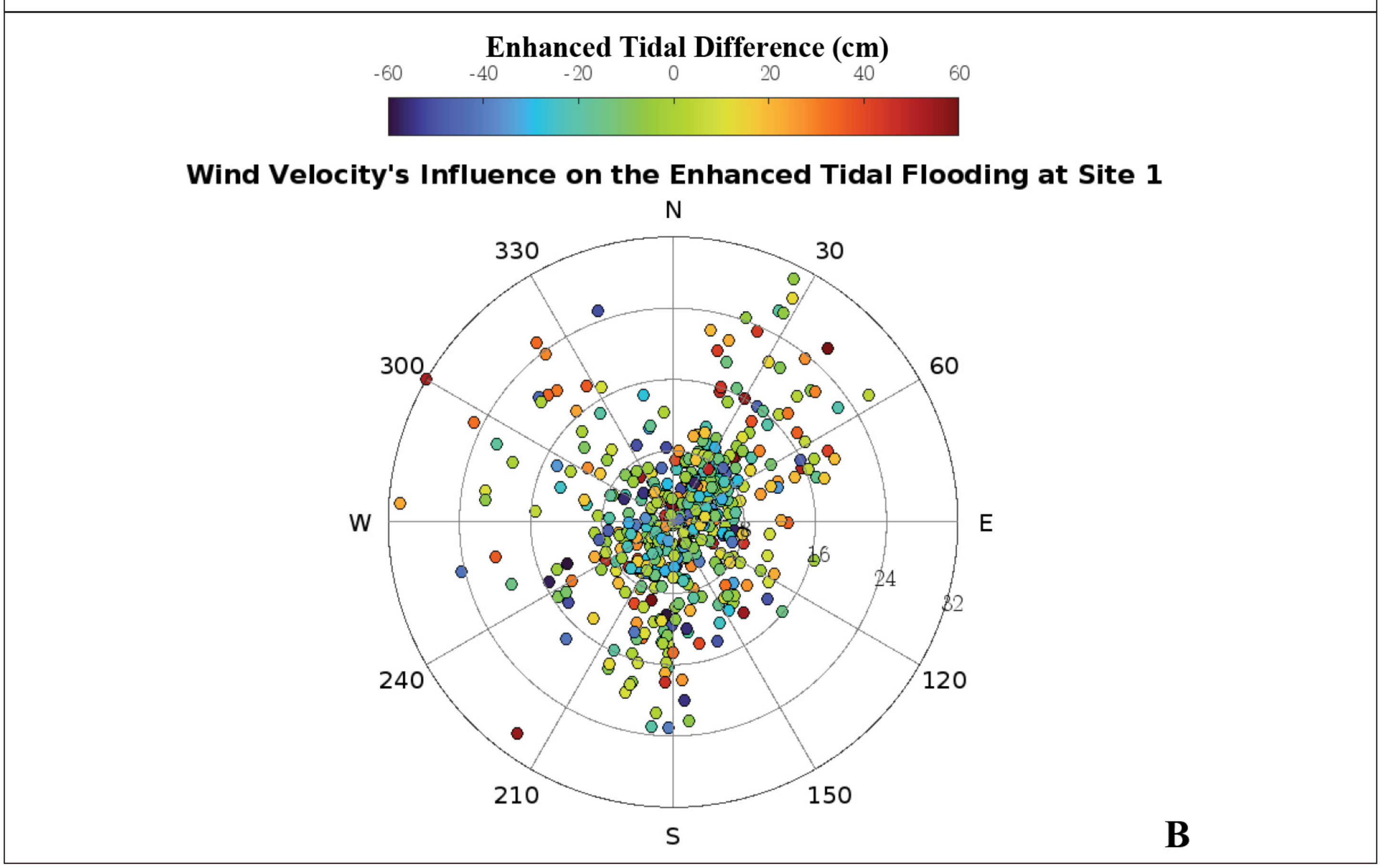

Figure 2. The effect of wind velocity on enhanced tidal flooding at the dock (**A**) and Site 1 (**B**) displayed as a windrose scatter plot. Notice that enhanced tidal flooding is most prominent when winds approach from the northeast, the direction of greatest fetch.

LEARNING HOW TO GROW PHYTOPLANKTON CULTURES WITH SPECIAL NEEDS: WHAT SOIL EXTRACTS FROM COASTAL GEORGIA DOES *LEVANDERINA FISSA* PREFER?

Dillon Doomstorm[1], Mallie Hunt[2], Jim Sanders[2], Catharina Alves-de-Souza[3], Charles Wingert[3], Sara Rivero-Calle[2]
[1]UGA Marine Sciences Department, Athens GA, [2]UGA Skidaway Institute of Oceanography, Savannah GA,
[3]UNCW Algal Resources Collection, Wilmington NC
Corresponding author: Sara Rivero-Calle (rivero@uga.edu)

REFERENCE: *Proceedings of the 2023 Georgia Water Resources Conference*, held March 30–31, 2023, at the University of Georgia.

Introduction. The Bio-Optical Oceanography Laboratory at Skidaway Institute of Oceanography is working on characterizing the optical properties of harmful algal bloom (HAB) species with the goal of using this information to identify them from space. As part of this project, a selection of HAB species need to be maintained in laboratory monocultures to test whether they can be optically distinguished based on hyperspectral scattering properties. One of the HAB species chosen was *Levanderina fissa*, which is an unarmored dinoflagellate characterized by delicate surface striations along its body **(Figure 1)** and present in saline, brackish, and freshwater systems. Since it was first described as *Gymnodinium fissum* by Levander in 1894, *L. fissa* has gone through multiple changes in name and classifications (Moestrup et al 2019). Today, *Spirodinium fissum*, *Gymnodinium fissum*, *Gyrodinium instriatum*, *Gyrodinium uncatenum* are considered synonyms (Moestrup et al 2019).

L. fissa is not necessarily a toxic species but its blooms can be harmful to fish and other wildlife by causing oxygen depletion. Frequent *L. fissa* blooms have been documented in the Pearl River estuary (China) for decades (Wang et al., 2017, Wang et al., 2019). Although blooms by this species are considered rare elsewhere (Tang et al. 2022), they have been observed in the Gulf of Guayaquil in Ecuador (Jiménez et al., 1993), in Hakozaki Fishing Port of Japan (Nagasoe et al., 2006), and Bahia de Acapulco, Mexico (Gárate-Lizárraga et al. 2013). *L.fissa* blooms have been associated with mass mortalities of farmed fish in Korea (Kim et al., 1995) and shrimp farms in Ecuador (Jiménez et al., 1993).

L. fissa's high salinity tolerance and ability to use organic phosphorus provide competitive advantages in brackish estuarine environments (Wang et al 2019), which could lead to dominance of an ecosystem and a harmful bloom. This high tolerance to a variety of environmental conditions means that, when grown in the lab, *L fissa* cultures can use a few different media compositions (ERD, F/2, L1) with a variety of salinity levels depending on the strain. Furthermore, some strains also require the addition of soil extract, which is not common for all phytoplankton species and often not well documented. For this project, *L. fissa* strain #277 from the University of North Carolina Wilmington Algal Resource Collection (ARC) was selected. It is assumed that this strain requires ERD media and the addition of soil extract but, to our knowledge, there is no published work comparing its growth rates with or without soil extract addition or even describing the properties of the soil extract per se. The need to identify a local source for this soil extract in Georgia and the lack of details in the literature on the composition of the extract further motivated this study. An experiment was designed to determine whether differences in soil extract affect *Levanderina fissa's* growth rates and which of three local sources provided the best results. An undergraduate student was tasked with this hands-on experiential learning opportunity as a faculty-directed independent research study during the Semester at Skidaway Program at the University of Georgia in the Fall of 2022.

Methods. To determine whether *L. fissa* has a preference in soil types, cultures were grown under three different soil treatments with triplicates for 20 days. Soil samples were collected from three locations in coastal Georgia: Priest Landing (PL), The Georgia Botanical Garden (BG), and Butter Bean Beach (BB) **(Figure 2)**. Selection of locations to collect soil were based on recommendations from a culture protocol by Starr and Zeikus (1993) and personal communication with Robert Anderson. According to this, the soil should be collected from areas close to the interface between land and water, but high enough to be above the water table to prevent the soil from being anoxic. In addition, the soil should not contain conglomerates, large amounts of clay particles or fertilizers. After soil collection, each individual soil sample needs to be examined to eliminate biotic matter (i.e. insects, worms, leaf litter, etc.) or other different sediment types, autoclaved, treated, and filtered to obtain a soil solution **(Figure 3)**.

The filtering process involved sieving each soil sample from 0.5 ϕ to 0.25 ϕ, and then placing the soil in a drying chamber for 24-48 hours. After initial drying, 1.5L of 30 salinity sea water and calcium carbonate were added in a 2L media bottle with a scoop from one of each individual soil samples and left overnight. The addition of calcium carbonate helped pull potential contaminants and other material out of the gathered soil, an extension of the filtering process. This was repeated three times, once for each soil sample. After this, another series of filtrations was performed. The first filtration was done with a coffee filter, followed by two series of filtrations through 0.4µm filters with the help of a vacuum pump, to eliminate any remaining organic material left in the mixture. Between filtrations, soil samples were autoclaved and kept in a refrigerator. After final filtration and autoclaving, each soil extract was labeled and kept in 2-liter glass bottles.

L. fissa cultures were grown in 75ml tissue flasks. Each flask was filled with 50 ml of Erdschreiber media (ERD2, which included 2.5ml of soil extract) and inoculated with 2ml of *L. fissa* culture. The ERD2 culture media was composed of 50ml of seawater at 15 salinity, 50µL of nitrate, 50µL of phosphate, 300µL of ERD trace metals, 25µL of vitamins, 50µL of manganese EDTA, and 2.5ml of one of the three soil extracts. The media of the control group cultures did not contain any soil extract. Triplicate cultures were grown for each of the three soil types and the control group, therefore the total number of cultures grown was twelve. Cultures were kept in an incubator at 19°C and a light cycle of 14hrs daylight:10hrs darkness.

Based on previous experience with *L. fissa* cultures and their growth rates, cell counts were started eleven days after inoculation. After the initial 11-day period, cell counts were recorded daily using a Sedgewick Rafter. A Sedgewick Rafter was chosen instead of a hemocytometer to accommodate the relatively large size of *L. fissa's* cells (~200µm). Due to the high concentrations obtained, dilutions were performed to avoid overcrowding the chambers of the Sedgewick Rafter and to facilitate counting. This involved adding 100µL of sample to 900µL of DI water to achieve the 1ml volume that the chambers can hold. Lugols were also added to paralyze the cells and facilitate cell counting. A hand-held clicker was used to keep track of cell counts. Care was taken to avoid counting dead or burst cells, counting cells on dividing lines, or double counting cells that were touching.

Results. Results show that when counting started (eleven days after inoculation), differences between treatments were not significant, while differences with the control group were significant **(Figure 4a)**. At the end of the experiment (~3 weeks after inoculation), all cultures treated with soil extract experienced growth, but those treated with soil extract from Priest Landing (PL) outperformed the rest **(Figure 4b)**. PL showed consistently higher concentrations on all days except day 11 and day 17 **(Figure 5)**. BB and BG followed a similar trend in growth for the duration of the experiment **(Figures 4, 5)**.

Discussion. The need of soil extract addition for increased growth in dinoflagellate cultures is well known since the 1960's (e.g., Sweeney 1961) but information in this regard remains mostly empirical, with few studies showing experimental data in this regard. This study shows that all cultures of *L. fissa* strain #277 can grow in ERD2 media, even without soil extract. However, when soil extract is added, growth is enhanced, multiplying culture concentrations by ~ 5. Maximum cell concentrations for the control group were ~500 cells/ml, while treated cultures reached 2,000cells/ml after 21 days. According to Kim et al., (1995), a cell density of 1,000 cells/ml is capable of killing fish in 2hrs, therefore the addition of soil extract triggers harmful bloom concentration levels. Nonetheless, based on cell count results, none of the cultures reached the stationary phase; they were all in the exponential phase. It would have been necessary to continue monitoring cell concentrations beyond 3 weeks to understand the complete life cycle of the cultures and the maximum concentration rates in the stationary phase.

The positive effect of soil extract has been related to the stimulatory effect of humic substances (Prakash and Rashid, 1968). Although all cultures treated with soil extract experienced greater growth rates than the control group, those treated with soil extract from Priest Landing outperformed the rest. The fact that there were differences in the response among soil treatments raises the question of what is unique about the composition of Priest Landing. Priest Landing and Butter Bean beach are very similar locations by river estuaries and marshlands, separated by less than 5 miles, while the Coastal Georgia Botanical Garden is located inland, 20 miles away from Skidaway Island. It would be expected that Priest Landing and Butter Bean Beach soil might be similar to each other and most different from the Botanical Garden soil, but results show that Butter Bean and Botanical Garden gave similar results and Priest Landing outperformed the rest. Reasons for these differences are unclear without performing a detailed analytical study of the soil composition, which was beyond the scope of this study. Nonetheless, in a similar experiment to examine the causes of an *L. fissa* harmful algal bloom in the Pearl River Estuary, nutrient composition was examined and *L. fissa's* growth was documented over a 22-day period under different phosphorus (P) and nitrogen (N) treatments (Wang et al., 2017). This study found that *L. fissa* is an adaptable dinoflagellate that can use both dissolved inorganic or organic forms of P and N. Inorganic sources provided the highest growth rates; *L. fissa* was not able to use DON, but it grew well under DOP. The ability to use organic P in the absence of inorganic P is an advantageous trait for *L. fissa* (Wang et al., 2017). Multiple factors contribute to the formation of a bloom but in the Pearl Estuary, the continuous supply of DIN, enrichment of DOP, warm and low salinity water may have driven the blooms (Wang et al., 2017). In addition to influences of both dissolved inorganic or organic P or N, the abundance of fulvic and humic acid could be a factor in cell growth. A study performed to understand humic substances effects on marine dinoflagellates found that blooms and their intensity may be correlated to humic substances entering the environment (Prakash and Rashid, 1968). Although there is debate on humic substances and their influences, the addition of humic and fulvic acid (soluble counter parts) had positive effects during Prakash and Rashid experiments on cell growth.

L. fissa strain #277 was isolated from New River (North Carolina) in 2009, which is a low salinity environment near soil sources, which explains why it is maintained in the lab under low salinity conditions and responds well to soil extract addition. Although this particular strain may be adapted to soil extract and low salinities, that is not necessarily the case for all strains of this species, and it cannot be assumed that one study on a particular strain can explain all future *L. fissa* blooms. At the moment, *L. fissa* is not common in Georgia, but understanding the mechanistic drivers conducive to a bloom of this species is important, as past research suggests that it is highly flexible and has characteristics of a HAB species (Nagasoe et al. 2006).

Conclusions and Future Work. This study shows that soil extract is in fact needed to enhance growth of *L. fissa* in the lab, especially if the goal is to reach bloom concentration levels. It is unclear what exactly is the compound that enhances growth but all the cultures with a soil extract treatment grew significantly faster, achieving bloom concentration levels. Out of the three soil extracts, that of Priest Landing outperformed the rest. If this work were to be repeated, daily cell counts should be extended beyond three weeks to capture all the phases of the culture (exponential, stationary, and decay). In addition, it would be valuable to analyze the phosphorus quantity and composition of soil extracts, and to identify the constituent(s) affecting growth rates. Identifying the different stages of growth and decay and the nutrient composition at each stage, could allow for clear evidence of which nutrients are available or limited in each soil extract. This information could allow to make predictions about where and how *L. fissa* might thrive in Georgia's rivers and estuaries and what conditions could lead to a harmful bloom.

Acknowledgements. This undergraduate research work was conducted as part of a faculty-led study during the Semester at Skidaway Program at the University of Georgia. This was an opportunity for the undergraduate to experience for the first time a real-world hands-on research experiment. Challenges and lessons learned from this experience include learning how to culture phytoplankton in the lab, experimental design, selecting locations for soil collection, following a protocol to produce soil extracts, learning how to monitor concentrations and growth rates, learning how to count large mobile cells in a counting chamber, the differences between a Sedgewick rafter and a hemocytometer, differences between using a compound instead of inverted microscope, the addition of Lugols to immobilize cells, selecting statistical analyses, and interpreting results. We would like to thank everyone at UNCW ARC for providing the *Levanderina fissa* strain used in this study and a wealth of information on how to grow phytoplankton cultures in the lab. We are grateful to everyone at UGA Skidaway, especially the coordinators, faculty and students that were part of the Semester at Skidaway in 2022. Special thanks to lab members of the Rivero-Calle group (Ben Lowin, Masud-Ul-Alam, Emma Goldsmith) for their feedback and continued support.

References:

Gárate-Lizárraga I., Sevilla-Torres G., Alvarez-Anorve M., Aguirre-Bahena F., Violante-Gonzalez J., Rojas-Herrera A. (2013). First Record of Red Tide Caused by *Gyrodinium Instriatum* (Dinophyceae: Gymnodiniales) in Bahía De Acapulco, Guerrero. *Cicimar. Oceánides* 28, 43–47. doi: 10.37543/oceanides.v28i1.120

Hakanen, Päivi & Hansen, Gert & Daugbjerg, Niels & Ellegaard, Marianne. (2014). On Levanderina fissa gen. & comb. nov. (Dinophyceae) (syn. Gymnodinium fissum, Gyrodinium instriatum, Gyr. uncatenum), a dinoflagellate with a very unusual sulcus.. Phycologia. 53. 265-292. 10.2216/13-254.1.

Jiménez, R., 1993. Ecological factors related to *Gyrodinium instriatum* bloom in the inner estuary of the Gulf of Guayaquil. In Smayda, T. J. & Y. Shimizu (Eds), Toxic Phytoplankton Blooms in the Sea. Proceedings of the 5th International Conference on Toxic Marine Phytoplankton, Newport, Rhode Island, U.S.A., 28 October–1 November 1991. Elsevier, Amsterdam: 257–262.

Kim H.G., Park J.S., Fukuyo H., Takayama K.H., Shim J.M., 1995. Noxious dinoflagellate bloom of an undescribed species of Gyrodinium in Chungmu coastal waters, Korea. In: Harmful Marine Algal Blooms, Lassus, P., Arzul, G., Erard, E., Gentien, P. and Marcaillou, C. eds., Lavoisier Tech. et Doc., Publish., 5964.

Nagasoe, S., Kim, D.I., Shimasaki, Y., Oshima, Y., Yamaguchi, M., Honjo, T., 2006. Effects of temperature, salinity and irradiance on the growth of the red tide dinoflagellate Gyrodinium instriatum Freudenthal et Lee. Harmful Algae 5, 20–25.

Øjvind Moestrup, Hakanen, Päivi, Gert Hansen, Niels Daugbjerg, and Marianne Ellegaard.(2014) On Levanderina Fissa Gen. & Comb. Nov. (Dinophyceae) (Syn. Gymnodinium Fissum, Gyrodinium Instriatum, Gyr. Uncatenum), a Dinoflagellate with a Very Unusual Sulcus." *Phycologia* 53: 265–92. https://doi.org/10.2216/13-254.1.

Starr, Richard C., and Jeffrey A. Zeikus. (1993): Utex—the Culture Collection of Algae at the University of Texas at Austin 1993 List of Cultures1. *Journal of Phycology* 29, no. s2: 1–106. https://doi.org/10.1111/j.0022-3646.1993.00001.x.

Sweeney, B. M. (1951). Culture of the Dinoflagellate *Gymnodinium* with Soil Extract. *American Journal of Botany*, 38(9), 669–677. https://doi.org/10.2307/2437913

Tang, Yali & Xie, Changliang & Jin, Xiaotong & Wang, Zhaohui & Hu, Ren. (2022). Inhibitory Effect of Isolated Bacteria from the Phycosphere of Levanderina fissa on the Growth of Different Microalgae. Frontiers in Marine Science. 9. 908813. 10.3389/fmars.2022.908813. https://www.frontiersin.org/articles/10.3389/fmars.2022.908813/full

Wang, Z., Zhao, J., Xiao, L., Lin, L. (2019). Interspecific Competition Between Levanderina fissa (Dinophyceae) and the Other Three Microalgal Species in Co-Cultures. Journal of Ocean University of China 18, 919–925. https://doi.org/10.1007/s11802-019-3951-1

Wang, Zhaohui, Xin Guo, Linjian Qu, and Langcong Lin. (2017). Effects of Nitrogen and Phosphorus on the Growth of Levanderina Fissa: How It Blooms in Pearl River Estuary. *Journal of Ocean University of China* 16, no. 1: 114–20. https://doi.org/10.1007/s11802-017-3080-7.

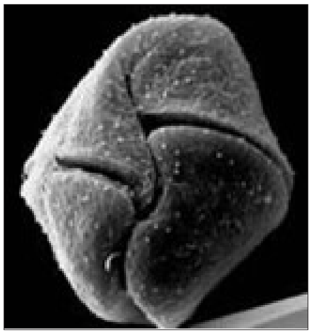

Figure 1. Levanderina fissa under an electron microscope with its outer shell displaying the segmentation used as a taxonomic indicator for the species. Credit: Hanaken et al., (2014).

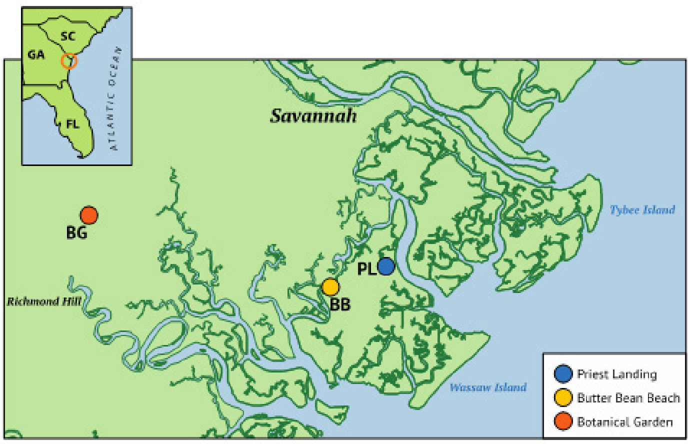

Figure 2. Soil samples were collected from three locations in coastal Georgia, from left to right: the Georgia Botanical Garden (BG), Butter Bean Beach (BB) and Priest Landing (PL).

Figure 3. a) Dillon Doomstorm learning how to identify and count species, b) the three soil extracts, c) Dillon Doomstorm performing the filtering of soil extracts.

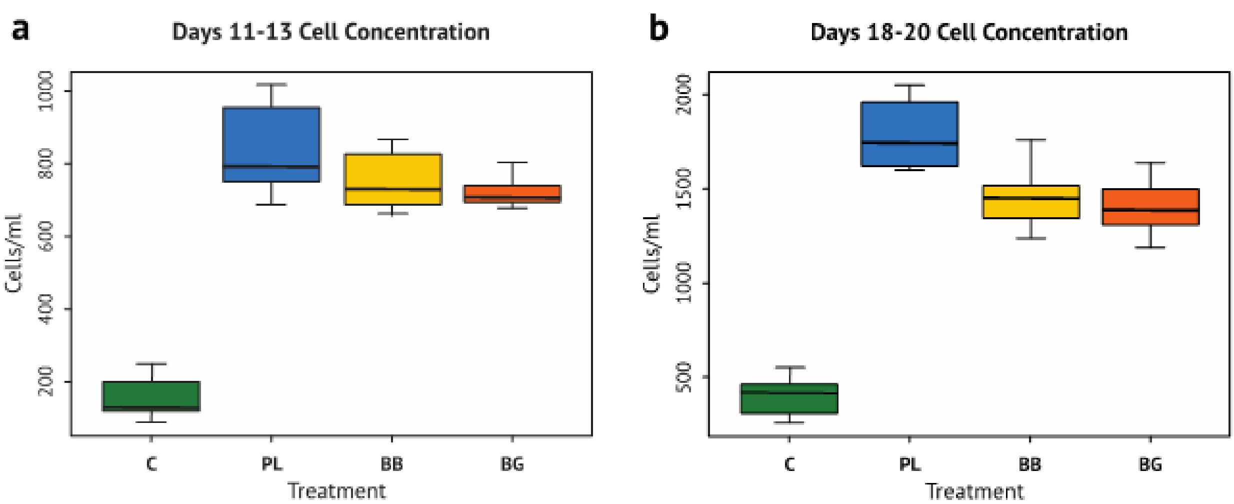

Figure 4. Statistical differences in cell density among treatments. Mean cell concentration per treatment averaged over: a) the first 3 days (days 11-13) and b) the last 3 days of the experiment (days 18-20). Error bars represent standard deviation. All treatments show significant differences with respect to the control. Differences among treatments with soil extract were only significant at the end of the experiment.

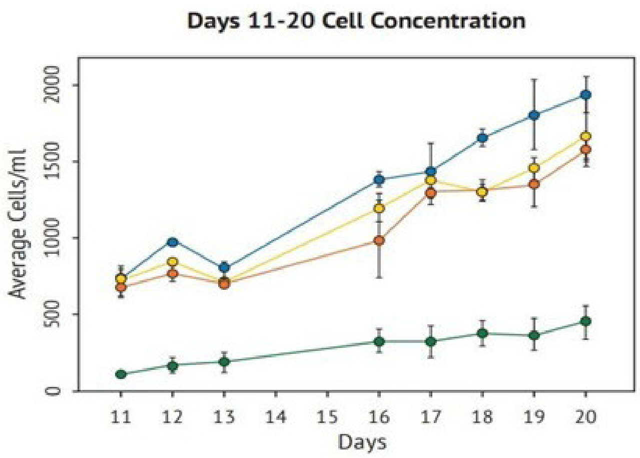

Figure 5. Time-series of Levanderina fissa daily average cell concentrations (cells/ml) between day 11 and day 20 for each of the treatments: Control (C, green), Priest Landing (PL, blue), Botanical Garden (BG, orange) and Butter Bean beach (BB, yellow). Error bars depict standard deviation. BG (orange) and BB (yellow) had similar cell densities and PL (blue) outperformed both. The control group without soil extraction (green) showed significantly lower concentrations throughout the experiment. No counts were done on Days 14 and 15.

ASSESSMENT OF AGRICULTURAL YIELD AND IRRIGATION DEMAND FOR THE ACF RIVER BASIN

Husayn El Sharif and Aris P. Georgakakos

REFERENCE: *Proceedings of the 2023 Georgia Water Resources Conference*, held March 30–31, 2023, at the University of Georgia.

Abstract. Biophysical crop models coupled with modern meteorological and soil data can support better crop planting strategies, more efficient irrigation water use, and more resilient drought management responses to climate variability and change. In this study, soil, crop, and meteorological gridded data are combined with the Decision Support System for Agrotechnology Transfer - Cropping System Model (DSSAT-CSM) [*Tsuji et al.*, 1994; *Hoogenboom et al.*, 2017] to assess the sensitivity of crop yield (peanuts, corn, soybeans, and cotton) and irrigation demand to historical climate conditions in the Apalachicola-Chattahoochee-Flint (ACF) River Basin. This assessment included normal, dry, and wet years. Then, using bias corrected General Circulation Model (GCM) climate projections, we estimate how crop yield and irrigation demand may materialize in the future.

For this study, the ACF is divided into 14 sub-basins as shown in **Figure 1**. Crop acreages for rainfed and irrigated peanut, corn, soybean, and cotton were obtained from the USDA Cropland Data Layer [*USDA NASS*, 2015] and the USDA Farm Service Agency. Annual crop yields and irrigation amounts for the control period 1980 – 2016 were simulated using the DSSAT-CSM model calibrated to the ACF region with the parameters listed in **Table 1**. Simulation results were then coupled with reanalysis climate data from the Climate Research Unit (CRU) to estimate typical crop yields and irrigation demand during dry, normal, and wet growing seasons as presented in **Tables 2** through **5**. Regression relationships were identified using these crop model runs between growing season precipitation, potential evapotranspiration, and modeled irrigation demand. These relationships were extended into the future using bias-corrected climate projections to assess the types of growing seasons, crop yield, and irrigation demand could materialize over the next thirty years to the end of the century.

Results based on the latest bias-corrected CMIP6 climate data indicate that over the next thirty years, the frequency of dry growing seasons will increase mildly throughout the ACF, and that after year 2050 dry growing seasons will constitute nearly half or more the growing seasons, suggesting that agricultural drought could become the “new normal” in the region (**Figure 2**). Crop model simulations assuming no change in irrigated acreages suggest that compensating for the increased frequency in dry seasons will require on average a 30 to 40 percent increase in irrigation volume over the next thirty years and a doubling or more of irrigation demand by the end of the century as illustrated in **Figures 3** and **4**.

Acknowledgements. This study was sponsored by the Georgia Water Resources Institute at Georgia Tech.

References:

Hoogenboom, G., et al. (2017), Decision Support System for Agrotechnology Transfer (DSSAT) Version 4.7, edited, DSSAT Foundation, Gainesville, Florida, USA.

Tsuji, G., G. Uehara, and S. Balas (1994), *DSSAT V3*, University of Hawaii, Honolulu.

USDA NASS (2015), USDA National Agricultural Statistics Service Cropland Data Layer, edited by USDA-NASS, Washington, DC. USA.

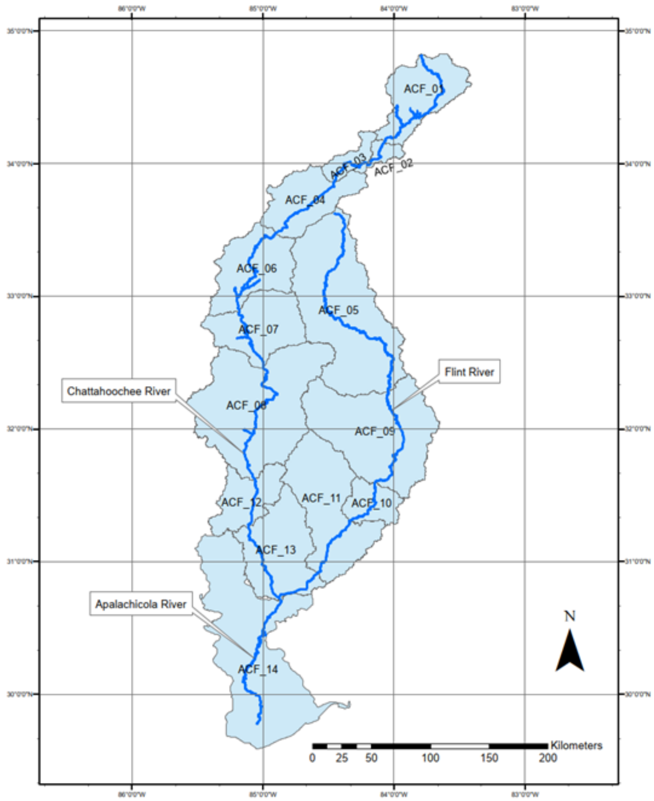

Figure 1. The Apalachicola-Chattahoochee-Flint (ACF) River Basin and its 14 sub-basins.

Table 1. Calibrated input parameters for DSSAT-CSM rainfed and irrigated crop simulations.

Model Parameter	Corn	Peanut	Cotton	Soybean
Planting Date (1980-2016)	March 29th	May 16th	May 5th	May 25th
Cultivar	B73 X MO17	Georgia Green	DP 555 BG/RR	DP 5634 (Maturity Group V)
Row Spacing	30 inches (76 cm)	36 inches (90 cm)	36 inches (90 cm)	30 inches (76 cm)
Plant Population	30,000 plants/acre (7.9 plants/m^2)	85,000 plants/acre (21 plants/m^2)	50,000 plants/acre (12.4 plants/m^2)	90,000 plants/acre (22.2 plants/m^2)
Irrigation: Soil Management Depth	12 inches (30 cm)	20 inches (50 cm)	12 inches (30 cm)	12 inches (30 cm)
Irrigation: Available soil water content threshold	50%	60%	50%	50%
Nitrogen Fertilizer	Nitrogen stress not simulated	Nitrogen stress not simulated	45 lbs/acre (50 kg/ha) of N fertilizer applied at 4 inch (10 cm) depth at planting and again at 46 days after planting	Nitrogen stress not simulated

Table 2. DSSAT-CSM Simulation results for rainfed and irrigated corn during typical dry, normal, and wet growing seasons in the ACF during the 1980-2016 control period.

ACF Basin	Corn								
	Rainfed Yield (kg/ha)			Irrigated Yield (kg/ha)			Irrigation Amount (mm)		
	Dry	Normal	Wet	Dry	Normal	Wet	Dry	Normal	Wet
1	6935	9413	12194	13696	13486	13772	196	147	78
2	5735	7508	11141	12064	12269	12751	212	169	99
3	5457	8064	11170	12191	12540	13153	211	160	105
4	4846	8104	10609	11263	11941	12254	216	146	90
5	3197	5579	9991	10527	10798	10895	261	189	93
6	5302	7607	11079	11332	11927	12319	216	156	89
7	5395	6842	10003	10294	10426	10347	186	147	86
8	4556	6269	9958	10859	11046	11378	237	170	104
9	3910	5936	9528	10494	10743	10303	253	179	100
10	4842	6525	8902	10319	10500	9861	230	158	113
11	4736	6746	9106	10492	10660	10047	230	159	104
12	4292	7227	9811	10514	11197	10507	231	152	99
13	4716	6532	8787	9887	10491	9616	224	162	105
14	5323	7675	8221	10317	10537	10458	200	143	116

Table 3. DSSAT-CSM Simulation results for rainfed and irrigated cotton in the ACF during typical dry, normal, and wet growing seasons in the ACF during the 1980-2016 control period.

ACF Basin	Cotton								
	Rainfed Yield (kg/ha)			Irrigated Yield (kg/ha)			Irrigation Amount (mm)		
	Dry	Normal	Wet	Dry	Normal	Wet	Dry	Normal	Wet
1	2206	2330	2414	2623	2700	2517	174	137	74
2	-	-	-	-	-	-	-	-	-
3	-	-	-	-	-	-	-	-	-
4	2273	2369	2564	2724	2723	2693	195	158	96
5	2272	2470	2971	2921	2959	3149	202	165	82
6	2250	2449	2580	2751	2764	2743	213	156	103
7	2230	2453	2655	2775	2800	2837	218	157	93
8	2250	2562	2756	2810	2872	2939	204	138	91
9	2336	2600	3116	3008	3072	3296	188	152	85
10	2618	2961	3154	3113	3261	3290	150	107	73
11	2582	2923	3114	3073	3223	3258	156	113	72
12	2383	2815	2907	2872	3013	2982	174	103	69
13	2562	2936	3070	3001	3205	3188	147	104	69
14	2644	2896	2916	2904	3039	2959	119	75	54

Table 4. DSSAT-CSM Simulation results for rainfed and irrigated peanut in the ACF during typical dry, normal, and wet growing seasons in the ACF during the 1980-2016 control period.

ACF Basin	Peanut								
	Rainfed Yield (kg/ha)			Irrigated Yield (kg/ha)			Irrigation Amount (mm)		
	Dry	Normal	Wet	Dry	Normal	Wet	Dry	Normal	Wet
1	3580	4128	5035	5297	5295	5292	197	166	91
2	-	-	-	-	-	-	-	-	-
3	-	-	-	-	-	-	-	-	-
4	-	-	-	-	-	-	-	-	-
5	2710	3237	4694	5222	5432	5337	274	221	122
6	2976	3682	4525	5445	5548	5693	272	205	136
7	2583	3385	4566	5295	5409	5509	287	213	128
8	2816	3804	4690	5259	5367	5395	266	185	125
9	2901	3544	4612	5165	5369	5271	253	202	121
10	3481	4228	4710	5191	5349	5293	212	157	111
11	3447	4189	4703	5187	5333	5269	218	162	106
12	3068	4319	4811	5227	5374	5313	240	157	100
13	3460	4328	4770	5070	5376	5252	210	152	101
14	3591	4547	4992	5116	5318	5305	201	123	84

Table 5. DSSAT-CSM Simulation results for rainfed and irrigated soybean in the ACF during typical dry, normal, and wet growing seasons in the ACF during the 1980-2016 control period.

ACF Basin	Soybean								
	Rainfed Yield (kg/ha)			Irrigated Yield (kg/ha)			Irrigation Amount (mm)		
	Dry	Normal	Wet	Dry	Normal	Wet	Dry	Normal	Wet
1	2057	2534	3222	3253	3344	3431	148	122	56
2	1651	2115	2815	3394	3358	3453	191	149	90
3	1689	2180	2848	3450	3348	3457	200	144	93
4	1735	2017	2603	3332	3331	3369	183	148	88
5	1485	1815	2501	3183	3210	3157	197	155	84
6	1550	2033	2486	3351	3356	3396	198	147	94
7	1419	1892	2481	3329	3276	3355	208	155	92
8	1393	1976	2455	3206	3143	3203	202	138	89
9	1522	1840	2376	3088	3113	3075	194	149	88
10	1817	2224	2550	3012	3017	3042	153	105	75
11	1629	2140	2539	3049	3052	3086	170	117	79
12	1501	2235	2560	3092	3035	3086	178	109	74
13	1841	2272	2558	2957	3006	3006	152	102	68
14	2067	2420	2781	3008	2921	3063	115	74	49

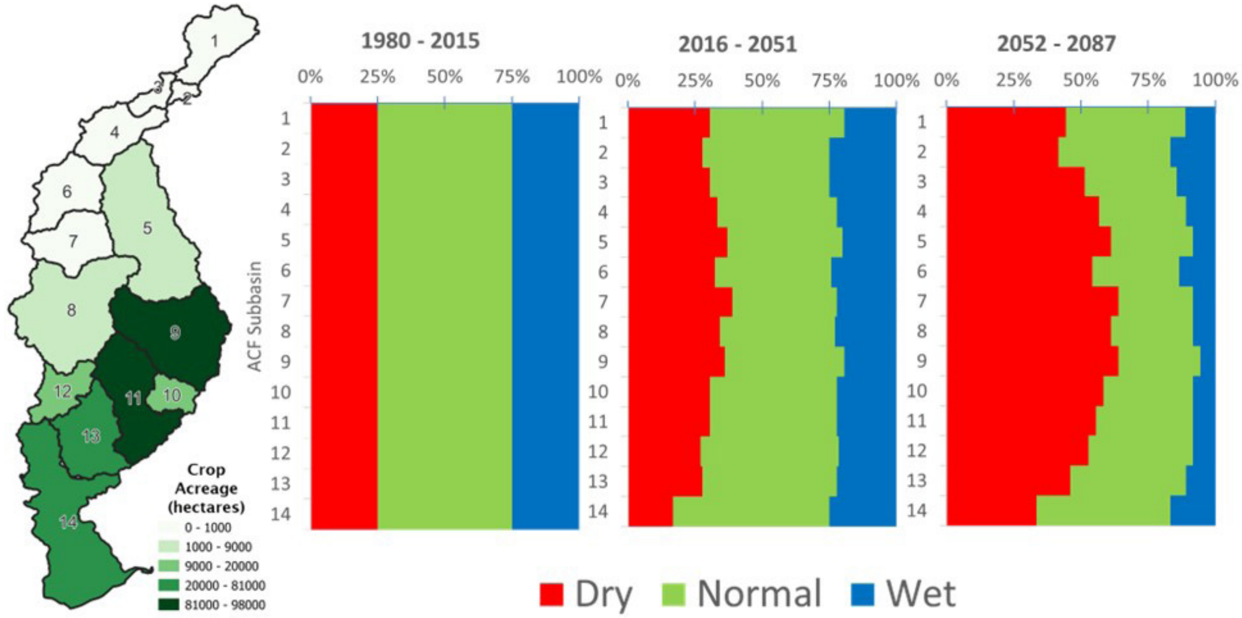

Figure 2. Classification of ACF growing seasons as dry, wet, or normal as a function of projected growing season precipitation and potential evapotranspiration.

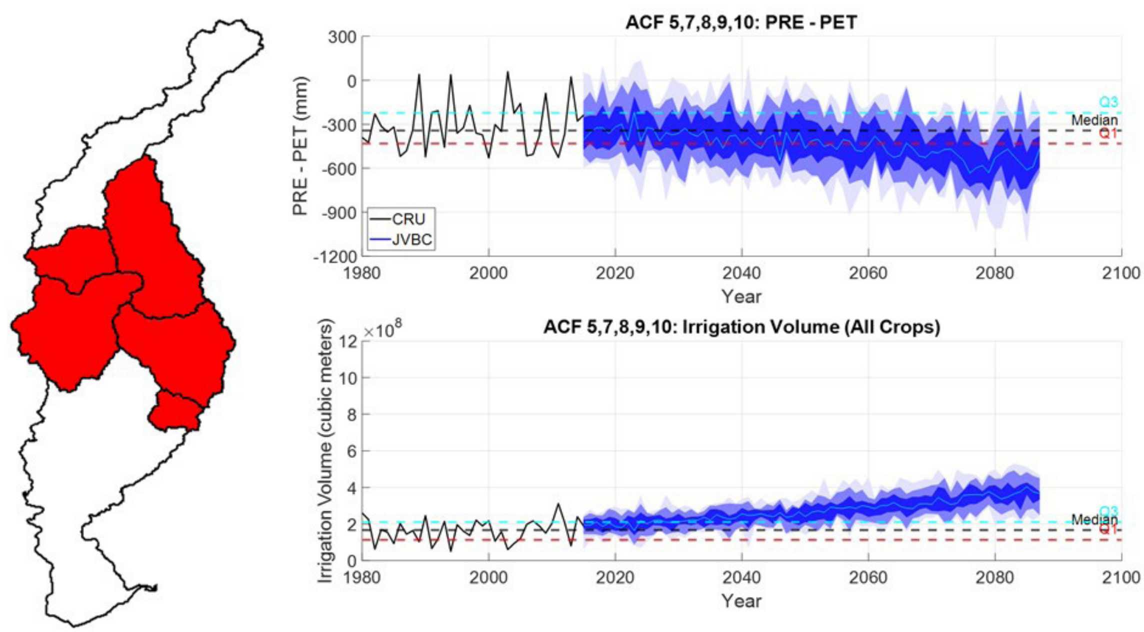

Figure 3. Projected irrigation volume for all crops (corn, cotton, peanut, and soybean) in the central ACF region as a function of projected growing season precipitation and potential evapotranspiration.

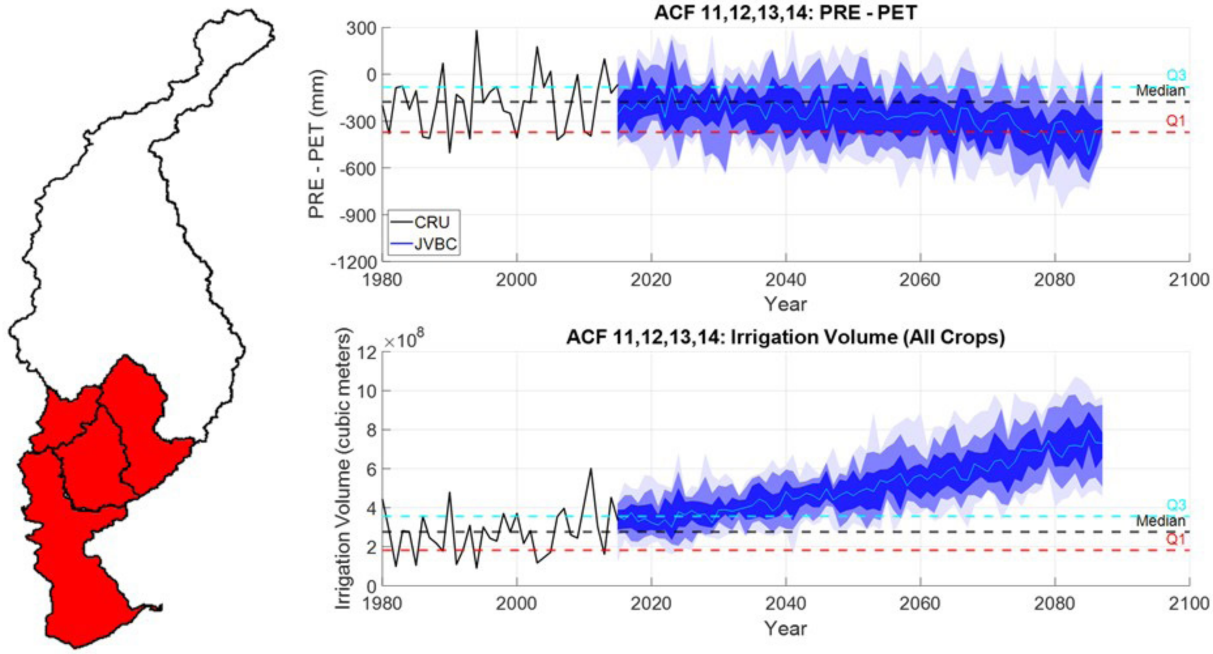

Figure 4. Projected irrigation volume for all crops (corn, cotton, peanut, and soybean) in the southern ACF region as a function of projected growing season precipitation and potential evapotranspiration.

FUTURE CLIMATE TRENDS IN GEORGIA

Husayn El Sharif and Aris P. Georgakakos

REFERENCE: *Proceedings of the 2023 Georgia Water Resources Conference*, held March 30–31, 2023, at the University of Georgia.

Abstract. According to the US EPA (2016), Georgia's climate is expected to usher in warmer temperatures and more severe floods and droughts in the coming years. Such changes can have critical impacts for the State's environment and economy, but the extent and severity of these impacts are still debated. In a separate article of this conference, the Georgia Water Resources Institute (GWRI) provided evidence that significant climatic shifts are clearly detectable in the State's historical data of temperature, precipitation, and potential evapotranspiration (Chougule *et al.*, 2023). In this study, we analyze the latest climate projections from 16 Global Circulation Models (GCMs) to assess whether the historical climate trends are likely to persist, intensify, or subside in the coming decades.

Our analysis of the future climate focuses on the monthly daily average temperature (TMP), monthly potential evapotranspiration (PET), monthly precipitation (PRE), and the difference between monthly precipitation and potential evapotranspiration (PRE - PET) projected to the end of the century under the Shared Socioeconomic Pathway 5 (SSP 5) fossil fuel emissions scenario (Nakicenovic *et al.*, 2014). The study assesses the climatic trends over three climatic Georgia regions: the Blue Ridge Mountain region in the north, the Piedmont plateau in the middle, and the coastal region in the south (**Figure 1**). Results are only presented for the Piedmont, but the identified trends are fairly similar for the Blue Ridge Mountain and the coastal regions. The GCM projections are analyzed at monthly, annual, bi-annual, and four-year time scales.

Systematic comparisons of the GCM-simulated climatic data for 1987–2014 versus the historical observations of the same period (Harris *et al.*, 2020; Climatic Research Unit, CRU, gridded data upscaled to the GCM spatial resolution) indicate that all GCMs contain significant biases that must be removed before any analysis of future climate trends can be undertaken. Bias correction is carried out via a new bias correction approach named Joint Variable Bias Correction (JVBC; Georgakakos and El Sharif, 2023, El Sharif and Georgakakos, 2023), designed to remove the simultaneous biases of statistically correlated climatic fields. The satisfactory performance of the JVBC algorithm is exemplified in **Figure 2**.

Figure 3 shows that all GCMs project rising temperature trends in the Piedmont region. Furthermore, the 1-, 2-, and 4-year rolling average sequences indicate that the interval (in years) during which temperatures *exceed* a specific threshold will rise sharply. For example, during the period from the 1980s to present, the 4-yr average temperature in the Piedmont region *never* exceeded 18 °C (64.6 °F). By contrast, all bias-corrected GCM projections indicate that beyond 2055, the region's 4-yr average temperatures will *always* exceed 18 °C. The rising temperature trends are expected to have important implications for agriculture, hydrology, water resources management, human health, and other socio-economic sectors.

The precipitation projections are shown on **Figure 4**. Precipitation is more variable (over all time scales) than temperature and PET, and its trends are more difficult to ascertain. However, the plots clearly indicate that heavy (maximum) precipitation is projected to increase considerably (see monthly and 1-yr plots), while average precipitation is expected to increase at a slower pace.

On the other hand, the Piedmont PET (**Figure 5**) is expected to rise sharply and outpace precipitation by 2040 (**Figure 6**). After 2040, the long-term difference between precipitation and PET (PRE - PET) is expected to exhibit growing deficits, more severe than any deficits experienced in the 1987–2014 historical period. This ominous trend implies adverse impacts for Georgia's agriculture, hydrology (surface and subsurface), and water resources management.

Bias-corrected climatic projections and similar assessments are currently been developed for all southeast river basins. GWRI plans to make this data publicly available through its website to facilitate detailed environmental and socio-economic impact studies.

Acknowledgements. This study was sponsored by the Georgia Water Resources Institute at Georgia Tech.

References:

Chougule, S., H. El Sharif, and A.P. Georgakakos (2023). Proceedings of the 2023 Georgia Water Res. Conference, held March 30–31, 2023, at the University of Georgia.

El Sharif, H., and A.P. Georgakakos (2023): A Bias-Corrected Climatic Projection Data Set for U.S. River Basins. Climatic Change, in review.

Georgakakos, A.P., and H. El Sharif (2023): Bias Correction of Correlated Climatic Variables. Climatic Change, in review.

Harris, I., Osborn, T. J., Jones, P., & D. Lister (2020). Version 4 of the CRU TS monthly high-resolution gridded multivariate climate dataset. Scientific Data, 7(1), 109. https://doi.org/10.1038/s41597-020-0453-3

Nakicenovic, N., Lempert, R. J., and A.C. Janetos (2014). A Framework for the Development of New Socio-Economic Scenarios for Climate Change Research: Introductory Essay, Climatic Change, 122, 351–361, https://doi.org/10.1007/s10584-013-0982-2.

U.S. Environmental Protection Agency, EPA (2016). What Climate Change Means for Georgia. US EPA. https://19january2017snapshot.epa.gov/sites/production files/2016-09/documents/climate-change-ga.pdf

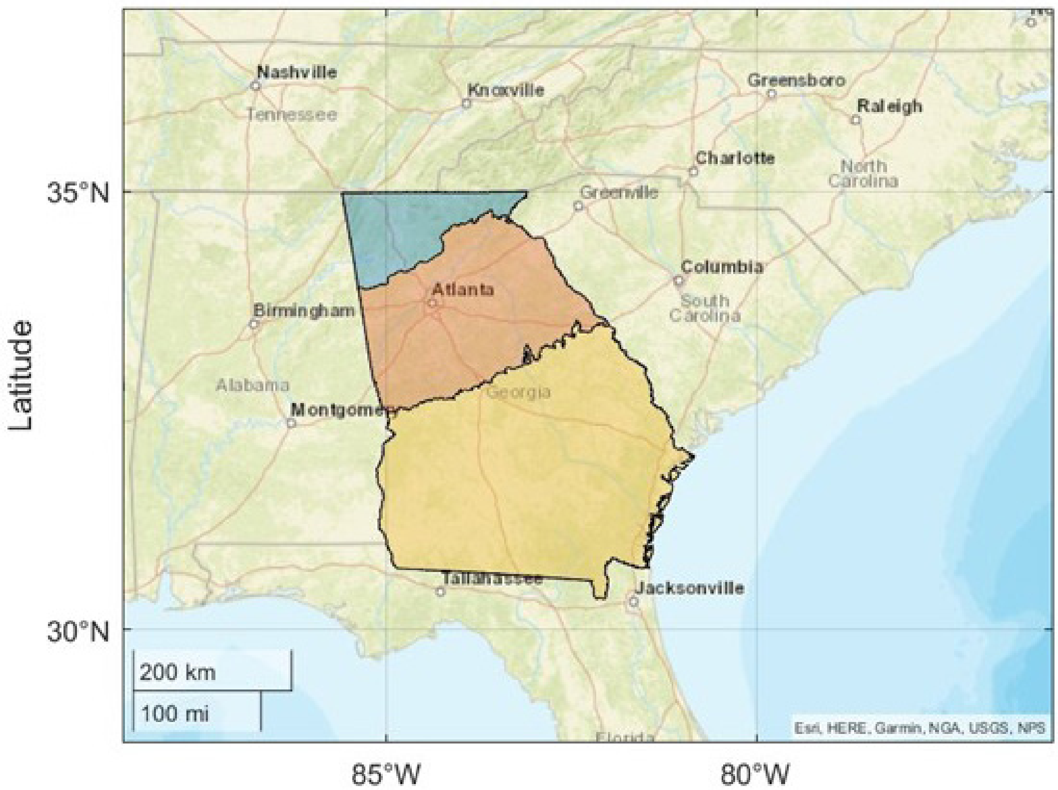

Figure 1. Three physiographic regions of Georgia: Blue Ridge Mountains (blue shading), Piedmont (orange shading), Coastal Plain (yellow shading).

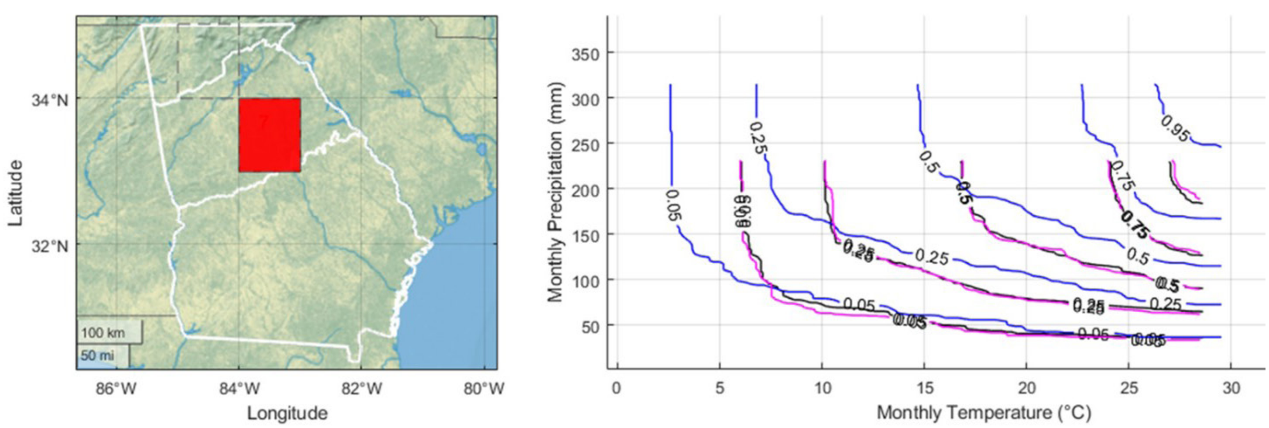

Figure 2. Typical Temperature-Precipitation joint cumulative distribution contours for a single GCM pixel (shown on the map) for the 1987–2014 historical period. Raw GCM contours without bias correction are plotted in blue, the target CRU-based contours in black, and the JVBC bias-corrected contours in magenta. These contours highlight the JVBC algorithm effectiveness in removing biases from raw GCM data.

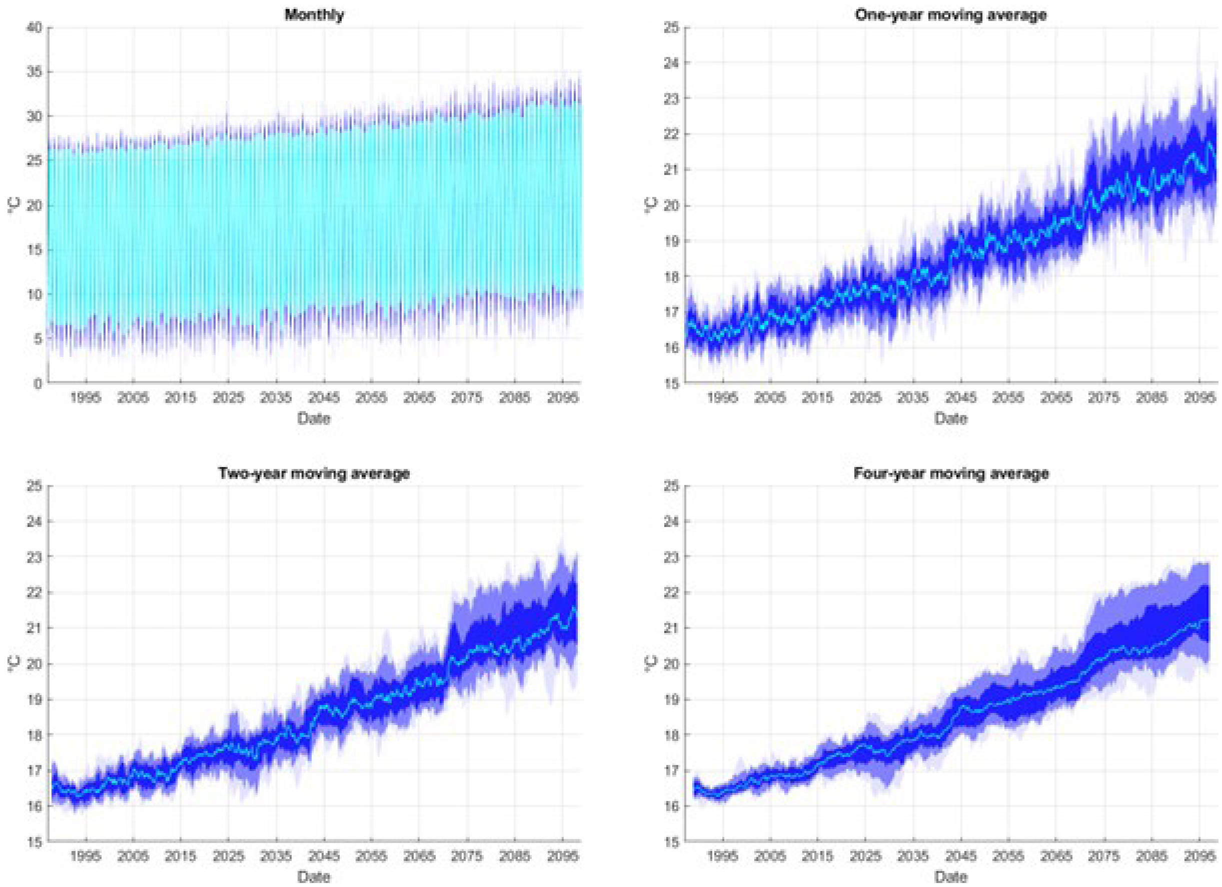

Figure 3. Time series of bias-corrected GCM monthly daily average temperature data for the Georgia Piedmont region. The shading delineates the 0th, 10th, 25th, 50th (cyan line), 75th, 90th, and 100th percentiles across 16 bias corrected CMIP6 GCM models under the aggressive SSP 5 emissions scenario.

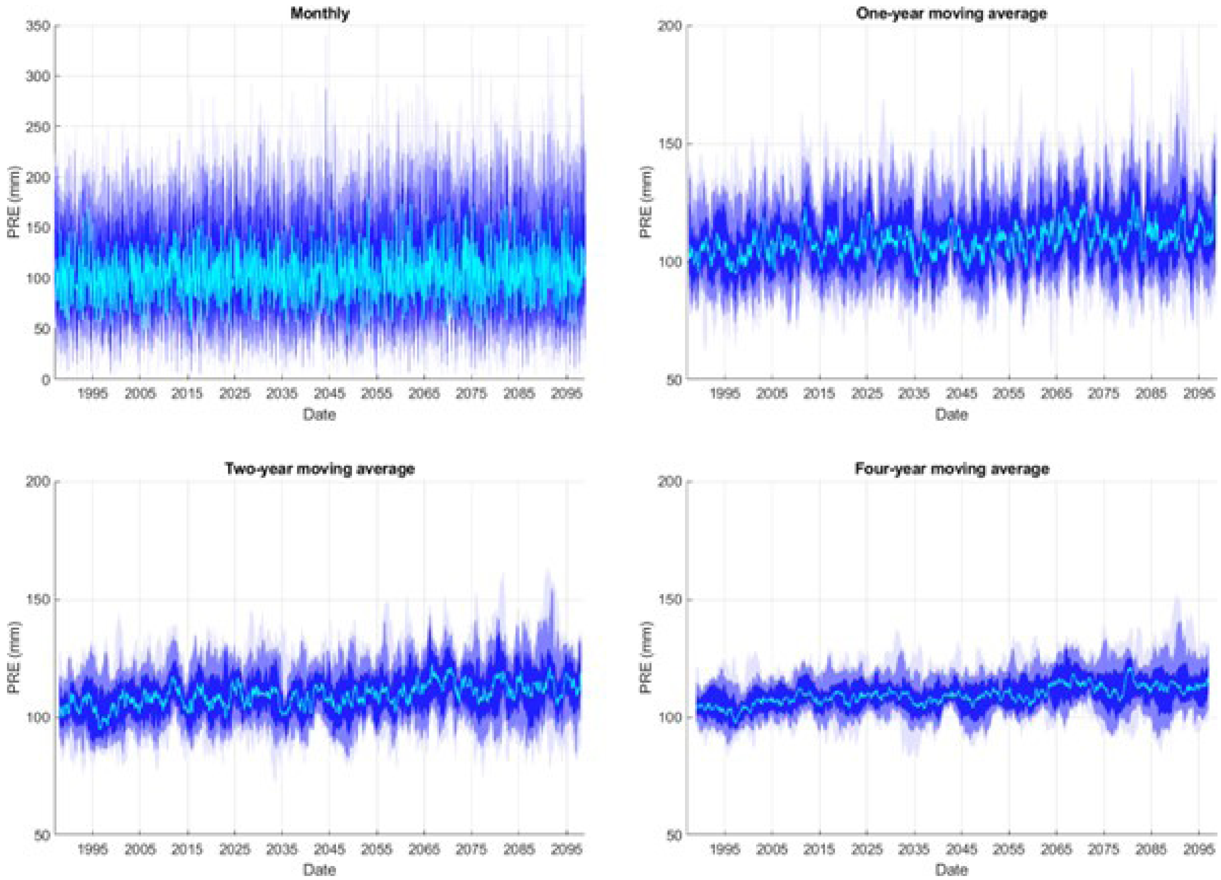

Figure 4. Time series of bias corrected GCM monthly precipitation (PRE) data for the Georgia Piedmont region. The shading delineates the 0th, 10th, 25th, 50th (cyan line), 75th, 90th, and 100th percentiles across 16 bias corrected CMIP6 GCM models under the aggressive SSP 5 emissions scenario.

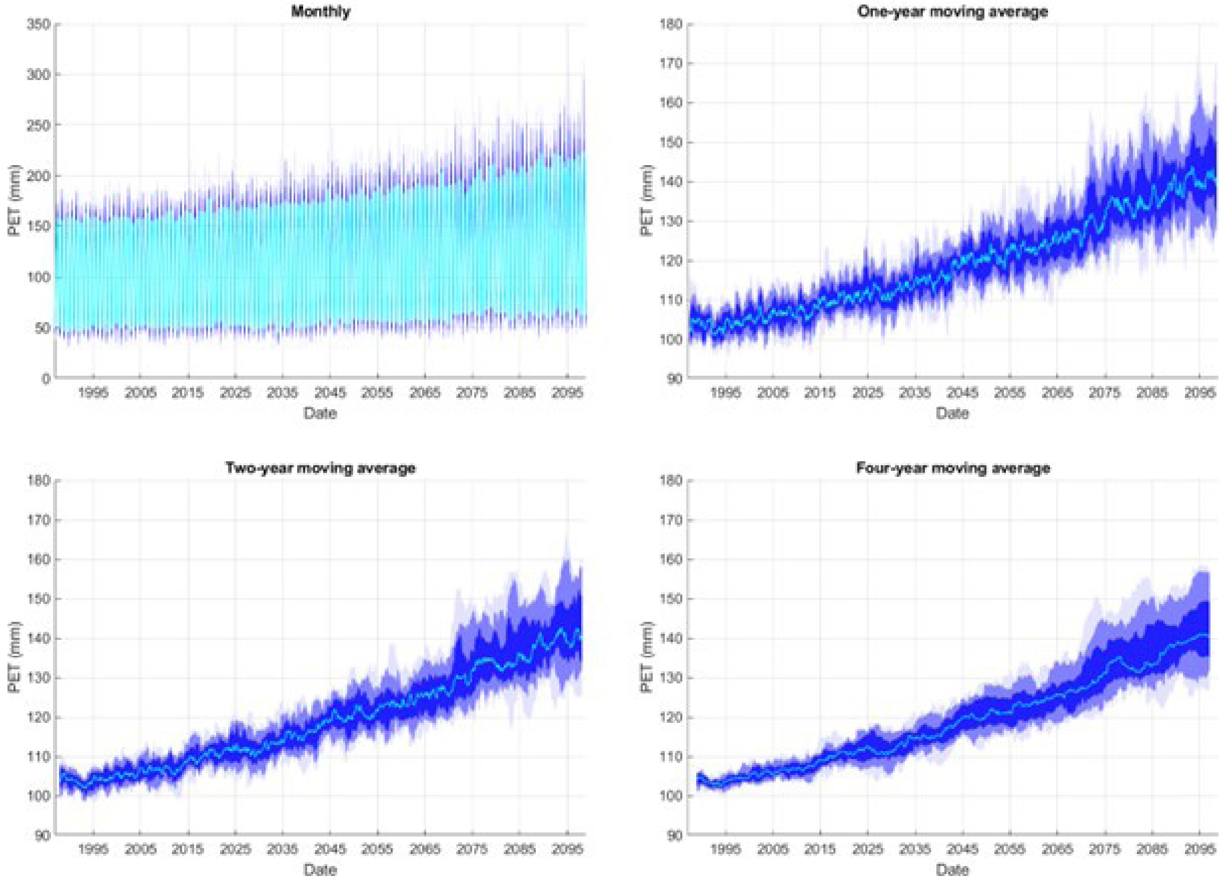

Figure 5. Time series of bias-corrected GCM monthly potential evapotranspiration (PET) data for the Georgia Piedmont region. The shading delineates the 0th, 10th, 25th, 50th (cyan line), 75th, 90th, and 100th percentiles across 16 bias corrected CMIP6 GCM models under the aggressive SSP 5 emissions scenario.

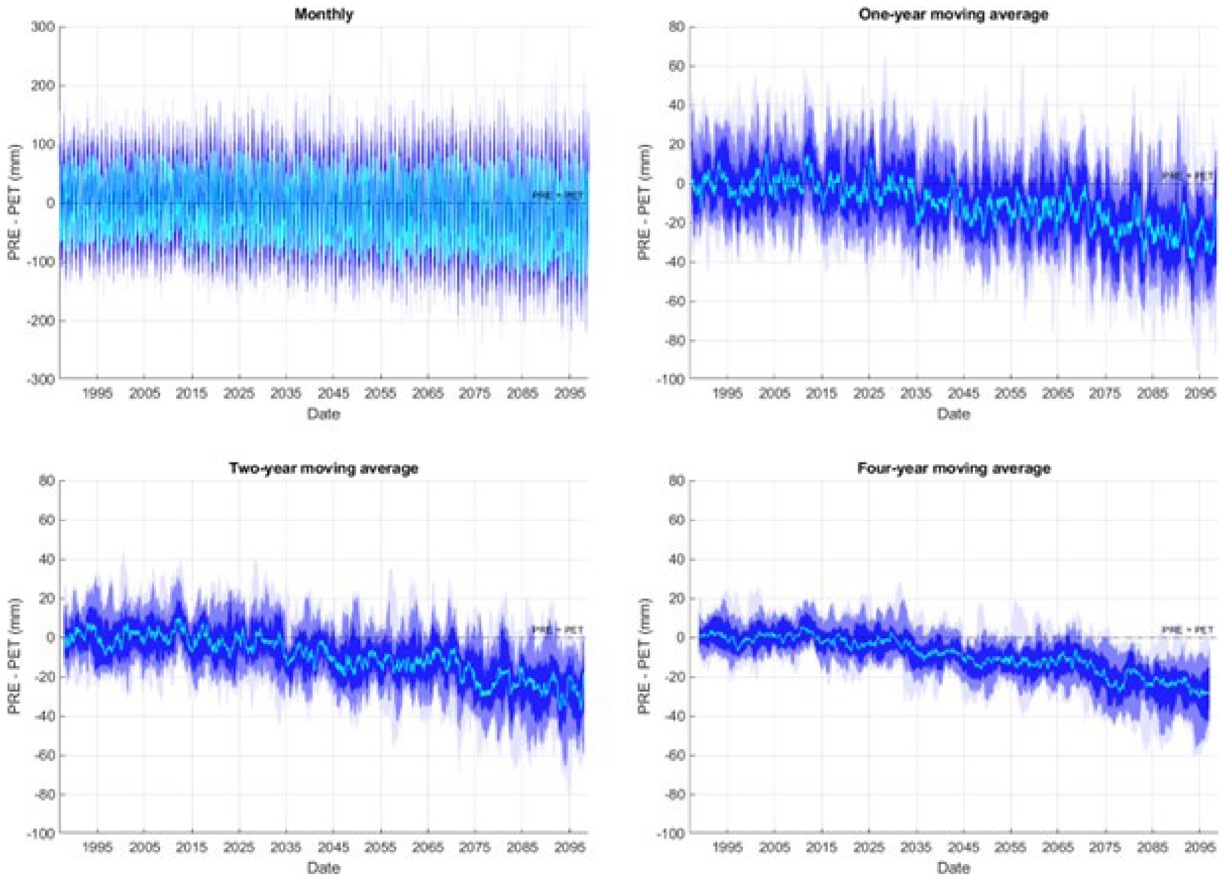

Figure 6. Time series of bias-corrected GCM monthly difference between precipitation and potential evapotranspiration (PRE ¬- PET) data for the Georgia Piedmont region. The shading delineates the 0th, 10th, 25th, 50th (cyan line), 75th, 90th, and 100th percentiles across 16 bias corrected CMIP6 GCM models under the aggressive SSP 5 emissions scenario.

AN UNEXPECTED LEARNING OPPORTUNITY ABOUT THE ETHICS OF SCIENTIFIC RESEARCH AND SAMPLING

Austin Heil and Anne Lindsay

University of Georgia Marine Extension and Georgia Sea Grant, Marine Education Center and Aquarium, Savannah, GA 31411

REFERENCE: *Proceedings of the 2023 Georgia Water Resources Conference*, held March 30–31, 2023, at the University of Georgia.

Who we are and how we teach. University of Georgia's Marine Extension and Georgia Sea Grant (UGA MAREX & GA SG) promotes marine science education using "hands on, feet in" experiential learning for all ages outside the typical classroom. As marine educators with UGA MAREX & GA SG, we teach PreK-12 students, teachers, college students, and the public about Georgia's coastal ecosystems, their importance, and encroaching issues that threaten them. In fact, we host nearly 75 school groups annually at the Marine Education Center and Aquarium (abbreviated UGA Aquarium) on Skidaway Island, near Savannah. Our educators teach *in the field and through experiences*. Salt marshes, maritime forests and barrier islands serve as our outdoor teaching spaces and our research vessels provide access to coastal waterways. This field-based experiential instruction is valuable for students' science learning as it fosters motivation, interest and content understanding (Djonko-Moore et al., 2018; Rukhsana et al., 2021; Weinberg et al., 2011).

Estaury trawls are unique opportunities. One of the most popular UGA MAREX & GA SG field-based experiential learning opportunity is an Estuary Trawl. Learners in grades 5-12 join educators aboard the 43 ft. R/V *Sea Dawg* to characterize the benthic communities found in tidal rivers and sounds near Savannah. While onboard and as an introduction, the group discusses maritime navigation, the dynamic nature of local ecosystems, water quality and the trawling process. We then deploy the cone shaped trawl net and tow it behind the vessel and along the tidal river's soft sediment bottom to capture benthic organisms. We place the organisms caught in a live well tank and discuss natural history, diversity and abundance of species found in coastal estuaries. Students then identify, sort, count, and record species, environmental, and positional data. The *intended* learning outcomes of the Estuary Trawl indicate learners should be able to:

- Describe how various parts of a trawl function
- Relate trawl operation to commercial shrimping
- Distinguish between vertebrates and invertebrates
- Demonstrate how anatomy of certain organisms represent adaptations
- Measure and record water quality parameters of seawater
- Record data that indicate diversity and abundance of local estuarine organisms
- Suggest ways in which natural fluctuations and human impact influence catch.

Estuary trawls serve coastal science and management. However, the Estuary Trawl also serves a different purpose for UGA MAREX & GA SG. Many of the organisms caught in the trawl will be used to feed animals held at the UGA Aquarium. The facility maintains a collection permit from the Georgia Department of Natural Resources to keep many of the organisms caught in the trawl for food or display. To comply with the permit, UGA MAREX & GA SG must record water quality data at the sample site (location data, temperature, salinity and dissolved oxygen levels) and report annually on species diversity and abundance of the catch. In fact, students help sort, count, and bag the catch from the trawl. In this way, students become active participants in scientific sampling. Although some organisms are returned to the river immediately and others are placed in a separate live well to be housed for exhibits, the majority of the organisms caught during the Estuary Trawl will die. In the process, students will observe organismal death happen in real time. The unique setting – aboard an active research vessel – provides an unexpected learning opportunity to discuss the ethics of scientific research and sampling with students. We use one such learning opportunity as a case study to explore how it was a product of the experiential learning environment, how we responded, and what we can learn from this experience and others like it.

Case study: Ethics of Scientific Research and Sampling. While aboard the R/V Sea Dawg with a middle school group in Fall 2022, a large catch was hoisted aboard and deposited into the waiting live well. The 8th graders set about the teamwork of identifying, sorting and counting organisms. One student turned and asked us, "Why do you kill the organisms you catch in the trawl?" We responded with our standard explanation that we maintain a special permit to collect organisms to feed the animals in our aquarium and to assist Department of Natural Resources in monitoring estuarine health as well as fish and invertebrate populations. This was something we always discuss with groups before we lower the trawl net. However, it was clear from the student's expression that this response was not sufficient given the magnitude of the catch. We continued our response by highlighting the importance of keeping diligent records of all organisms we catch for scientific purposes. Again, the student pressed us, "So, you get to keep all of them just because you count them?" At this point, other students were waiting to hear our response to his question. We used this learning moment to explain to the students that, as scientists, it is important to collect samples to document changes, patterns, and responses in our ecosystems. Sometimes animals die in that process and in a way those few deaths allow us to learn more about how other animals live and how humans can lessen their impact on the ecosystem in which they live. We also offered that rather than purchasing food for the captive animals on display in the UGA Aquarium, we instead gather native species as food for those animals. We are also providing natural food items for those captive animals in a sustainable fashion, rather than relying on non native or imported food sources.

While our responses were accurate, it became evident to us that it was equally important in that moment to acknowledge and validate the student's emotional responses to death. This led us, as educators, to consider our objectives for trawling. We asked ourselves: what is the best way to explain to students that death is often a necessary part of science? In the past, educators have responded to similar questions with the adage "we are sacrificing for science." Yet, this didn't ring true to us. Instead, it led us to acknowledge that there are ethical tensions for educators and researchers when sampling in science and participating students might be grappling with these same tensions too. With hindsight, there were words we wished we used to meet this learning moment. For instance, clear opportunities were missed to talk about the importance of subsamples and acknowledge the ways science is a human endeavor. We discuss how this case study fits within the larger conversation about death in science education and what was learned from this experience.

Discussion. In the case study provided above, middle school students engaged in an authentic, field-based experiential learning opportunity aboard a research vessel. During this experience, students started to question the ethics of aquatic science sampling and research. This instance was not only an unexpected learning moment for the students but also for us educators. We learned it is imperative to recognize students' moral processes during death-related discussions in science. Researchers classified similar conversations surrounding death into one of two categories: *good death and bad death* (Oliveira et al., 2014). Good death represents dying of natural causes while bad death is often unnecessary and caused by humans. Yet, our instance falls somewhere in the middle. Organisms were dying for science and to feed other organisms but they were still dying as a result of human intervention. We posit that this middle ground provided a rich setting for an unexpected learning opportunity about the ethics of scientific research which could only be realized in the field while *doing science*.

Further, it is important to acknowledge that students see fish, shrimp, and squid alive and then watch them die during the trawl. The position statements of the National Science Teachers Association (NSTA) and National Association of Biology Teachers (NABT) supports including live animals as part of instruction in the K-12 science teaching because "observing and working with animals firsthand can spark students' interest in science as well as a general respect for life while reinforcing key concepts" (NSTA, 2008). Guidance from prominent national science education organizations provides best practices for teaching with either live *or* dead animals (NABT, 2019; NSTA, 2008). No such guidance exists for how educators should respond when teaching with animals as they are dying. Our case study highlights the need for aquatic science educators to be prepared for unexpected conversations about the ethics of scientific research and teaching with dying organisms during experiential learning. We hope our case study ignites conversation within the aquatic science education community to discuss ethical concerns that arise during authentic experiential learning events. It reminds students and us that science is a human endeavor and subject to that unique perspective.

References:

Djonko-Moore, C. M., Leonard, J., Holifield, Q., Bailey, E. B., & Almughyirah, S. M. (2018). Using culturally relevant experiential education to enhance urban children's knowledge and engagement in science. *Journal of Experiential Education*, 41(2), 137-153.

National Association of Biology Teachers. (2019). *Position statements*. https://nabt.org/Position Statements-The-Use-of Animals-in-Biology-Education

National Science Teaching Association. (2008). Responsible use of live animals and dissection in the science classroom. https://www.nsta.org/nstas-official-positions/responsible-use-live-animals-and dissection-science classroom#:~:text=NSTA%20opposes%20regulations%20or%20legislation,humanely%2C%20res ponsibly%2C%20and%20ethically

Oliveira, A. W., Reis, G., Chaize, D. O., & Snyder, M. A. (2014). Death discussion in science read- alouds: Cognitive, sociolinguistic, and moral processes. *Journal of Research in Science Teaching*, 51(2), 117-146.

Rukhsana, B., Naeemullah, M., & Rehman, S. (2021). Effect of Experiential Learning on Students' Motivation and Interest at Elementary Level in the Subject of General Science. *International Research Journal of Education and Innovation*, 2(2), 41-53.

Weinberg, A. E., Basile, C. G., & Albright, L. (2011). The effect of an experiential learning program on middle school students' motivation toward mathematics and science. *RMLE Online*, 35(3), 1-12.

UTILIZING DATA FROM THE US EPA'S PRELIMINARY HEALTHY WATERSHED ASSESSMENT (PHWA) PROJECT TO COMPARE THE HEALTH AND VULNERABILITY OF WATERSHEDS IN GEORGIA

Don Lane
Elachee Nature Science Center

REFERENCE: *Proceedings of the 2023 Georgia Water Resources Conference*, held March 30–31, 2023, at the University of Georgia.

The Elachee Nature Science Center is responsible for the management of the 1,440-acre Chicopee Woods Nature Preserve. While the nature preserve is protected by a conservation easement, land surrounding the preserve is subject to increasing human activities that may have an impact on the larger watershed. A study was undertaken to compare the preserve's surrounding watershed with another watershed of similar characteristics using the Preliminary Healthy Watershed Assessment (PHWA).

The PHWA (developed in 2017 and updated in 2021) is a set of statewide and ecoregional-scale assessments that score watershed health and vulnerability in the contiguous United States. The PHWA focuses on six key attributes of watershed health. These attributes are Landscape Condition, Hydrologic, Geomorphology, Habitat, Water Quality, and Biological Condition. The PHWA also includes a Watershed Vulnerability Index which is derived from Land Use Change, Water Use, and Wildfire sub-index scores.

The PHWA data are divided into four categories: "Base Indicators", "Ecological Indicators", "Stressor Indicators" and "Social Indicators. Base Indicators are reference metrics such as HUC12 Unit Code, watershed name, area of the watershed, and other metrics. Ecological Indicators can be thought of as positive metrics while Stressor Indicators can be thought of as negative metrics. Social Indicators include (but are not limited to) metrics of water quality, drinking water, and community content.

The Upper Walnut Creek Watershed (HUC12 030701010104, hereafter referred to as "UWC") was chosen as the Watershed of Interest as it is the watershed which contains the Chicopee Woods Nature Preserve. UWC has an area of approximately 65,136,600 square meters, is a headwater watershed, and the entirety of its area lies in Ecoregion 45-Piedmont.

The watershed chosen to use as a comparator was Yellowdirt Creek (HUC12 031300020405, hereafter "YDC"). YDC has approximately the same area as UWC, is a headwater watershed, and lies entirely within Ecoregion 45. Therefore, YDC is approximately the same size, same type (i.e. headwater watershed), and lies within the same ecoregion as UWC.

Following are comparisons of the various Indexes, the Sub-Indexes that are used to derive the Indexes, and the Indicators used to derive the Sub-Indexes. A 'significant difference" between any two values is a percent difference of the two values greater than, or equal to 10%. Each section will contain paraphrased EPA definitions followed by the result of the specific comparison.

Watershed Health Index (WHI) and Watershed Vulnerability Index (WVI). The WHI score is an integrated measure of watershed condition that combines Landscape Condition, Hydrologic, Geomorphology, Habitat, Water Quality, and Biological Condition Sub-Index scores. Higher scores correspond to greater potential for a watershed to have the structure and function in place to support healthy aquatic ecosystems.

The WVI score characterizes the vulnerability of aquatic ecosystems in a watershed to future alteration based on Land Use Change, Water Use Change, and Wildfire Vulnerability Sub-Index scores. Higher scores correspond to greater potential vulnerability of aquatic ecosystems to future degradation.

The percent difference between the two WHI's were within 10%. However, YDC's WVI exceeded UWC by approximately 39%.

WHI Sub-Indexes. Landscape Sub-Index: combines multiple measures of the extent and connectivity of natural land cover in a watershed. Higher scores correspond to greater extent and connectivity of natural land cover.

Hydrology Sub-Index: combines multiple measures of the potential for streams in the HUC12 to support natural flow regimes, including the relative magnitude of impoundments, the prevalence of forest, wetland, and impervious cover, the number of road-stream crossings, and the amount of farmland on hydric soils.

Geomorphology Sub-Index: combines multiple measures of the potential for the HUC12 to maintain fluvial geomorphic processes within their natural range, including the density of dams and roads, the area drained by surface ditches, and the prevalence of urban and cropped lands in the riparian zone.

Habitat Sub-Index: characterizes the potential for a HUC12 to support high quality stream habitat based on multiple measures of watershed attributes that were determined to be relevant to fish habitat quality, including the extent of urban and agricultural land cover types, human population density, road length, number of road-stream crossings, number of dams, number of mine operations, number of facilities with National Pollutant Discharge Elimination System (NPDES) wastewater discharge permits, number of sites in the EPA Toxic Release Inventory program, and number of sites on the Superfund National Priorities List.

Biological Sub-Index: measures the likelihood for high-quality stream biological communities in the HUC12, based on a predictive model of stream biological condition that uses watershed attributes as inputs.

Water Quality Sub-Index: considers information on impaired waters in a HUC12, defined as rivers, lakes, or other waterbodies that are not meeting surface water quality standards due to excess pollution. The Water Quality Sub-Index is measured from: (1) the percentage of the HUC12 containing impaired waters, relative to the area of the HUC12 that has been assessed for water quality standards attainment; and (2) the number of unique causes of impairment (i.e., types of pollutants or other issues causing impairment). Higher scores correspond to a greater proportion of waters attaining surface water quality standards and a lower number of impairment causes.

Three sub-indexes differed significantly: Habitat, YDC higher; Biological, UWC higher; and Water Quality, YDC higher.

WVI Sub-Indexes. Land Use Vulnerability Sub-Index: characterizes the vulnerability of aquatic ecosystems in a HUC12 to land use change based on recent (2001-2011) land use change, projected changes in impervious cover, and the extent of protected lands in the watershed.

Water Use Vulnerability Sub-Index: characterizes the vulnerability of aquatic ecosystems in a HUC12 to future increases in water use based on recent (2005) estimates of agricultural, domestic, and industrial water use in the HUC12.

Wildfire Vulnerability Sub-Index: characterizes the vulnerability of aquatic ecosystems in a HUC12 to the effects of intense wildfires based on a predictive model of wildfire risk in the HUC12.

Three sub-indices differed significantly: UWC was higher in Land Use and Water Use Vulnerability. YDC was higher in Wildfire Vulnerability.

Landscape Sub-Index Indicators. % Natural Cover in Watershed. Percent of the HUC12 classified as natural land cover (excluding barren land) by the National Land Cover Database (NLCD). Natural land cover classes in include forest, wetlands, shrubland, and grassland; NLCD codes 41 through 43, 52, 71, 90, and 95.

% Natural Cover in Hydro-Active Zone (HAZ) in HUC12. Percent of the HUC12 that is in the Hydrologically Active Zone (HAZ) and classified as natural land cover (excluding barren land).

Population Density in Watershed. Human population density in the land area of the HUC12 (persons per square kilometer).

Population Density in Riparian Zone (RZ). Human population density in the land area of the RZ of the HUC12 (persons per square kilometer).

Mining Density in Watershed. Density of all coal mines, coal mining support activity sites, mineral mines, and mineral processing plants in the HUC12 (count per square kilometer).

Three of the five indicators showed a significant difference. UWC exceeded YDC in HAZ Natural Land Cover, and also exceeded YDC in both Population Density Indicators. There was no significant difference in natural cover, and no mining was reported to take place in either watershed.

Hydrology Sub-Index Indicators. Percent Agriculture on Hydric Soil in Watershed. Percent of the HUC12 with agriculture on hydric soils.

Dam Storage Ratio in Watershed. The ratio of dam storage volume in the HUC12 to pre-development annual streamflow at the HUC12 outlet (acre-feet/acre-feet per year).

% Forest Remaining in Watershed. Percent of forest cover remaining relative to pre-development forest cover in the HUC12.

% Wetlands Remaining in Watershed. Percent of wetland cover remaining relative to pre-development wetland cover in the HUC12.

% Imperviousness in Watershed. Percent of the HUC12 with developed impervious surface cover.

Road Stream Crossings Density in Watershed. Density of road-stream crossings in the HUC12 (number of crossings per square kilometer).

Four of six indicators differed significantly. UWC has more remaining wetlands than YDC, but also exceeded YDC in impervious cover, stream crossings and dam storage. There was no significant difference in remaining forest and no agricultural activities on hydric soils reported in either watershed.

Geomorphology Sub-Index Indicators. Dam Density in Watershed. Density of dams in the HUC12 (dam count per stream kilometer).

% Ditch Drained Area in Watershed. Percent of the HUC12 that is drained by artificial surface ditches. Surface ditches collect and convey water from the surface of agricultural fields.

Roads Density in Riparian Zone. Density of all roads in the Riparian Zone (RZ) of the HUC12 (kilometer per square kilometer).

% High-Intensity Land Cover in Riparian Zone. Percent of the HUC12 that is in the Riparian Zone and classified as 'Developed, High Intensity' (NLCD code 24).

Three of four indicators differed significantly. UWC exceeded YDC in dam density, RZ road density, and high intensity land cover. There was no ditch drainage reported in either watershed.

Habitat Sub-Index Indicator. Mean National Fish Habitat Partnership (NFHP) Habitat Condition Index Local Watershed. Mean Habitat Condition Index (HCI) score for the HUC12 from the NFHP 2015 National Assessment. Scores range from 1 (high likelihood of aquatic habitat degradation) to 5 (low likelihood of aquatic habitat degradation) based on land use, population density, roads, dams, mines, and point-source pollution sites.

There was no significant difference between the watersheds.

Biological Sub-Index Indicators. Mean Probability of Good Biological Condition. Mean probability that perennial stream reaches in the HUC12 would be rated as having 'good' biological condition under the EPA National Rivers and Streams Assessment (NRSA). Probabilities range from 1 (high likelihood of good biological condition) to 0 (low likelihood of good biological condition).

Biological (Aquatic) Condition Score at Watershed Outlet. Probability that the perennial stream reach at the HUC12 outlet would be rated as having 'good' biological condition under the EPA National Rivers and Streams Assessment (NRSA). Probabilities range from 1 (high likelihood of good biological conditions) to 0 (low likelihood of good biological conditions).

One of two indicators differed significantly. UWC exceeded YDC in the condition score at the watershed outlet. There was no significant difference in aquatic condition.

Water Quality Sub-Index Indicators. % Assessed Supporting Minus Impaired Stream length. Percent of the Assessed Area of the HUC12 containing Impaired Waters. The Assessed Area is the portion of the HUC12 containing surface water features that have been assessed for attainment of surface water quality standards under Section 305(b) of the Clean Water Act. Impaired Waters are surface water features that are not attaining water quality standards.

% Assessed Supporting Minus Impaired Waterbody Area. Count of unique Impairment Causes in the HUC12. An Impairment Cause is a pollutant or related parameter that is causing non-attainment of surface water quality standards.

There was a significant difference in both indicators. UWC exceeded YDC in both.

WVI Sub-Indexes. % Human Use Change in Watershed (2001-2011). Change in the percentage of the HUC12 with human use land cover (including barren land) from 2001 to 2019. Human use cover classes included are 'Developed, Open Space', 'Developed, Low Intensity', 'Developed, Medium Intensity', 'Developed, High Intensity', 'Barren Land (Rock/Sand/Clay)', 'Pasture/Hay', and 'Cultivated Crops' cover classes; NLCD codes 21 through 24, 31, 81, and 82. Positive values denote an increase in Human Use Change; negative values denote a decrease in Human Use Change.

% Human Use Change in Riparian Zone (2001-2011). Change in the percentage of the HUC12 with human use land cover (including barren land) in the RZ from 2001 to 2019. See above for human use cover classes.

Projected Change in Impervious Cover (2010-2050). The projected change in the percentage of impervious surface cover in the HUC12 from 2010 to 2050.

% Protected Lands in Watershed. Percent of the HUC12 that is designated as a protected area.

There was significant difference in all four sub-indexes. UWC exceeded YDC in all.

Water Use Sub-Index Indicators. Agricultural Water Use in Watershed. Daily agricultural water use in the HUC12 (million gallons per day). Agricultural water use includes surface and groundwater that is self-supplied by agricultural producers or supplied by water providers (governments, private companies, or other organizations). Water used in a HUC12 may originate from within or outside the HUC12.

Domestic Water Use in Watershed. Daily domestic water use in the HUC12 (million gallons per day). Domestic water use includes indoor and outdoor household uses, such as drinking, bathing, cleaning, landscaping, and pools. Domestic water can include surface or groundwater that is self-supplied by households or publicly supplied. Water used in a HUC12 may originate from within or outside the HUC12.

Industrial Water Use in Watershed. Daily industrial water use in the HUC12 (million gallons per day). Industrial water use includes water used for chemical, food, paper, wood, and metal production. Only includes self-supplied surface water or groundwater by private wells or reservoirs. Industrial water supplied by public water utilities is not counted. Water used in a HUC12 may originate from within or outside the HUC12.

There were significant differences in all three indicators. YDC exceeded UWC in agricultural water use and WDC exceeded YDC in domestic and industrial water use.

Wildfire Sub-Index Indicators. Mean Wildfire Risk in Watershed. Mean wildfire hazard potential in the HUC12. The Wildfire Hazard Potential dataset depicts the relative potential for the occurrence of wildfire that would be difficult for suppression resources to contain. Values range from 1 (very low risk of wildfire) to 100,000 (very high risk of wildfire).

% Watershed High or Very High Wildfire Risk. Percent of the HUC12 with high or very high wildfire hazard potential. That is, the relative potential for the occurrence of wildfire that would be difficult for suppression resources to contain.

There were significant differences in both indicators. YDC exceeded UWC in both.

Conclusions. The PHWA can be a useful tool in identifying various components of a heathy and/or vulnerable watershed. However, the comparison of to (or more) watersheds must be conducted with care. A comparator watershed which has no significant differences in the following categories: area, number of upstream watersheds, and ecoregion.

Any sub-index where a significant difference is noted can become a list where actionable priorities can be established for the protection, restoration, enhancement, or mitigation of water, riparian, and forest resources within the watershed.

LAKE LANIER WATER QUALITY AND ECOLOGY MODEL

Xiaofeng Liu and Aris P. Georgakakos

REFERENCE: *Proceedings of the 2023 Georgia Water Resources Conference*, held March 30–31, 2023, at the University of Georgia.

Abstract. In 2020 and 2022, Lake Lanier was listed on Georgia's 305(b)/303(d) list for not meeting the Chlorophyll *a* standards(Georgia EPD, 2020, 2022), indicating declining water quality trends and raising important sustainability concerns and questions: Are the recent exceedances of water quality standards episodic events or are they part of a longer term trend? Which are the main nutrient sources to the lake and what are their individual and collective impacts on lake water quality? What management alternatives can be adopted to improve lake water quality conditions?

Lake monitoring is essential in assessing local water quality conditions, but it cannot anticipate future lake responses nor answer management questions like those stated above. This is the agency of water quality models.

In theory, water quality models can serve both as diagnostic *and* as predictive tools and can inform lake management investigations in several important ways: (i) "fill in" limited observational data across the lake domain; (ii) provide in-depth understanding of the physical, chemical, and biological processes at work; (iii) quantify lake responses to external lake inputs and changes; (iv) reconstruct the historical water quality conditions *and* project future conditions under specific management and hydroclimatic scenarios (Dekker et al., 1996); and (v) identify the most effective management options for a sustainable lake future. In practice, however, water quality models can serve these purposes *only if* they exhibit sufficient accuracy. But high model accuracy is difficult to achieve for large lakes like Lanier due to their extensive spatial domain, the many interacting physical and bio-chemical processes involved, and the need for sufficient field data. As a result, water quality models had limited use in lake water quality assessments and management. In particular, previously developed water quality models for Lake Lanier do not exhibit sufficient accuracy (and spatial resolution) to address important management questions.

The objective of the water quality program at the Georgia Water Resources Institute (GWRI) at Georgia Tech is to overcome this limitation and develop a coupled hydrodynamic-biogeochemical model for Lake Lanier that is accurate enough to inform environmental management decisions. The GWRI Lake Lanier model has been built based on the Delft3D Flexible Mesh (Delft3D FM) modeling system (Deltares, 2021). **Figure 1** shows the model grid network, which features a variable horizontal resolution (from 20 m to 200 m) and up to 25 vertical layers of 2 m average thickness. The number of spatial grid cells at the surface layer is 20,069, while the number of grid cells in the entire lake domain exceeds 130,000.

The hydrodynamic model simulates the lake flow and thermal response to hydroclimatic factors and is calibrated to match the simulated lake water level and water temperature against observed data. The water quality/ecology model simulates the spatiotemporal changes and transformations of lake nutrients, organic matter, and dissolved oxygen as well as the biological response of the lake algae **(Figure 2)**. The water quality model is calibrated by fine-tuning the process parameters such that model-simulated results agree with available observations, including Chlorophyll *a* (Chl-a), Dissolved Oxygen (DO), Total Nitrogen (TN), Total Phosphorus (TP), and Total Organic Carbon (TOC).

Figure 3 compares the simulated with the observed lake levels (measured near Buford Dam, above sea level) over the two-year study period and shows that the hydrodynamic model is accurate within 5-10 cm. **Figure 4** compares the simulated (red lines) with the observed (black lines) temperature profiles at Browns Bridge, one of Georgia EPD's monitoring locations. These results indicate that the simulated temperature profiles agree well with *in situ* temperature measurements across all seasons. The error standard deviations at all sites range from 0.83 to 1.23℃, and the average error mean from -0.13 to 0.53℃. Lastly, **Figure 5** (upper panel) shows that there is also good agreement between model-simulated (black line) and satellite-estimated (red circles; Sharif et al., 2023) photic zone Chl-a concentrations at Browns Bridge. The agreement is similar at all locations where data is available. The lower panel of **Figure 5** depicts the model-estimated algae biomass composition sequences for diatoms, green algae, and blue-green algae, indicating that green algae dominate during the warm season, while diatoms proliferate during late winter and early spring and blue-green algae during fall.

Additional results (not shown) demonstrate that the profiles of other water quality parameters (e.g., total nitrogen, total phosphorus, and associated compounds) are also simulated with similar accuracy, suggesting that the Lake Lanier water quality model is well suited for lake water quality management investigations. The model is currently employed to assess a range of management issues, including the relative impact of nutrient sources, the effectiveness of alternative management interventions, and the development of best management strategies for lake sustainability.

Acknowledgements. This study was sponsored by the Georgia Water Resources Institute and the Gwinnett County Department of Water Resources.

References:

Dekker, A.G., ZamuroviĆ-Nenad, Hoogenboom, H.J., Peters, S.W.M., 1996. Remote sensing, ecological water quality modelling and in situ measurements: a case study in shallow lakes. https://doi.org/10.1080/02626669609491524 41, 531–547. https://doi.org/10.1080/02626669609491524

Deltares, 2021. D-Flow_FM_User_Manual. Georgia EPD, 2022. Water quality in Georgia 2020-2021, 2022 Integrated 305b/303d Report.

Georgia EPD, 2020. Water quality in Georgia 2018-2019, 2020 Integrated 305b/303d Report.

Sharif, H. El, Liu, X., Georgakakos, A.P., 2023.Satellite-based lake Chlorophyll-a assessment.

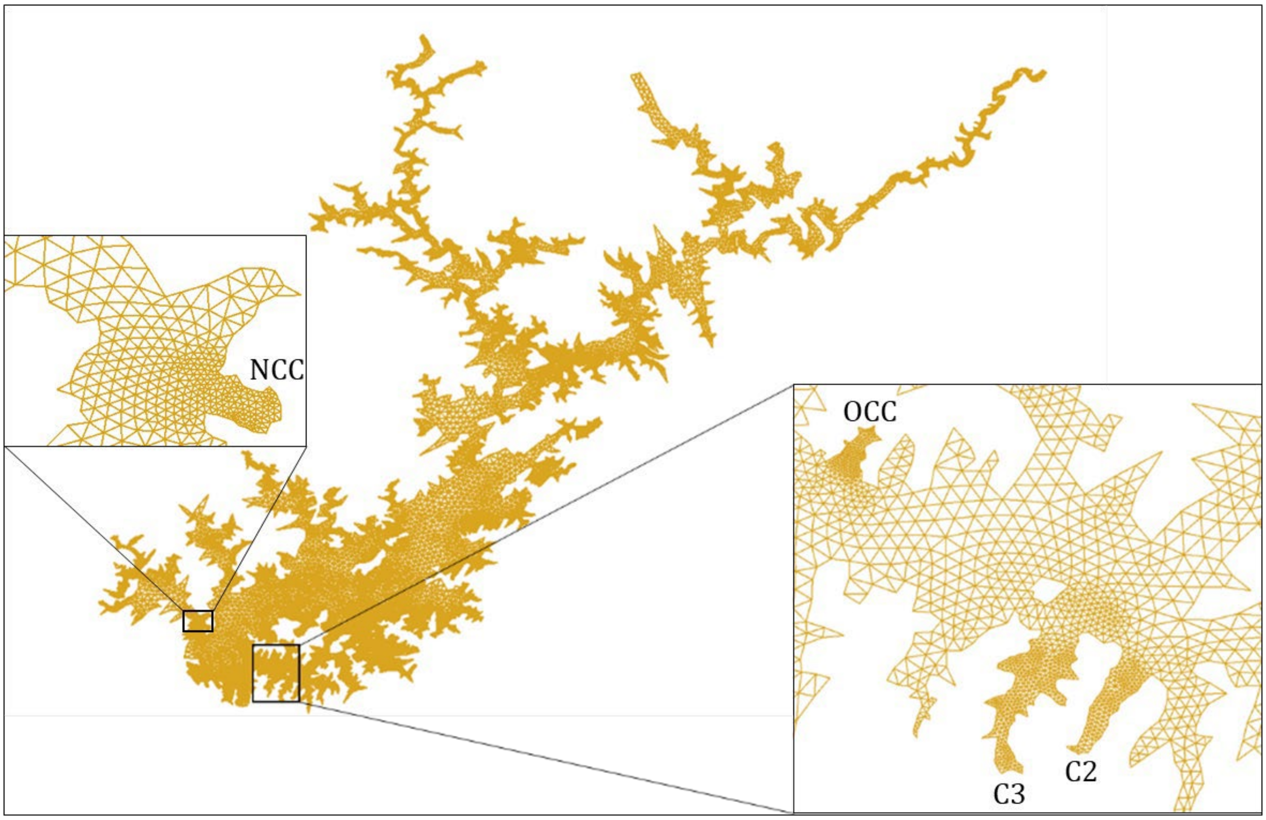

Figure 1. Lake Lanier Delft3D FM unstructured grids, with refined resolutions in coves C2, C3, OCC, and NCC.

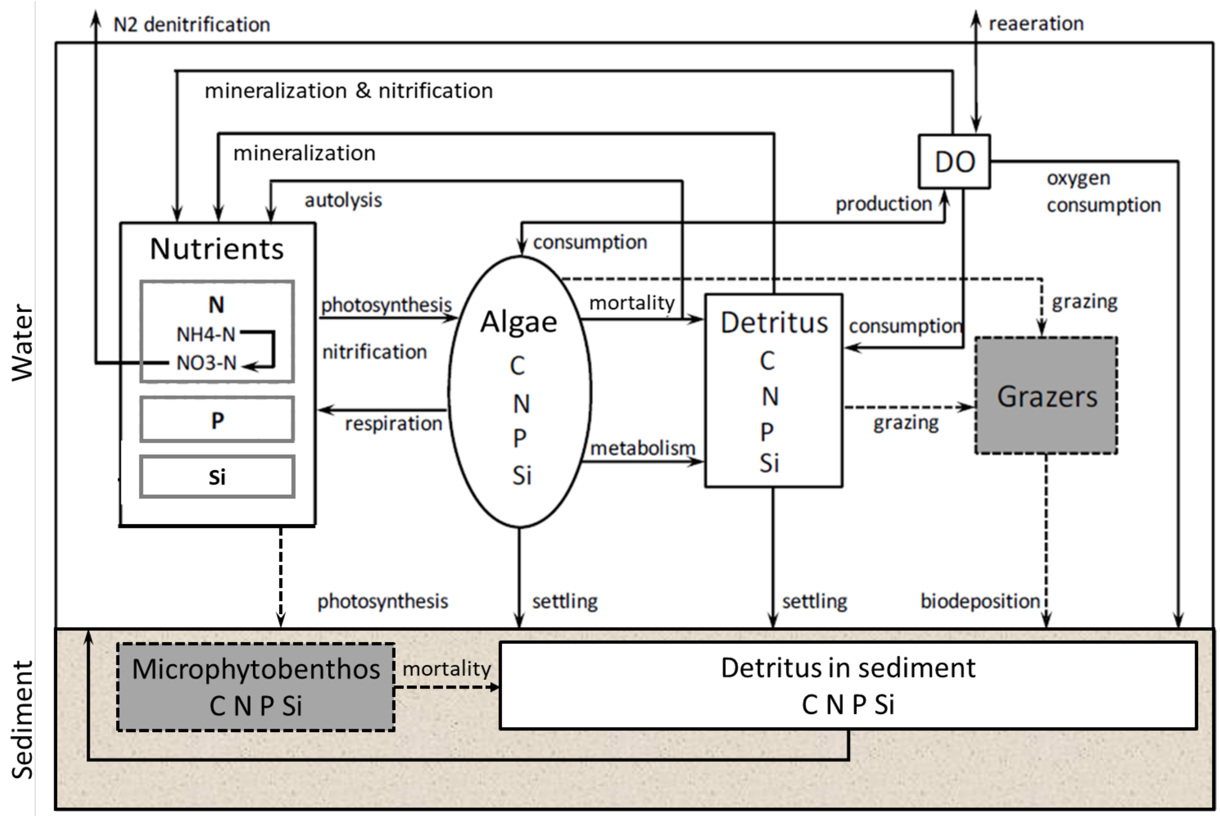

Figure 2. Substances and processes simulated in the Lake Lanier water quality and ecology model.

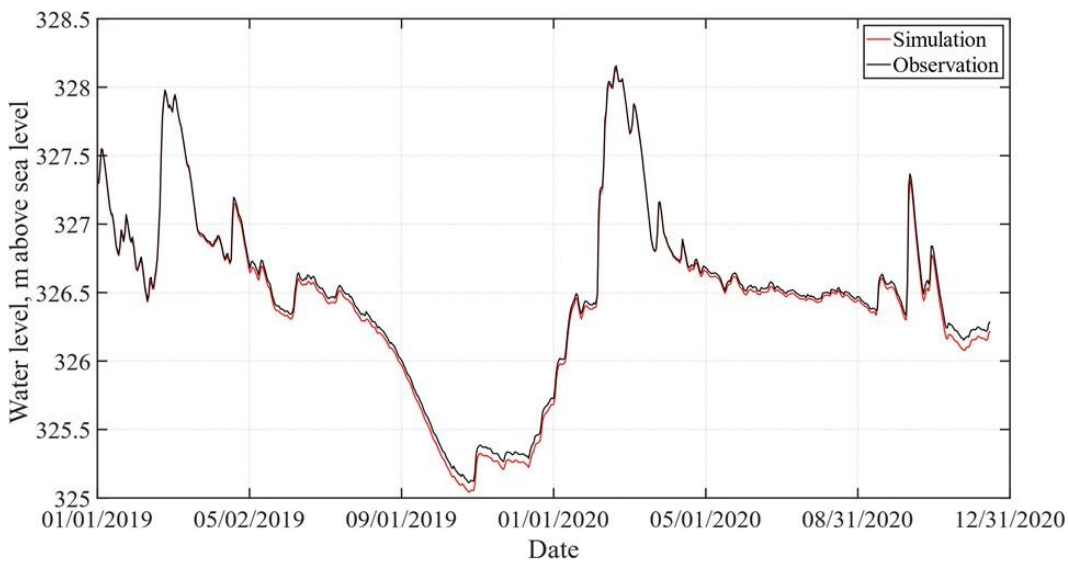

Figure 3. Comparison of simulated (red line) and observed (black line) Lake Lanier water levels for 2019 and 2020.

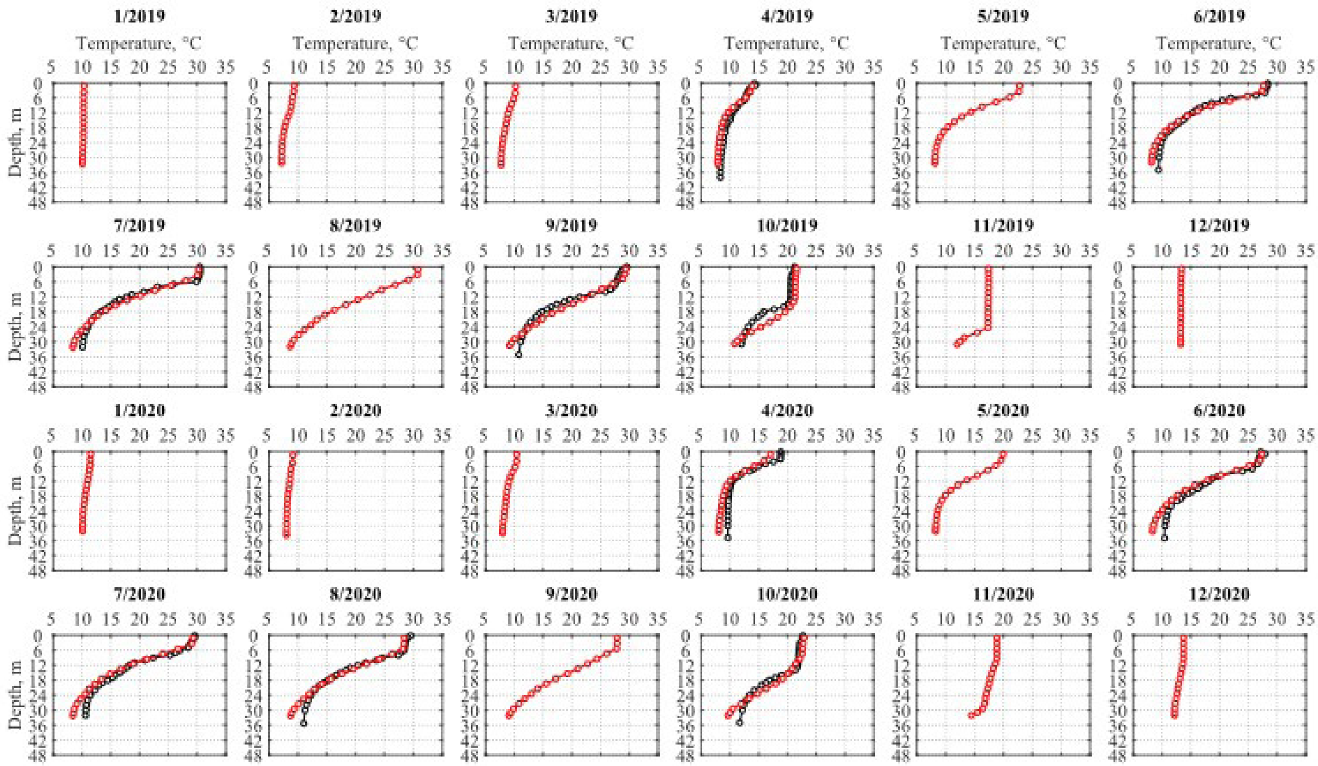

Figure 4. Observed (black) and modeled (red) water temperature profiles at Browns Bridge in 2019 and 2020.

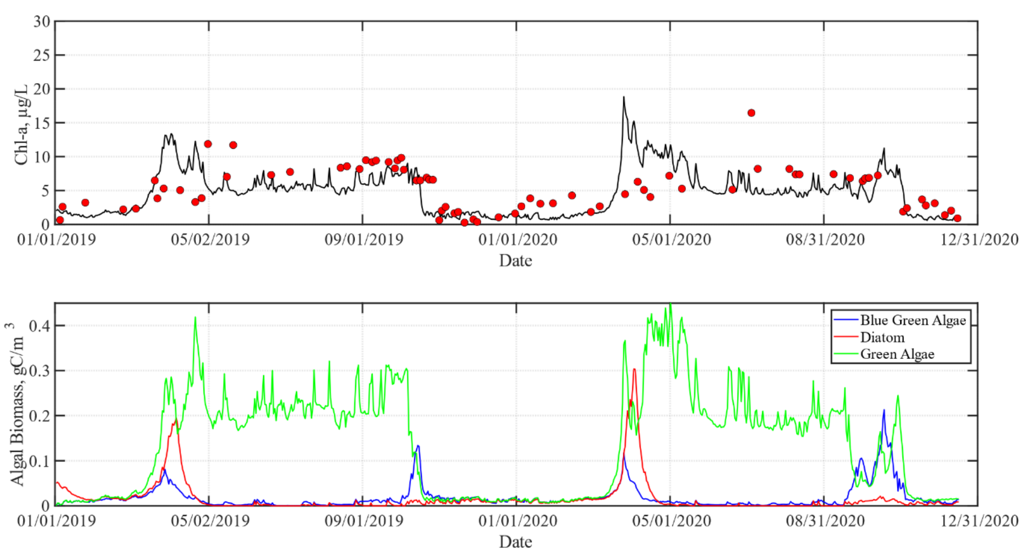

Figure 5. (Upper panel) Simulated (black line) versus satellite-estimated (red circles) photic zone Chl-a concentrations at Browns Bridge. (Lower panel) Model-simulated photic zone algae species at Browns Bridge.

REPEATABILITY OF A TERRESTRIAL LIDAR SURVEY OF A STREAM CHANNEL: BALUS CREEK, OAKWOOD, GA

Jacob M. Bateman McDonald, Drake Nye, Sammy Lee Hand, Michael Hartman, Michael McGee, Eric Odum, William Strand, Joshua Teague, Michael Wild
University of North Georgia

REFERENCE: *Proceedings of the 2023 Georgia Water Resources Conference*, held March 30–31, 2023, at the University of Georgia.

Abstract. The Laser scanning or LiDAR (light detection and ranging) systems offer the opportunity to collect nearly continuous data along a surface. As long as site control is established, repeated LiDAR surveys of a study area can quantify the rate at which an entire landform or landscape is changing. The purpose of this experiment was to determine the replicability of a terrestrial LiDAR survey of a stream channel on the University of North Georgia's Gainesville campus. Additionally, these data were used to determine the amount of weekly change that took place from mid-January through early-March (2023). Semi-permanent benchmarks were installed near the study site to provide a consistent initial setup (benchmark) and back-sight locations. For each weekly survey, a temporary point was installed and surveyed relative to the benchmark. A Trimble SX10 laser scanning total station was set up on that week's temporary point (using the permanent benchmark as the backsight) and the entire stream channel was scanned. To determine the accuracy of the reflectorless ranges (LiDAR returns), at least 30 points were surveyed from the temporary point using the total station functionality of the Trimble SX10. Control points were either randomly distributed within the surveyed area or chosen to delineate the wetted edge of the stream channel and the morphology of in-channel bars. The results of this study indicate that as long as care is taken to set up the site properly and a standard operating procedure is followed for each survey, actual change can be detected and uncertainty can be minimized.

Introduction. Erosional events are episodic and the exact location where bank erosion is going to occur can be difficult to predict. While total station surveys and erosional pins can provide an understanding of how spots are changing, laser scanning or LiDAR (light detection and ranging) systems offer the opportunity to collect nearly continuous data along a surface. As long as site control is established, repeated terrestrial laser scan (TLS) surveys of a study area can quantify the rate at which an entire landform or landscape is changing.

The purpose of this experiment was to determine the replicability of a TLS survey of a stream channel using temporary benchmarks on a point bar. This experiment was done as part of the ENVE 4401K – Terrestrial LiDAR Methods course in spring 2023. Three TLS surveys were completed on a small segment (~30m) of Balus Creek, in the Tumbling Creek Woods adjacent to the University of North Georgia's Gainesville campus. In addition to developing an understanding of the replicability (and associated uncertainty) of TLS surveys, this project sought to understand the potential issues involved with TLS surveys and how to minimize error.

Study Area. The This study surveyed a small incipient meander on Balus Creek on the University of North Georgia's Gainesville campus. The creek is fairly entrenched. Running along river left (approximately 5m away from the river left channel full bank top) is a sewer line that doubles as a walking/bike trail. River right out-of-channel slowly slopes up to the hillslope. Riparian vegetation on both banks is dominantly privet and there are many overhanging branches. Canopy cover is thick.

A point bar has developed on river left. This bar grades up into a relatively high inset surface. This inset surface rises up to the sewer line/historical terrace level. The river right bank is steep and relatively high (~1.8m). A good portion of the river right bank is either vegetated or covered by mosses. The downstream portion of the river right bank in this area is heavily undercut. A medium-sized tree relatively recently toppled into the reach (from just downstream) and has created conditions that have simultaneously increased erosion on both sides of the stream (through undercutting on river right and significant loss of point bar volume on river left) as the large wood has bisected the flow (and changed the direction of deflection during storm events).

During the study period Jan. 20 – Feb. 7, 2023, there was only one very large storm that took place between the first (Jan. 20th) and second (Jan. 27th) surveys. No large precipitation events hit the area between the 2nd and 3rd surveys.

Methods. A Trimble SX10 laser scanning total station (SX10) was used to conduct this experiment. This section will describe how the site was setup, how the temporary (scanning) location was chosen, where the validation points were placed, and how the scan was conducted.

Semi-permanent benchmarks were installed near the study site to provide a consistent initial setup (benchmark; BM) and back-sight (BS) location. The location of the BM was chosen to be stable, off the walking trail (sewer line), and have a clear view into the stream. The BS location was also placed in a stable location way from the walking trail. The BM and BS were separated by at least 50m to reduce the possibility of errors in horizontal angles during the initial station setup influencing the rest of the survey.

For each weekly survey, a temporary point was installed (or reused if found) and surveyed relative to that week's initial setup on the benchmark. The temporary point location was chosen to maximize the visibility of stream banks while being within the channel (not in the water).

To determine the accuracy of the reflectorless ranges (LiDAR returns) from the eventual scan on the temporary point, at least 30 validation points were surveyed from the initial setup (on BM) using the total station functionality of the Trimble SX10. Validation points were either randomly distributed within the surveyed area or chosen to delineate geomorphic features (e.g., the wetted edge of the stream channel and the morphology of in-channel bars). No validation points were captured during the first survey because the methods for the experiment hadn't yet been finalized.

After the SX10 was set up on that week's temporary point (using the BM as the backsight) and the entire stream channel (and surrounding riparian vegetation) was scanned using 'full dome' 'coarse' resolution settings. While the 'full dome' was not needed, these data were collected with a secondary purpose of creating a library of TLS scans for training purposes. A better choice for scanning geometry would have been to draw a 'polygon' that captured just the channel and the near-channel full height area. A coarse scan was chosen to expedite the scans and as a test for what can be expected from relatively short range (~15m) coarse TLS scans.

Data were downloaded from the tablet controller and imported into Trimble Business Center (TBC). The scan data were auto-classified (into high vegetation and ground) by TBC and then manually sifted through to correct misclassifications and classify the points that were not able to be classified. Once the classifications were verified, the ground-classified portion of the point cloud were exported as a .las and imported into ArcGIS Pro (added to an LAS dataset). The validation points were also exported from TBC and imported into ArcGIS Pro.

In ArcGIS Pro, the las dataset from each survey day was converted into a raster (DEM) with pixel size at least twice average point spacing (average pixel size of 0.07 m). Each day's validation points were attributed that day's DEM elevation to determine the DEM's RMSE. DEMs of difference were created by subtracting the older survey(s) from the younger survey(s).

Potential areas of change were determined taking into account the average RMSE from the surveys. Individual RMSE for each survey could not be used because no validation points were collected during the first survey. Areas ephemerally covered by the stream were cut out from the DEMs of difference, as the SX10 cannot penetrate water.

Results. The vast majority of the 'change' observed between time 1 (T1) and time 2 (T2) was either well below the expected accuracy of the surveys or due to differences in the areas actually surveyed **(Figure 1)**. The one area that may have changed is in the middle of the reach on river left where there may have been slight aggradation on the point bar surface right next to the stream. The roughness of the DEMs produced by these scans indicate there are quite a few very low vegetation points included in the 'ground' classified points.

Similar to the T1 to T2 comparison, the 'change' observed between time 3 (T3) and T2 was not actual change. The area with the most 'change' was on river right near the small mid-channel bar **(Figure 2)**. This area had significant vegetation cover and any change is likely due to how the raw point cloud was classified. Also similar to T1 to T2, there appears to be some changes occurring on river left on the edge of the point bar. Considering this area was identified as changing from T1 to T2 and from T2 to T3, there may actually be some storage of sediment on this portion of the point bar.

The two validation point surveys showed similar differences **(Figure 3)**. These differences were on the order of +/- a few millimeters where the scans captured that ground location. Residuals can get relatively high when the validation point falls on a location with interpolated elevation. Much larger residuals were observed during T3. These larger residuals were due to these areas being obscured by large wood or because the point was too close to the water and the laser scanner did not accurately capture that specific point.

Discussion/Conclusion/Lessons Learned. A temporary point can be used as a scanning station and repeat surveys can be successfully done using different temporary points. The amount of error associated with these surveys is dependent on the stability of the TLS setup. Shifting gravels and sands that compose point bar sediments in Balus Creek can become unstable during a scan. The movement of the TLS during its scan can cause tripod legs to move and tilt errors can accumulate. While conducting these scans the first two setups had slight tilt errors (5mm at 50m) while the 3rd setup was in a more stable location.

The laser scanner has a blind spot beneath it. If only the bank is important then setting up on a temporary point on the point bar will work for you. If you are interested in how the whole stream is changing, have multiple setups out of the channel that together can tell the whole story. It is unclear in our analysis whether the changes that were identified were due to actual change or was a result of differences in the way that the point clouds were classified. Overhanging vegetation and small stems and roots make it difficult to consistently capture bank points if your TLS only captures single returns.

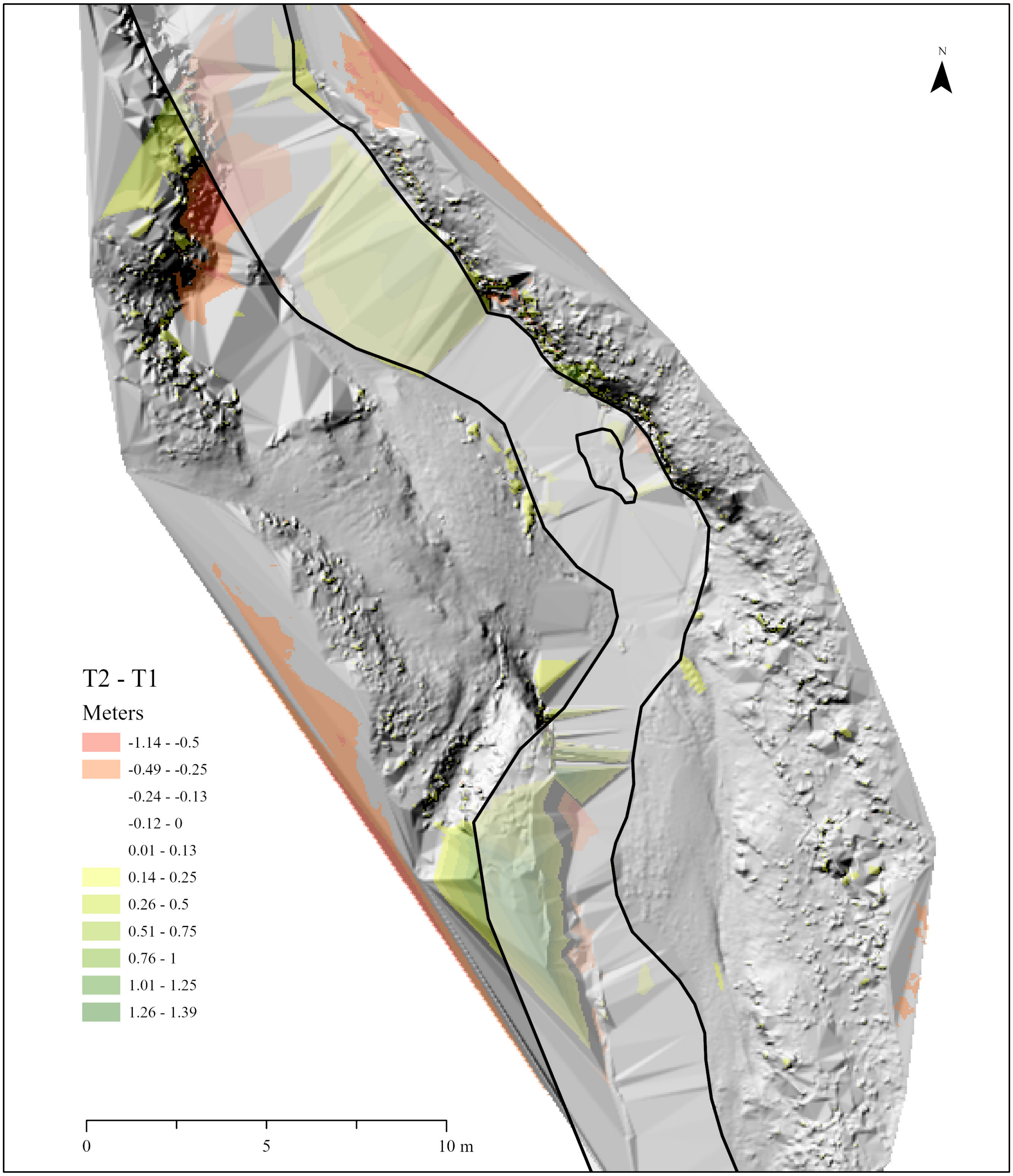

Figure 1. DEM of Difference comparing the elevations from T2 and T1. Reds indicate losses and yellows and greens represent additions

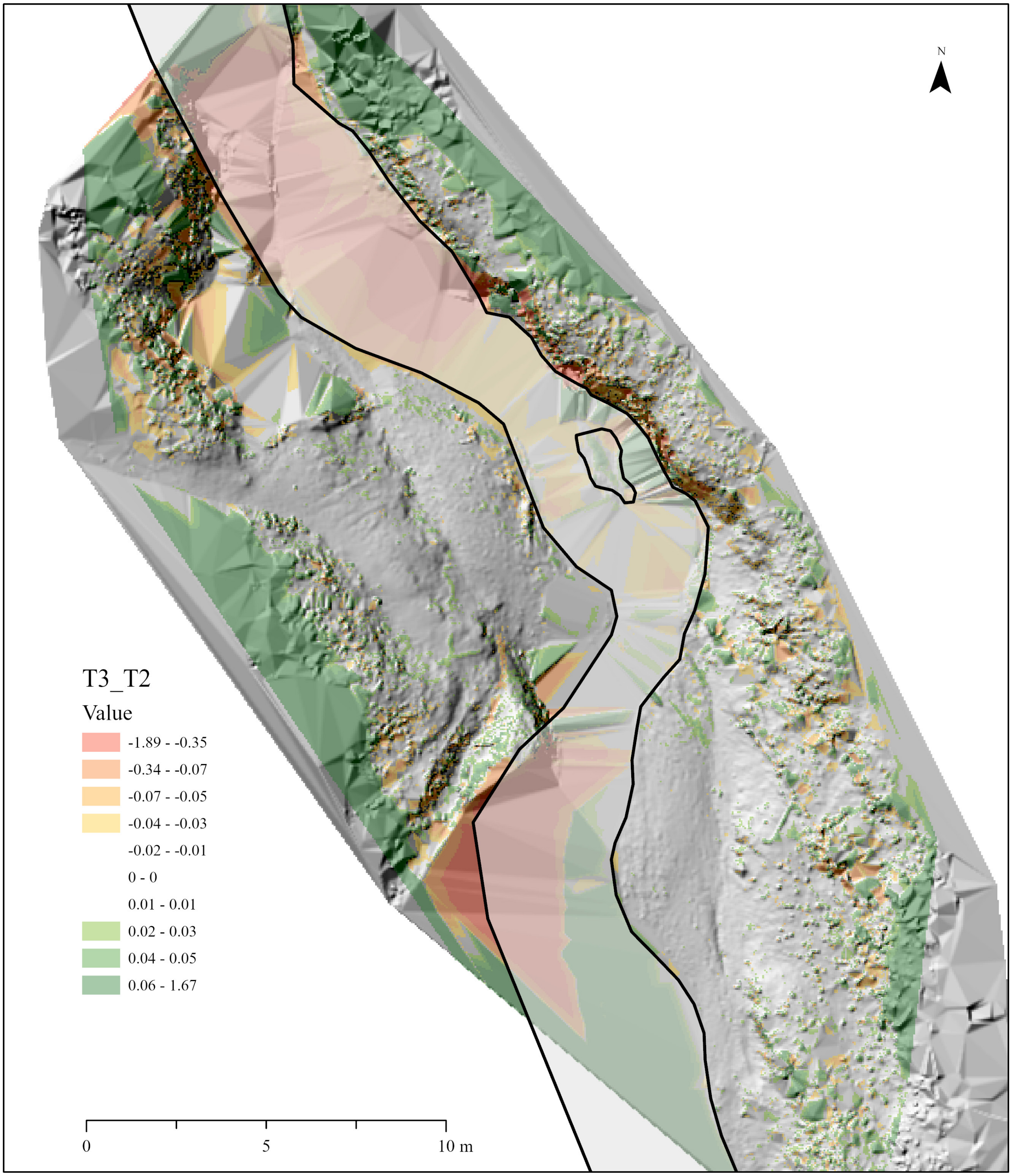

Figure 2. DEM of Difference comparing the elevations from T3 and T2. Reds indicate losses and yellows and greens represent additions.

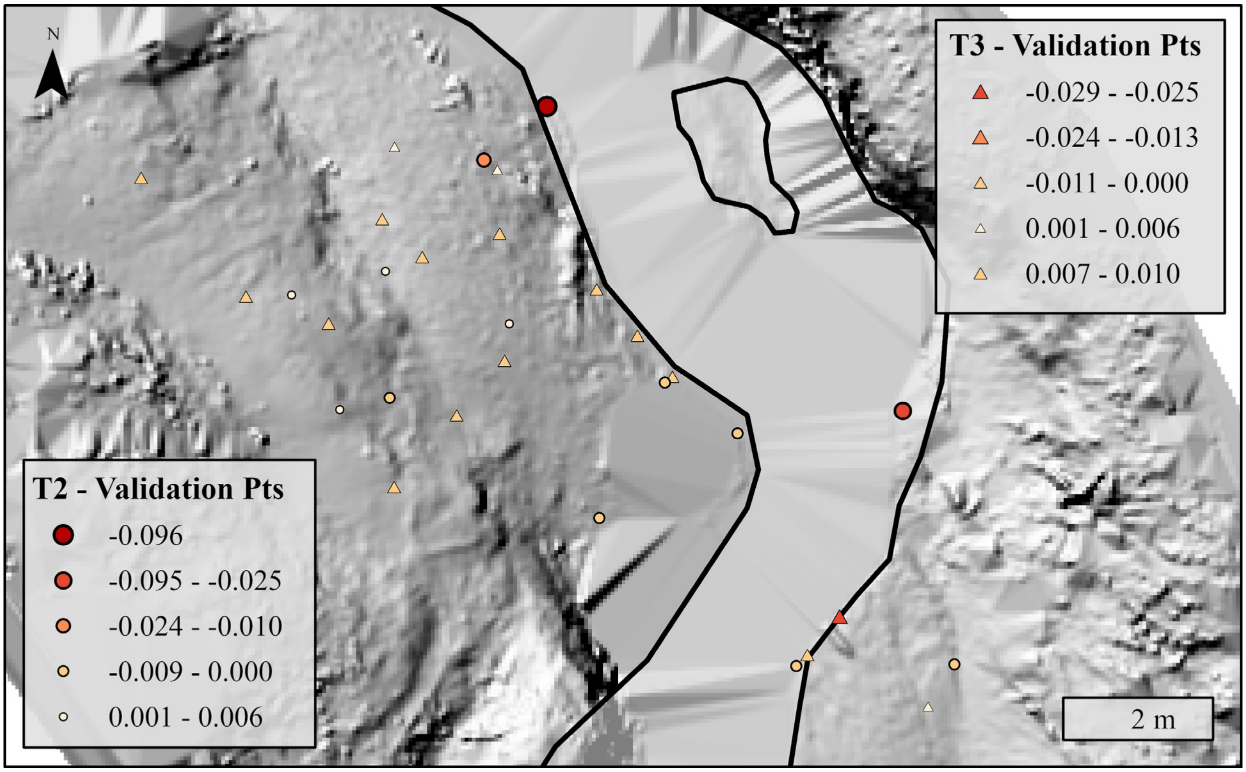

Figure 3. Map showing the elevation errors observed in the validation point surveys for T2 and T3. Validation points were not taken during T1. The color and size of the points indicates the magnitude of the error.

SEPTIC SYSTEM DRAIN FIELD DENSITIES IN ATHENS-CLARKE COUNTY, GEORGIA

Sonrisa Reed, Madison Rollins, Emma Vail, Jacob M. Bateman McDonald
University of North Georgia

REFERENCE: *Proceedings of the 2023 Georgia Water Resources Conference*, held March 30–31, 2023, at the University of Georgia.

Abstract. Athens-Clarke County (ACC) maintains one of the most comprehensive spatial databases of septic systems in the southeastern US. Previous analyses of the potential environmental impacts of these systems suggest system age (< 12 years old and > 49 years old) is likely a greater environmental threat than landscape position (i.e., soil type, slope, and distance to stream). Additionally, while the majority of septic systems in ACC are 'environmentally compliant,' once ephemeral and intermittent streams are taken into account, there are many more potentially environmentally impactful septic systems than previously considered. This research builds upon previous studies to create a potential stream risk (of pollution) map. Septic drainage fields were digitized from installation or repair records in five smaller watersheds spread out across ACC. These watersheds were chosen because 100% of these watersheds' drainages are within ACC. Once the drainage fields were delineated, a simple model was created that used system age and distance to the nearest ephemeral flowpath to estimate risk. Risk maps were created using septic tank locations and septic field locations to determine how these two datasets influence risk potential. The results of this analysis indicate that it is vital that septic drainage fields and ephemeral drainages be taken into account when determining nonpoint source pollution risk.

Introduction. The contamination of surface water by residential septic systems poses a variety of risks to water quality and health. Contamination of surface and ground water from septic systems which are damaged, poorly located, poorly maintained or placed with inadequate consideration of the geological and geochemical conditions of the site are well documented (Wilcox et al., 2010; Rhan, 2011; Schneeberger et al., 2015). Soil type, slope and distance to streams impact contamination levels of water, but age of septic systems was found to pose a much greater risk in Athens-Clarke County (ACC) where about 70% of septic systems are more than 25 years old (Capps et. al., 2020). While well-managed onsite wastewater treatment systems can be a practical and cost effective option for many areas and more than 17% of new single family homes in the south are built with individual septic systems (U.S. Census Bureau, 2022), many such systems are not well-maintained and septic tank systems are the third most common source of the contamination of groundwater (Office of Water, Environmental Protection Agency, 2003).

Furthermore, environmental compliance of septic system locations often involves a minimum distance from the septic tank or drainfield to bodies of water, however, these distances do not consider ephemeral or intermittent streams. Systems near or on one of these flowlines represent unaccounted for risks of contamination of surface water. Possible contaminants from septic system effluent include E-coli which can cause dangerous diarrheal illness; pharmaceuticals that pass relatively unchanged through the human body and may negatively impact sensitive aquatic ecosystems and enter drinking water sources; and antibiotics which can contribute to antibiotic resistant pathogens (Huang et al., 2019).

The burdens on human health and ecosystems increase with increasing density of septic systems. Borchardt et al. (2003) found increased rates of diarrheal disease amongst children in areas where septic systems were more concentrated. Additionally, human waste contains high amounts of nitrogen, which can be harmful to babies at even small concentrations in drinking water, and phosphorus which, like nitrogen, contributes to the eutrophication of water bodies, creating conditions that can foster the growth of toxic algal blooms such as cyanobacteria which has been responsible for multiple illnesses and pet deaths (Environmental Protection Agency, 2021). Our study assessed the age, area, and density of septic system drainfields in sub-watersheds within Athens-Clarke County. Using these data, we created a predictive model to identify potential biogeochemical hotspots for water testing. With many aging septic systems and expanding suburban development, identifying these hotspots of potential water contamination is a vital part of monitoring and protecting the surface water and ground water of Athens-Clarke County and could inform cost effective management plans of onsite wastewater treatment systems that meet public health needs.

Study Area/Data. The data used to conduct our analysis were in the form of a spatial geodatabase of septic systems obtained from the Athens-Clarke County (ACC) Department of Public Works (DPW). This geodatabase included ages and point locations of existing septic systems accompanied by scanned copies of installation or repair forms which included a hand-drawn map of each drainage field and their dimensions, total linear feet, and total area. A 1.25m digital elevation model (DEM) was obtained from the ACC DPW and was used to calculate the environmental variables.

Though there are 18 named watersheds/sub-watersheds in ACC, this analysis focused on five watersheds that are fully contained within ACC's boundary. These watersheds included Brooklyn Creek, Carr Creek, Hunnicutt Creek, Malcolm Creek, and Tanyard Branch. The analysis focused on these watersheds so that if any area of potential concern is identified, ACC has the jurisdiction to potentially ameliorate these conditions/issues.

Methods. To effectively map the locations and footprints of the drainage fields, the scanned, hand-drawn maps included in the septic geodatabase were manually digitized as linear features, and the existing point locations were adjusted, if necessary, to accurately portray the septic tank and drainfield on the parcel (based on map dimensions and a ACC buildings layer also obtained from the ACC DPW).

Once the linear drainage lines were drawn into the geodatabase, the OID (object identifier) which corresponded to the accompanying septic tank (data point in geodatabase) for the drainfield was added to the attribute table of the newly digitized drainfield in order to manage our dataset and determine if there is a correlation between age and area. Drainage lines were then buffered (1 ft on each side) to approximate the drainage pipe area. These buffered drainage lines were then used to determine the system and environment characteristics (distance to ephemeral and perennial streams, slope, etc) of each field.

The digitized field areas were compared to the on-the-form 'absorption areas' for each system to determine if there was a relationship between age and absorption area and if the digitized fields were representative of the data that were provided. Additional analyses were done using just the septic tank locations and the absorption area listed for each tank to get an overall understanding of the spatial distribution and density of septic drainfields throughout ACC. These data were then used to determine which watersheds in ACC have the potential to be the most impacted by septic system contamination of surface waters.

Streams were created from the 10 m DEM using the flow accumulation method for determining the initiation point of the stream or ephemeral flowline. A 20ha threshold was used to approximate the location of perennial streams (in the Appalachian Piedmont, 20ha correlates well with the USGS 'blue lines') and a 2ha threshold was used to approximate the location of ephemeral drainages/flowlines.

A stream risk map was created by determining the age and environmental compliance status (i.e., distance from stream) conditions of the septic systems within each stream pixel's watershed. The variables were attributed to each stream point and a stream risk map was created by assigning weights to the different variables and calculating a relative risk score. Age risk was classified as 2 if the system was younger than 12 years old or older than 49 years old. Distance to stream risk was classified as 4 if less than 30 meters from the 2ha stream network, 2 if between 30 and 50m, and 1 for all other systems. Overall risk was then calculated by multiplying distance to stream risk by age risk.

Results. This analysis classified the potential risk of septic effluent contamination for approximately 113 km of stream network spread out across five relatively small watersheds in Athens-Clarke County (ACC) **(Figure 1)**. Within the analyzed stream network, approximately 53% (~60 km) were classified as "No Risk" due to not having septic systems in the watershed **(Table 1)**. Approximately 20% (~23 km) were "Low Risk" and 25% (~28 km) were "Medium Risk". Of the analyzed stream network, 2% was classified as "High Risk" (1.3 km) or "Extreme Risk" (0.9 km). Incorporation of septic drainage field data in the analysis of the Brooklyn Creek and Malcolm Creek watersheds increased the areas identified as at-risk. Each watershed had unique spatial patterns of risk related to its history of development. The following subsections describe the classified potential risk within the five watersheds.

Brooklyn Creek. The majority of this watershed is on sewer, but there are a few spots in the southwestern portion of the watershed that may be at-risk if any of these systems were to fail **(Figure 1)**. Approximately 60% of the streams in Brooklyn Creek have no septic tanks/fields in their subwatershed **(Table 1)**. Approximately 32% of the streams in Brooklyn Creek were classified as "Medium Risk" due to either having age risk or systems within 50m from the stream. Addition of the septic drainage field data increased the percent of "Extreme Risk" from 1% to 2% **(Table 1)** and substantially broadened the area classified as high risk on the southwestern side of the watershed. 'Hotspots' that had not been identified using the septic tank location data, became evident with the septic drainage field location data. Overall, approximately 38% (9 km) to 40% (10 km) of the stream network in the Brooklyn Creek watershed faces potential risk from a failing septic system.

Carr Creek. Of the study watersheds, Carr Creek had by far the highest density of septic systems and the longest length of stream potentially at-risk. While a few small areas along the 20ha stream network were at-risk, all four of the high density areas in Carr Creek's watershed were directly drained if not underlain by the 2ha network **(Figure 1)**. Only 40% of the stream network in the Carr Creek watershed had no risk from septic. Even without having the drainage field data for this watershed, 1.5% of the stream network was classified as having "Extreme Risk" for impacts from septic systems. Overall, approximately 59% (22 km) of the stream network in the Carr Creek watershed has the potential to be affected by a failing septic system.

Hunnicutt Creek. The 2nd highest density of septic systems was found in Hunnicutt Creek's watershed (northwestern corner). Both the 20ha and 2ha stream networks had areas at-risk near this septic hotspot. As we found in the other watersheds, even in areas with low density of septic systems, there are many potentially at-risk 2ha flow lines that might provide a quickflow pathway for effluent. Approximately 52% of the stream network in the Hunnicutt Creek watershed had no risk from septic **(Table 1)**. Of the stream network that was at-risk, the majority of the stream pixels were classified as "Medium Risk". A small percentage of stream pixels were classified as "High Risk" (0.9%) or "Extreme Risk" (0.3%). Overall, approximately 48% (14 km) of the stream network in the Hunnicutt Creek watershed has the potential to be affected by a failing septic system.

Malcolm Creek. There were only a few septic systems in this watershed. While there were systems near the 2ha flow network, a number of systems were near the watershed divide and may influence adjacent watersheds (depending on local subsurface flow conditions). Slightly below 50% of the stream pixels in Malcolm Creek's watershed were classified as "No Risk" **(Table 1)**. The majority of the at-risk stream pixels were classified as "Low Risk". The addition of the septic drainage field data increased the "Medium Risk" and "High Risk" classes a total of 5% **(Table 1)**. This 5% increase represents an additional 0.5 km of potentially at-risk stream **(Figure 2)**. Overall, approximately 50% (5 km) to 54% (6 km) of the stream network in the Malcolm Creek watershed has the potential to be affected by a failing septic system.

Tanyard Branch. This watershed only had three septic systems. Of those systems, two of them are concerningly close to a 2ha flowline, which puts 17% (approximately 2 km) of the Tanyard Branch stream network at-risk for pollution from a failing septic system.

Discussion/Conclusion. This analysis provides an understanding of the spatial distribution of potential biogeochemical hotspots that are hydrologically connected to the stream network. Further work is needed to refine the relative risk score and determine how these scores correlate to real world variations in water quality. While nearly 50% of the stream network within the study area is not impacted (no septic tanks) or not significantly at-risk due to septic systems, most of the parcels in these watersheds are also serviced by sewers (being closer to central Athens), and a follow-up study incorporating sewer lines and the pollution risk they pose into the analysis is needed. Though there were not many areas with "High" to "Extreme" risk due to septic systems, each watershed had areas of concern.

Incorporating the 2ha flow network provided a much better picture of areas directly at-risk. While there are portions of the 2ha flow network that are just artifacts of the way the network was delineated in GIS, these flow lines represent relatively quick pathways for contaminants to flow into our surface water. Additionally, the largest federally recognized stream inventory, NHD (National Hydrography Dataset), is woefully unrepresentative of headwater streams (Elmore et al., 2013; Fritz et al., 2013; Christensen et al., 2022). Using the 2ha flow network allowed for a more representative understanding of water flow within each watershed.

This research revealed the importance of determining the spatial distribution of septic drainage fields when determining pollution risk. While the vast majority of septic tanks are compliant with regards to distance to stream (Capps et al., 2020), many septic drainage fields lie within restricted areas. Finally, we found that the addition of the septic drainage field data more than doubled the length of stream classified as "Extreme Risk" in the two watersheds we compared **(Figure 2)**. Future work will continue to build upon this dataset.

References:

Borchardt, M. A., Po-Huang Chyou, DeVries, E. O., & Belongia, E. A. (2003). Septic System Density and Infectious Diarrhea in a Defined Population of Children. *Environmental Health Perspectives*, 111(5), 742. https://doi.org/10.1289/ehp.5914

Capps, K. A., Bateman McDonald, J. M., Gaur, N., & Parsons, R. (2020). Assessing the socio-environmental risk of onsite wastewater treatment systems to inform management decisions. *Environmental Science & Technology*, 54(23), 14843–14853. https://doi.org/10.1021/acs.est.0c03909

Christensen, J. R., Golden, H. E., Alexander, L. C., Pickard, B. R., Fritz, K. M., Lane, C. R., Weber, M. H., Kwok, R. M., and Keefer, M. N., 2022, Headwater streams and inland wetlands: Status and advancements of geospatial datasets and maps across the United States: Earth-Science Reviews, v. 235, 104230.

Environmental Protection Agency. (August 11, 2022). Nutrient pollution. EPA. https://www.epa.gov/nutrientpollution/issue#:~:text=Too%20much%20nitrogen%20and%20phosphorus%20in%20the%20water%20causes%20algae,aquatic%20life%20need%20to%20survive.

Elmore, A. J., Julian, J. P., Guinn, S. M., and Fitzpatrick, M. C., 2013, Potential stream density in mid-Atlantic U.S., watersheds: PLoS One, v. 8, n. 8, e74819.

Fritz, K. M., Hagenbuch, E., D'Amico, E., Reif, M., Wigington, P.J., Leibowitz, S. G., Comeleo, R. L., Ebersole, J. L., and Nadeau, T. L., 2013, Comparing the extent and permanence of headwater streams from two field surveys to values from hydrographic databases and maps: Journal of the American Water Resources Association, v. 49, n. 4, 867-882.

Huang, F., Zou, S., Deng, D., Lang, H., Liu, F. (2019). Antibiotics in a typical karst river system in China: Spatiotemporal variation and environmental risks. *Science of The Total Environment*, 650(1),1348-1355. https://doi.org/10.1016/j.scitotenv.2018.09.131.

Office of Water, Environmental Protection Agency. (2003). *Voluntary national guidelines for management of onsite and clustered (decentralized) wastewater treatment systems*. EPA. Retrieved February 25, 2023, from https://www.epa.gov/septic/septic-systems-reports-regulations-guidance-and-manuals

Rahn, P. H. (2011). Sickness Caused by Septic Disposal Systems in the Black Hills. *Proceedings of the South Dakota Academy of Science*, 90, 51–66.

Schneeberger, C. L., O, D. M., Humphrey, C., Henry, K., Deal, N., Seiber, K., Hill, V. R., & Zarate-Bermudez, M. (2015). Fate and Transport of Enteric Microbes From Septic Systems in a Coastal Watershed. *Journal of Environmental Health*, 77(9), 22–31.

U.S. Census Bureau. (2022). *Sewer*. U.S. Department of Commerce. Retrieved July 10, 2023, from https://www.census.gov/construction/chars/current.html

Wilcox, J., Gotkowitz, M., Bradbury, K., & Bahr, J. (2010). Using Groundwater Models to Evaluate Strategies for Drinking-Water Protection in Rural Subdivisions. *Journal of the American Planning Association*, 76(3), 295–304. https://doi.org/10.1080/01944361003742403

Table 1. Percent of stream pixels classified as "No-Risk" to "Extreme-Risk".

Watershed	Total Steam Pixels	Data Used	No Risk (0)	Low Risk (1)	Medium Risk (2)	High Risk (4)	Extreme Risk (8)
Total	11332	Tank	53%	20%	25%	1%	1%
	3534	Field	56%	15%	26%	1%	2%
Brooklyn	2464	Tank	62%	4%	32%	1%	1%
		Field	60%	4%	32%	1%	2%
Carr	3782	Tank	41%	35%	21%	2%	1%
Hunnicutt	3006	Tank	52%	15%	32%	1%	0%
Malcolm	1070	Tank	50%	41%	8%	0%	1%
		Field	46%	40%	11%	2%	1%
Tanyard	1010	Tank	82%	0%	17%	0%	0%

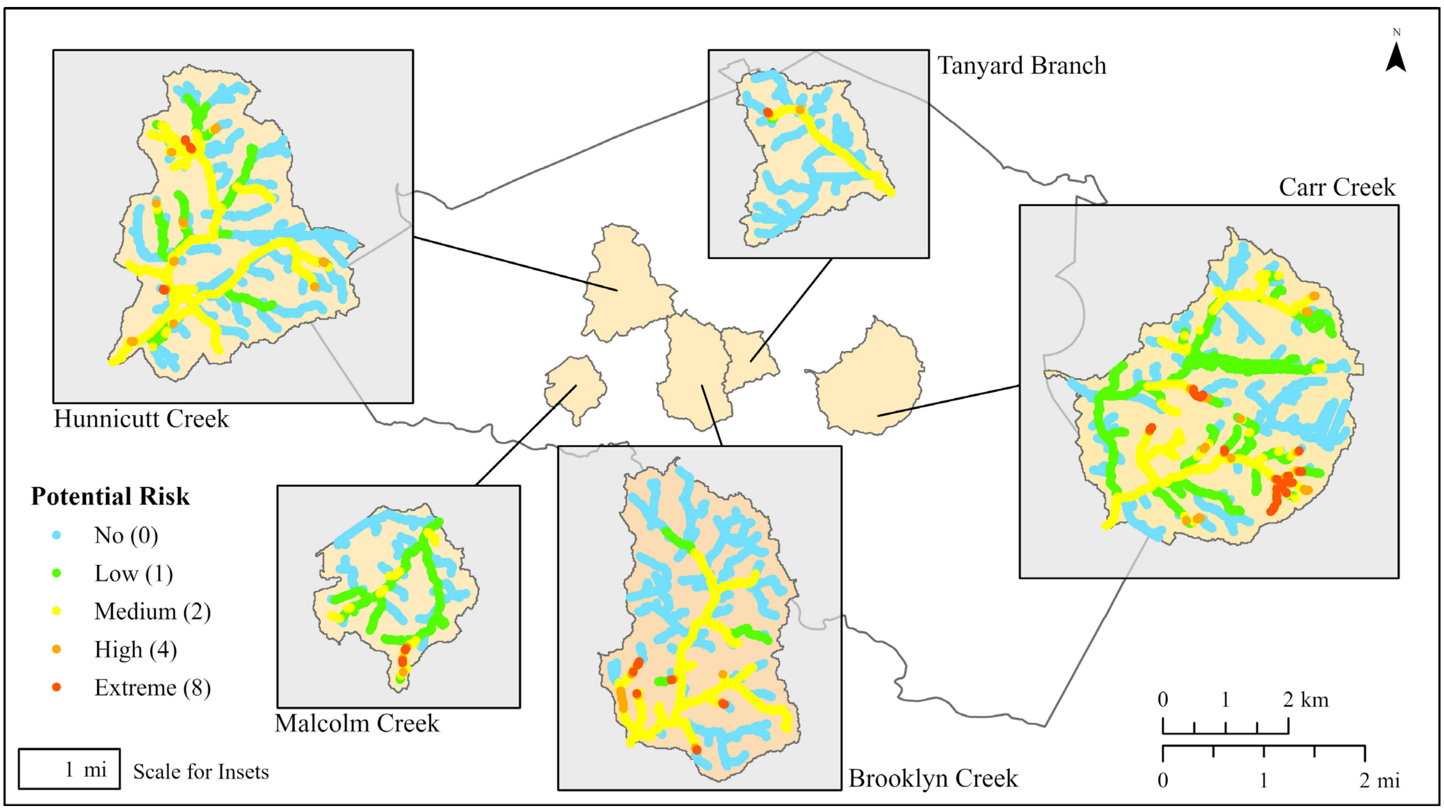

Figure 1. Potential risk maps for the five watersheds analyzed in this study.

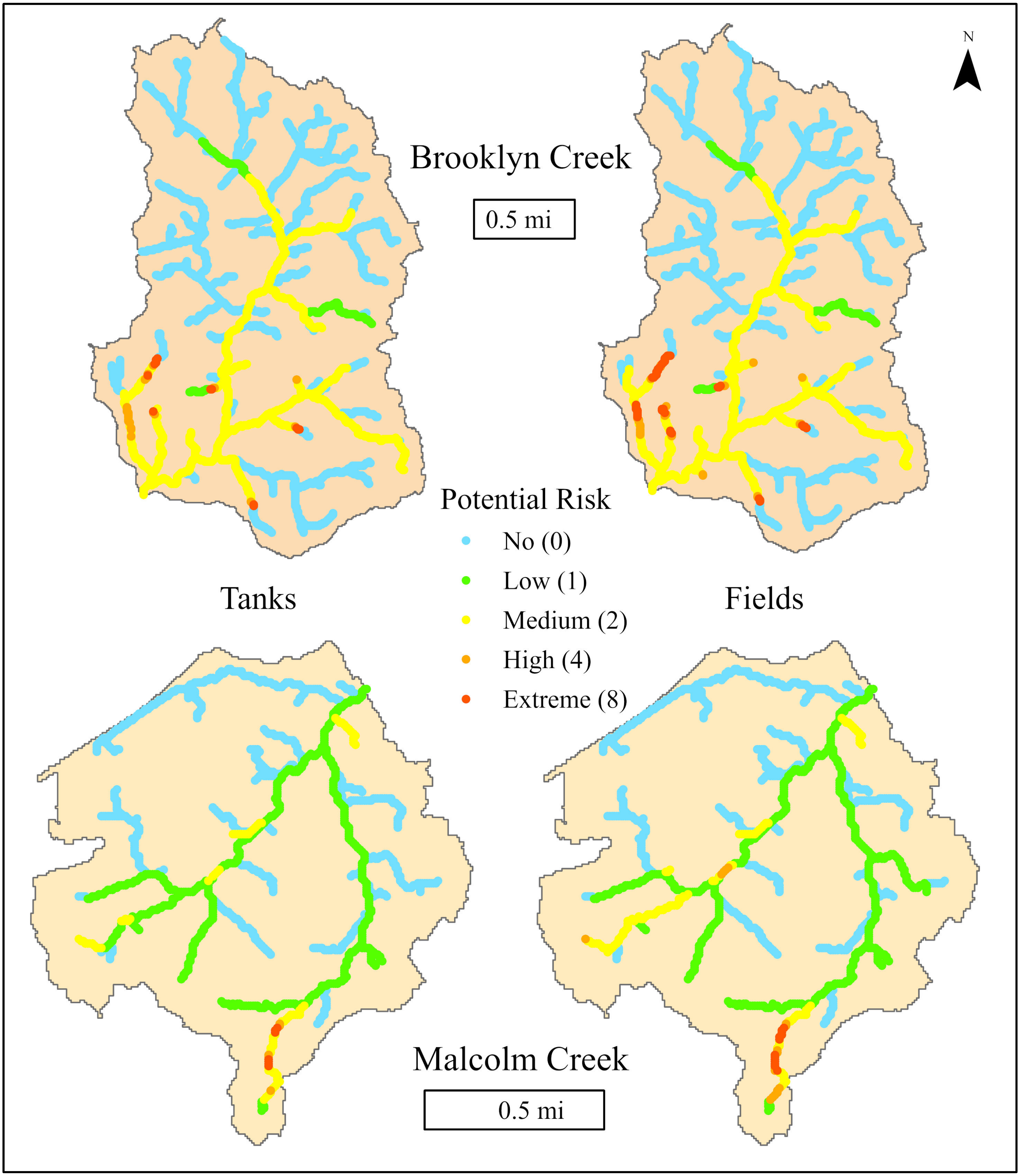

Figure 2. Comparisons between the risk maps created using the septic tank locations versus the septic drainage field locations.

USING WATER QUALITY TO ASSESS THE ACTIVITY OF WILD PIGS IN A PILOT MANAGEMENT STUDY

L.C. Sweeney[1], S.W. Golladay[1], J.L. Smith[1,2], F.E. Kruis[1,2], M.T. Mengak[2], L.M. Conner[1]
[1]The Jones Center at Ichauway, Newton, GA 39870, [2]Warnell School of Forestry and Natural Resources, University of Georgia, Athens, GA 30602

REFERENCE: *Proceedings of the 2023 Georgia Water Resources Conference*, held March 30–31, 2023, at the University of Georgia.

Abstract. Wild pigs (*Sus scrofa*) can cause significant agricultural and environmental damage, however previous research to determine their effects on water quality has yielded variable results. We collaborated on a wild pig removal study to assess selected water quality parameters as indicators of pig activity. Monthly grab samples from tributaries in agricultural and conservation lands were collected and analyzed for parameters including total suspended solids (TSS), NO_3-N, NH_4-N, soluble reactive phosphorus (SRP), and eDNA. Three continuous water quality sensors were installed to measure temperature, specific conductance, and turbidity at 15-minute intervals. Monthly water samples showed tributaries in agricultural areas with dense wild pig populations had elevated TSS and slightly elevated SRP. Environmental DNA (eDNA) was detectable across the study area but in low concentration. Sensor data suggest specific conductance and turbidity are useful for detecting instances of instream wildlife disturbances. Our future work will utilize measures of wild pig density for further interpretation of water quality response to wild pig management.

Introduction. Wild pigs are a highly invasive and economically costly species. Due to property damage including crops, pastures, fences, and equipment, it is estimated wild pigs cost Georgia agricultural producers over $150 million annually (Mengak 2016). Their presence also raises concern for water quality because they frequent riparian areas where they defecate and disturb soil by rooting for food and wallowing (Strauch et al. 2016). Although visual evidence of riparian disturbance is often evident, prior research has shown variable success at detecting water quality degradation from pig activity (Doupe et al. 2009; Dunkell et al. 2011; Brooks et al. 2020; Bolds et al. 2021). Increases in *Escherichia coli* have commonly been detected, but the effects on parameters such as suspended solids and nutrients have been inconsistent.

Coordinated pig removal efforts occurred in the Albany, GA area as part of the Feral Swine Eradication and Control Pilot Program (https://www.nrcs.usda.gov/feral-swine-eradication-and-control-pilot-program). Pig removal occurred on ~12,150 ha of private lands that are predominantly agricultural (cotton, corn, peanuts, and pecans), forested, and wetland. Demonstrating success in wild pig management is difficult. Removal counts from corral traps, tracking, and aerial gunning were recorded, but the fast maturation and high reproductive rate of wild pigs (Choquenot et al. 1996) make removal counts an ineffective metric. Therefore, in addition to pig removal counts and crop damage assessments, we collaborated on the Pilot Program to assess selected water quality parameters as indicators of pig activity and their removal. Our specific objectives were: 1) Expand an existing sampling network to evaluate differences in water quality in areas of intensive agriculture and in forested conservation management areas, 2) Test the efficacy of continuous water quality sensors for specific conductance, turbidity, and temperature in detecting changes in water quality potentially associated with pig activity, and 3) Relate water quality parameters to seasonal and annual variations in stream discharge.

Methods. *Monthly Grab Samples.* Twelve sites along six tributaries (i.e., Ichawaynochaway Creek, Market Branch, Horse Lot Branch, Chickasawhatchee Creek, Keel Creek, and Little Spring Creek) were selected for monthly sampling (**Figure 1, top**). Nine sites are within or near the boundaries of the Pilot Program study area (collectively referred to as agriculture sites), and three sites are within the Chickasawhatchee Wildlife Management Area (collectively referred to as conservation lands). Sample collection was from August 2020 to August 2022 where monthly 1-L surface grab samples were placed on ice, taken to the laboratory, and stored at 2º C until processing. An additional 1-L sample was collected at each site and delivered to the Tifton Veterinary Diagnostic Laboratory for detection of wild pig enteric environmental DNA (eDNA).

Processing was completed within 48 hours of collection and included determination of pH and alkalinity with a Mettler Toledo DL15 Titrator and filtration through pre-weighed 0.7 µm pore size glass fiber filters. Filtered and unfiltered aliquots were stored at 2º, -4º, and -20º C for nutrient analyses. Filters from processing were dried, weighed, placed in a muffle furnace at 500ºC, and reweighed to determine total suspended solids (TSS) and fine particulate organic matter (FPOM). A Shimadzu TOC-L Total Carbon Analyzer was used to measure dissolved organic (DOC) and inorganic carbon (IC), and a Lachat QuikChem 8500 was used to measure NO_3-N, NH_4-N, soluble reactive phosphorus (SRP), unfiltered total nitrogen, and unfiltered total phosphorus.

Continuous Data Loggers. In January of 2022, YSI EXO3 Multiparameter Water Quality Sondes were installed along Little Spring Creek in three locations of varying pig removal efforts (**Figure 1, bottom**). Two sondes, HDitch and HReservoir, were placed in the Pilot Program pig removal area. HDitch was in a channel with nearby visual evidence of hog disturbance. HReservoir was below the outfall of an irrigation reservoir, which potentially allowed material processing and sediment deposition prior to reaching the sonde. H62, the third sonde, was downstream of private land outside of the Pilot Program study area and was likely receiving the least wild pig removal effort. The sondes measured temperature, specific conductance (dissolved ions), and turbidity (light scattering) at 15-minutes intervals. Monthly maintenance was performed to download data, change batteries, and calibrate sensors. Gage height and discharge measurements for Little Spring Creek were obtained from USGS Gage 02354475 downstream from the project area.

Data Analysis. Water quality samples were summarized by site and date. A principal component analysis (PCA) was created in R Statistical Software (R Core Team 2021) with package ggbiplot (Vu 2011) to look for patterns in water quality parameters across the study area over time.

Site and date averages for water quality parameters were used to generate site specific box plots for the study period. A one-way ANOVA on ranks was used to compare differences across sites (Sigmaplot V14, Systat Software Inc). In this manuscript summaries are limited to total suspended solids based on interpretation of PCA (below).

The continuous sonde data were adjusted by changing the turbidity values under the detection limit to 0. Additionally, the sondes periodically recorded turbidity values much greater than the calibration standard of 124 FNU. Therefore, values greater than 136 FNU (10% above the calibration) were truncated at 136 FNU. Dynamic time series graphs were created in R Statistical Software (R Core Team 2021) with package dygraphs (Vanderkam et al. 2018).

Results. *Monthly Grab Samples.* Two axes of the PCA explained 59.1% of the variation in the data (**Figure 2**). Axis 1 was positively correlated with groundwater as shown by having greater alkalinity and pH, both indicating the presence of carbonates originating in the upper Floridan aquifer. Suspended solids (FPOM and TSS) were negatively correlated with axis 1. While there was a broad overlap between conservation lands and agricultural lands, generally streams in agricultural areas had greater and more variable TSS concentrations. Inorganic nitrogen and phosphorus species, common agricultural contaminants, showed little influence on the distribution of sites in the PCA. However, SRP tended to be slightly greater in samples from agricultural lands, especially at sites with high TSS (data not shown).

Lands in conservation status, i.e., Wildlife Management Areas (WMAs), tended to have lower and less variable TSS concentrations compared to agricultural lands (**Figure 3**). One exception was LS_Res, a reservoir outfall within the project area. TSS at LS_Res were consistently lower and less variable than at other sites. Sites that had the greatest or most variable TSS concentrations (e.g., Horse55, CR62, and CRMag) were near the project boundary with uncontrolled agricultural areas upstream. Likewise, sites outside of the project area with uncontrolled areas upstream also showed greater TSS concentration and variability (e.g., CR234 and LS62).

Wild pig eDNA was detectable, but generally found in low concentrations at all sites throughout the study (**Figure 4**). Preliminary analyses showed great variability in eDNA levels across sampling dates. There did not appear to be a relationship between eDNA detection and stream discharge.

Continuous Data. All sonde sites had daily specific conductance cycles that peaked in mid-morning. H62 had daily cycles of turbidity that peaked in the middle of the night, while HDitch and HReservoir only cycled occasionally. Increases in discharge caused decreases in specific conductance and increases in turbidity. Many spikes in turbidity were also observed during periods of stable or no flow, and the specific conductance did not decrease (**Figure 5**).

Discussion. *Monthly Water.* Our study showed differences in water quality parameters associated with wild pig activity across the study area, but results need to be put in the context of regional geology and historic patterns of land use. Our sites span the transition between two physiographic districts, the Fall Line Hills and Dougherty Plain. The Fall Line Hills has greater stream drainage density, somewhat greater topographic relief, and greater surface runoff. The Dougherty Plain has lower relief with carbonate bedrock and greater subsurface flow (Hicks et al. 1981). A majority of agricultural land in our study area was found in the Fall Line Hills. Greater drainage density would increase the susceptibility of streams to both agricultural runoff and wild pig activity. Small 1-3 order streams represent a majority of stream length in many watersheds serving as collecting areas for potential contaminants (Freeman et al. 2007).

Elevated TSS and SRP are often associated with agricultural production and surface runoff, but the levels at agricultural sites in our study were likely exacerbated by the disruptive activities of pigs. Wild pig tracking during the study indicated that population density was high along stream corridors adjacent to the agricultural fields. Riparian areas across our study tended to be densely vegetated with flood tolerant hardwood species and a dense understory of shrubs and vines that act as buffers for the creeks. When riparian areas were near agricultural fields, they also offered cover for wild pig populations in near proximity to a food source (crops). Additionally, precipitation was above normal, and streamflow was above median levels during the first year of our study. During that period, wild pigs were likely not limited by the availability of water in the landscape. The elevated levels of TSS and SRP in agricultural sites compared to conservation sites became more prominent during seasonal dry periods when surface runoff had decreased, and riparian corridors became a source of both cover and water for pigs.

While evidence of nutrient and sediment runoff from agriculture and wild pigs was detectable in our study, levels were generally modest. Site averages for NO_3-N ranged from 0.13 to 1.30 mg/L and NH_4-N was generally less than 0.10 mg/L. Likewise, SRP concentration was generally less than 0.05 mg/L. These levels do not suggest widespread impairment of instream conditions (https://www.epa.gov/nutrient-policy-data/ecoregional-nutrient-criteria-rivers-and-streams). As agriculture intensified in the region, center pivot irrigation became essential to insure crop production.

This resulted in a consolidation of crops in the uplands and subsequent regrowth of stream-side forests which are now reaching maturity (Craft and Casey 2000). While acting as cover for wild pigs and their destructive ways, streamside forests also provide a significant buffer absorbing potential contaminants from uplands prior to runoff entering streams (Lowrance et al. 1984).

Our results show that eDNA is potentially useful for detecting the presence of wild pig activity in streams. However, in our study area, detection was highly variable, and results suggested that concentrations are very low at our study sites. This is consistent with other studies of eDNA which have shown that it degrades rapidly in natural settings and the likelihood of collecting eDNA is low unless large volumes of water can be concentrated (Davis et al. 2018). Still, when combined with other water quality parameters and information on wild pig populations from terrestrial monitoring, eDNA appears to be a useful parameter because it is very specific.

Isolating Wild Pig Activity in Continuous Data. Discharge can complicate identifying wild pig induced changes to water quality parameters, but our preliminary results show that our selected water quality parameters appear useful for detecting wild pig or other wildlife effects. Spikes in turbidity paired with a simultaneous lack of decrease in specific conductance seem indicative of wildlife, presumably wild pig, disturbance. Many of these peaks were at dusk or dawn, further suggesting wildlife origin. We plan to combine our results with measures of wild pig activity to provide for more detailed interpretations of water quality responses to wild pig management.

Conclusions. Wild pig activity appears to pose a significant threat to water quality across our study area. Assessing the magnitude of wild pig influence is complicated by substantial variations in their abundance and distribution over space and time (F.E. Kruis and J.L. Smith, personal observation). We have found that total suspended solids, turbidity, and eDNA are all useful for determining wild pig effects. Unfortunately, there is no single absolute indicator of wild pig presence and abundance, and a suite of indicators appears most useful for detection of water quality effects. Sonde sensors, while expensive, show much promise in distinguishing direct (actual instream activity) and indirect (disturbed soils eroded during precipitation) effects.

Streams are linear features crossing landscapes and encountering a mosaic of land uses. Water quality taken at a single point represents not only local conditions but integrates processes and disturbances occurring upstream. All the streams we sampled originated or flowed through land outside of the project area. This confounds our ability to evaluate the effectiveness of control efforts to enhance water quality. If water quality is the primary objective of wild pig control efforts, then a watershed approach is likely to be most effective. We recognize that this may not be realistic in areas dominated by private land ownership as individuals will have diverse management objectives and views on the presence of wild pigs.

Acknowledgements. This research was supported by the Flint River Soil and Water Conservation District and the Jones Center at Ichauway.

We'd like to thank Brian Clayton, Bryan Cloninger, Chelsea Smith, Jamie Rogers, Maxine Hauser, Jeneil Patel, and Natalie Horn for their contributions to field and laboratory work.

References:

Bolds, S. A., B. G. Lockaby, S. S. Ditchkoff, M. D. Smith, and K. C. VerCauteren. 2021. Impacts of a large invasive mammal on water quality in riparian ecosystems. Journal of Environmental Quality **50**: 441–453. doi:10.1002/jeq2.20194

Brooks, J. P., R. K. Smith, C. A. Aldridge, B. Chaney, A. Omer, J. Dentinger, G. M. Street, and B. H. Baker. 2020. A preliminary investigation of wild pig (Sus scrofa) impacts in water quality. Journal of Environmental Quality **49**: 27–37. doi:10.1002/jeq2.20036

Choquenot, D., J. McIlr, and T. Korn. 1996. Managing Vertebrate Pests: Feral Pigs, Bureau of Resource Sciences, Australian Government Publishing Service.

Craft, C. B., and W. P. Casey. 2000. Sediment and nutrient accumulation in floodplain and depressional freshwater wetlands of Georgia, USA. Wetlands **20**: 323–332. doi:10.1672/0277-5212(2000)020[0323:SANAIF]2.0.CO;2

Davis, A. J., K. E. Williams, N. P. Snow, K. M. Pepin, and A. J. Piaggio. 2018. Accounting for observation processes across multiple levels of uncertainty improves inference of species distributions and guides adaptive sampling of environmental DNA. Ecology and Evolution **8**: 10879–10892. doi:10.1002/ece3.4552

Doupe, R. G., J. Schaffer, M. J. Knott, and P. W. Dicky. 2009. A description of freshwater turtle habitat destruction by feral pigs in tropical north eastern Australia. Herpetological Conservation and Biology **4**: 331–339.

Dunkell, D. O., G. L. Bruland, C. I. Evensen, and C. M. Litton. 2011. Runoff, sediment transport, and effect of feral pig (Sus scrofa) exclusion in a forested Hawaiian watershed. Pacific Science **65**: 175–194. doi:10.2984/65.2.175

Freeman, M. C., C. M. Pringle, and C. R. Jackson. 2007. Hydrologic Connectivity and the Contribution of Stream Headwaters to Ecological Integrity at Regional Scales. JAWRA Journal of the American Water Resources Association **43**: 5–14. doi:10.1111/j.1752-1688.2007.00002.x

Hicks, D. W., R. E. Krause, and J. S. Clarke. 1981. Geohydrology of the Albany area, Georgia. 80–1296. 80–1296 U.S. Geological Survey.

Lowrance, R., R. Todd, J. Fail Jr., O. Hendrickson Jr., R. Leonard, and L. Asmussen. 1984. Riparian Forests as Nutrient Filters in Agricultural Watersheds. BioScience **34**: 374–377. doi:10.2307/1309729

Mengak, M. T. 2016. Landowner Opinions Regarding Wild Pigs in Georgia, USA. Proceedings of the Vertebrate Pest Conference **27**. doi:10.5070/V427110567

R Core Team. 2021. R: A language and environment for statistical computing.

Strauch, A. M., G. L. Bruland, R. A. MacKenzie, and C. P. Giardina. 2016. Soil and hydrological responses to wild pig (Sus scofa) exclusion from native and strawberry guava (Psidium cattleianum)-invaded tropical montane wet forests. Geoderma **279**: 53–60. doi:10.1016/j.geoderma.2016.05.021

Vanderkam, D., J. Allaire, J. Owen, D. Gromer, and B. Thieurmel. 2018. dygraphs: Interface to “Dygraphs” Interactive Time Series Charting Library.

Vu, V. 2011. ggbiplot: A ggplot2 based biplot.

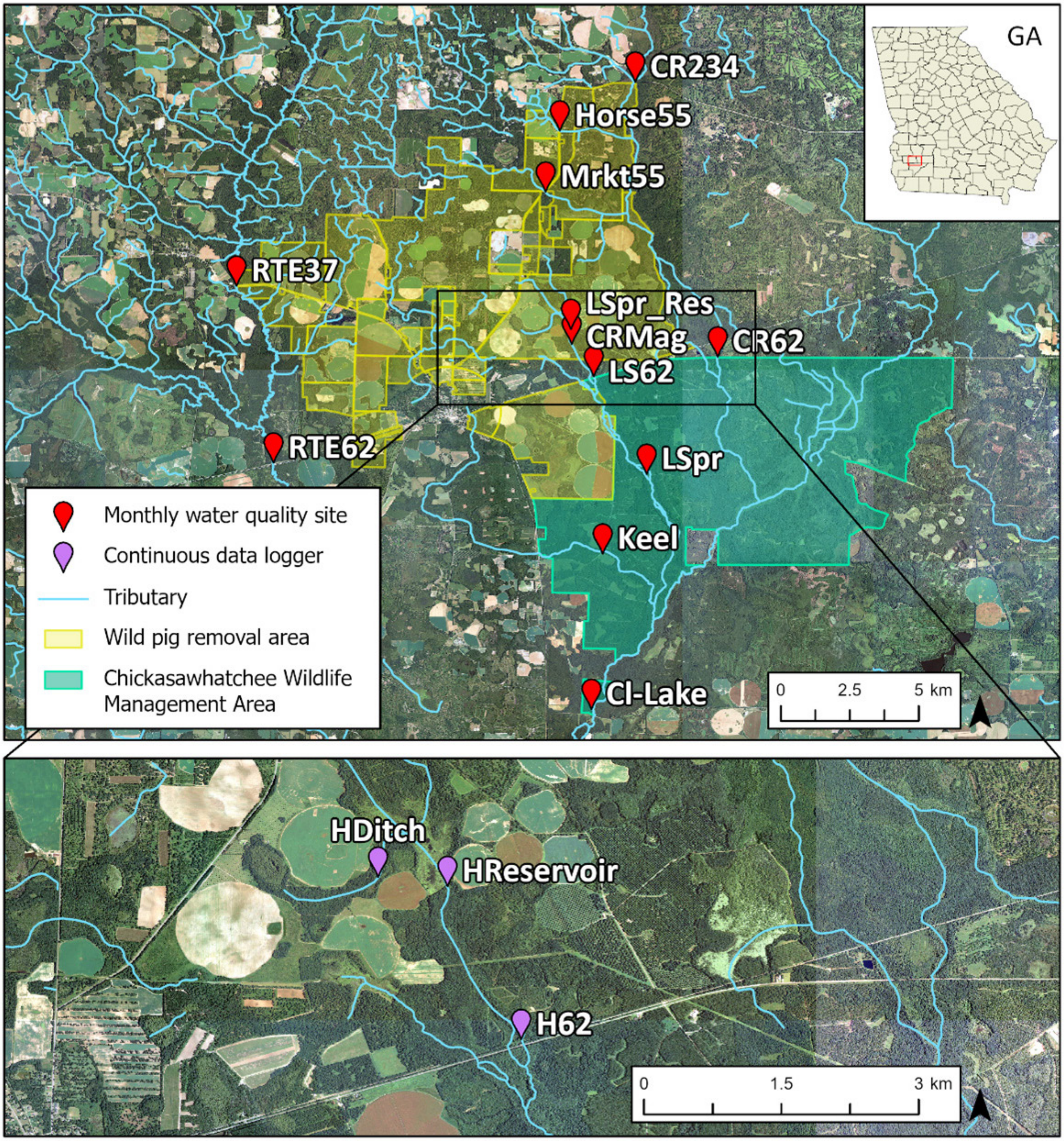

Figure 1. Map of the study area (top panel) and map of sonde locations (bottom panel). The site labeled 'HReservoir' in the bottom panel corresponds to LS-Res in the top panel. Aerial imagery courtesy of the U.S. Geological Survey.

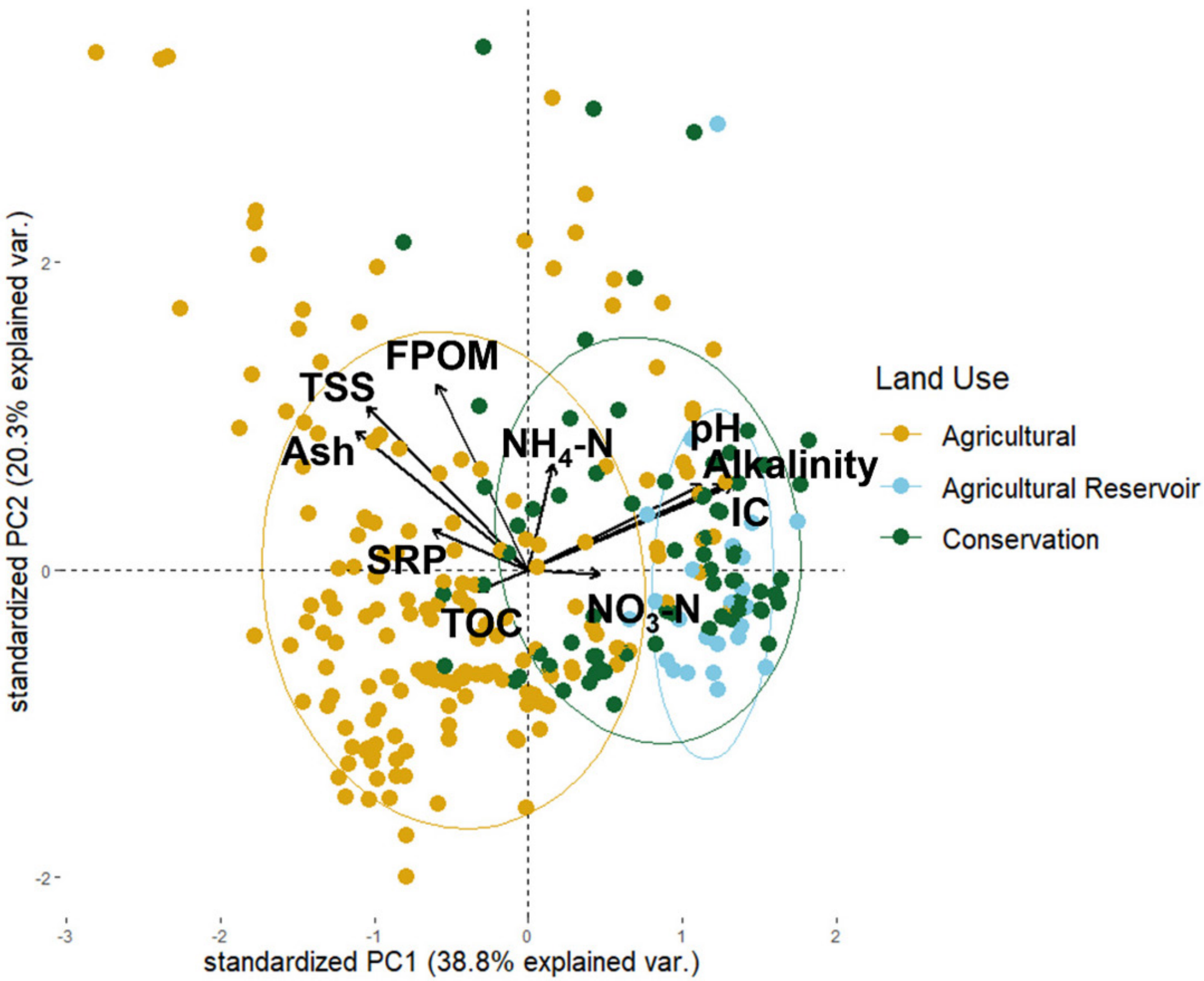

Figure 2. Principal component analysis of water quality data from the study.

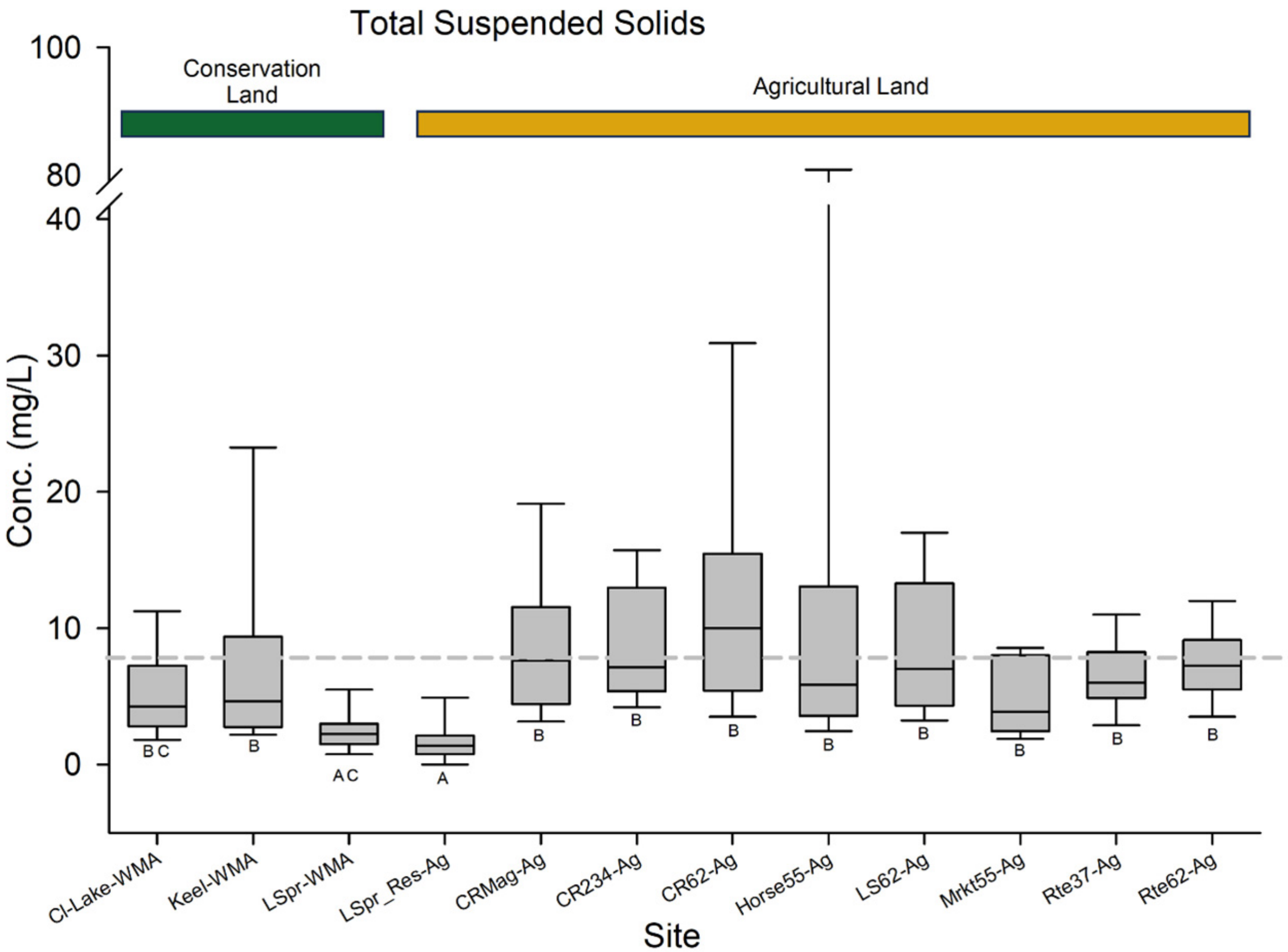

Figure 3. Total suspended solids concentrations at sites across the wild pig project area. Dashed line represents the median value of all site date combinations. Sites were compared by a one-way ANOVA on ranks followed by pairwise comparisons, p<0.05 for comparisons deemed different (see letter codes).

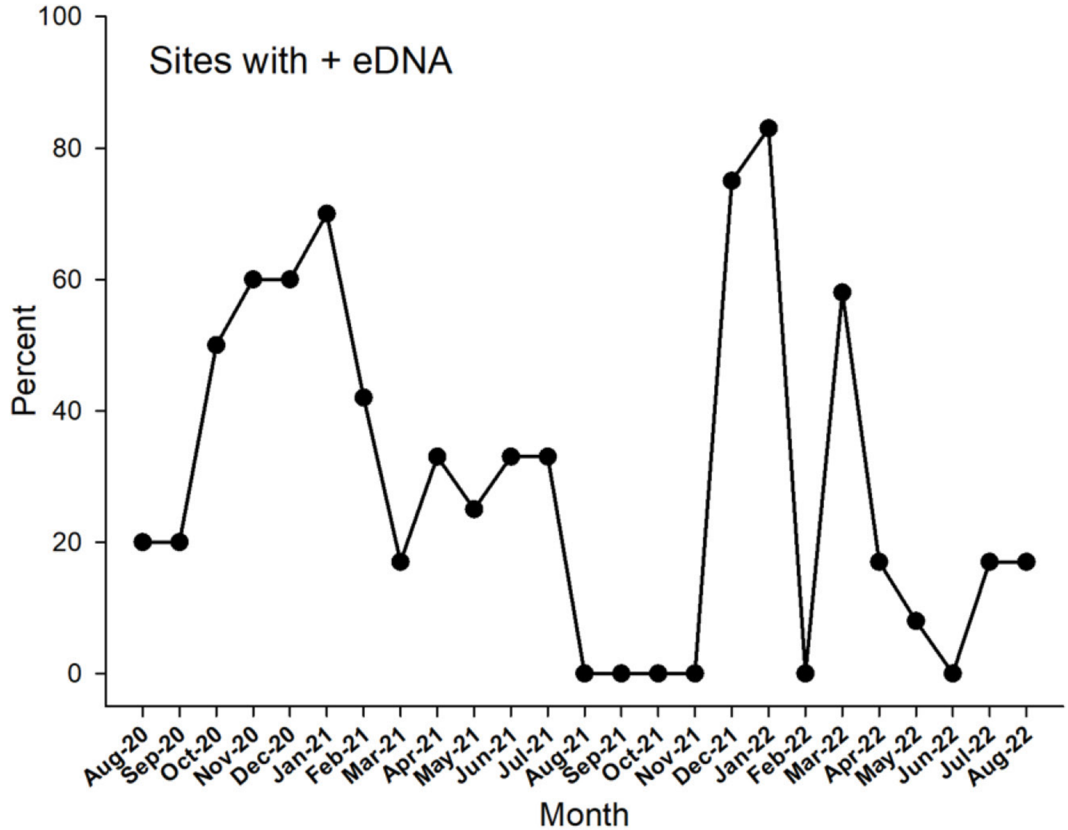

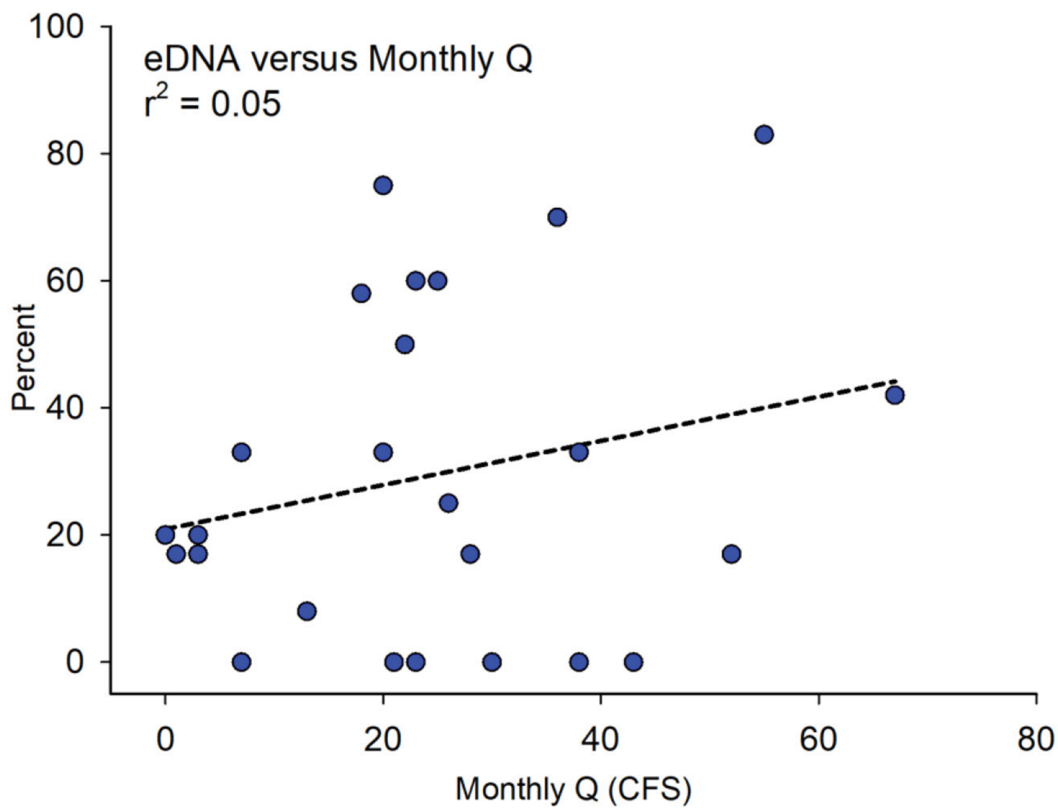

Figure 4. Percentage of sites with positive detections for wild pig eDNA (top), and percentage of sites with positive detections of wild pig eDNA versus stream discharge (bottom).

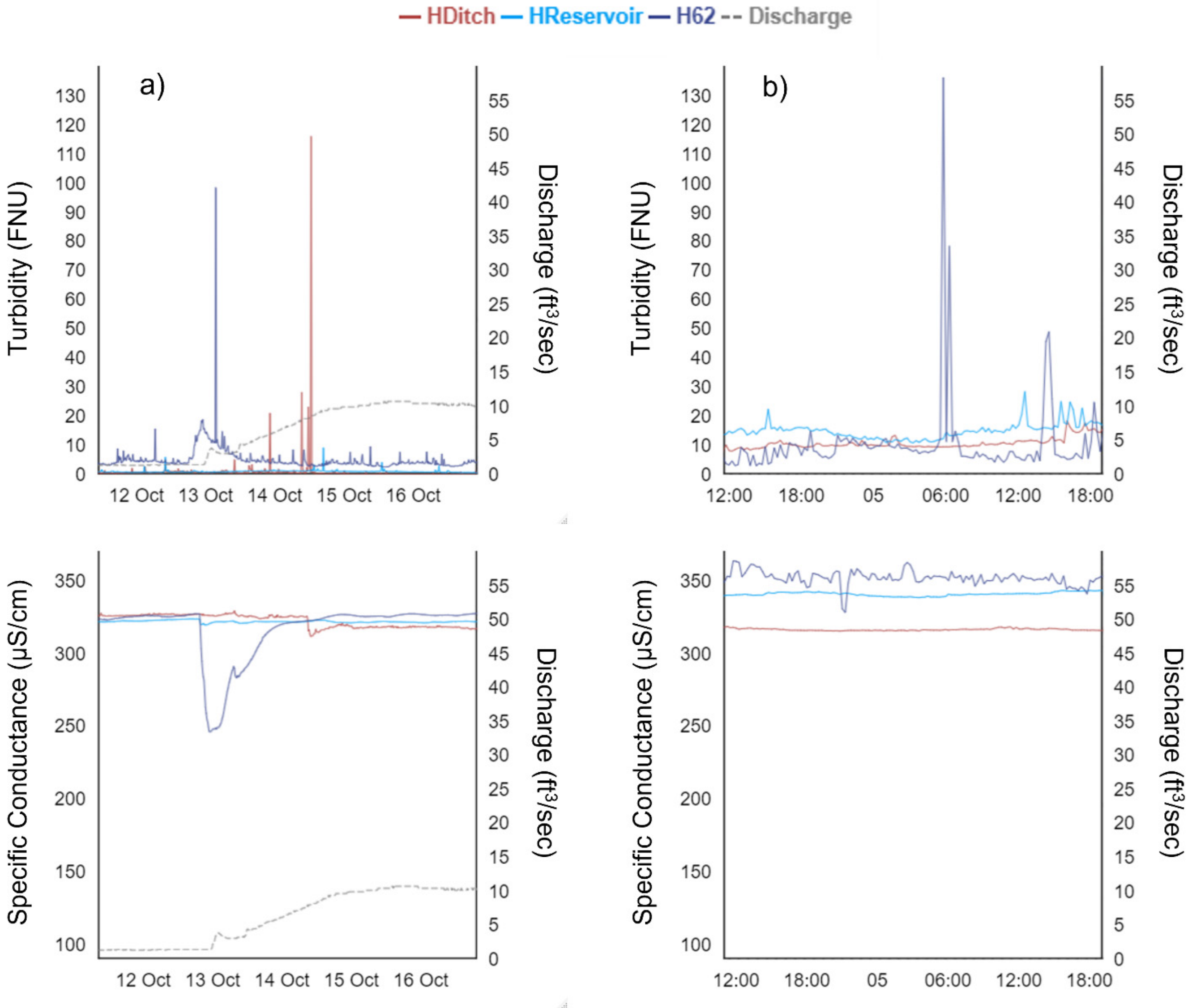

Figure 5. Turbidity and specific conductance measurements during (a) an increase in discharge and (b) stable flow conditions

COASTAL SEDIMENT BUDGETING TO MATCH SEDIMENT SUPPLIES, DREDGING VOLUMES, AND NATURAL INFRASTRUCTURE ENHANCEMENT NEEDS FOR SEA-LEVEL RISE ADAPTATION

Caleb Sytsma[1], Rhett Jackson[2], Mark Risse[3], Margaret Kurth[4], Clark Alexander[6], Matthew V. Bilskie[7], Oscar Villegas[7], Ellis Kaladjian[1]

[1]ORISE Research Fellow, US Army Corps of Engineers, Engineer Research and Development Center, [2]University of Georgia, Warnell School of Forestry and Natural Resources, [4]US Army Corps of Engineers, Engineer Research and Development Center [5]University of Georgia, Marine Extension and Georgia Sea Grant, [6]University of Georgia, Skidaway Institute of Oceanography, [7]University of Georgia, College of Engineering

REFERENCE: *Proceedings of the 2023 Georgia Water Resources Conference*, held March 30–31, 2023, at the University of Georgia.

Introduction. Coastal communities and ecosystems are at increasing risk from flood damages as climate change and sea level rise bring the combined impacts of heightened storm surges and increased beach, marsh, and dune erosion (Nicholls and Leatherman 1996; Cazenave and Cozannet 2014). Combating these risks traditionally requires significant investments in grey infrastructure like sea walls, but research has found such approaches have unintended negative impacts on surrounding ecosystems and the stability of beaches they are placed behind (Pilkey and Wright 1998; Dugan et al. 2018). Additionally, grey infrastructure approaches lack inherent resilience, meaning additional money and labor are required for periodic repairs and reconstruction following major storms. These costs are expected to increase as environmental conditions at our coasts grow more extreme (Temmerman et al. 2013). Natural Infrastructure (NI) projects show both theoretical promise and experimental success as viable alternatives for managing these risks while delivering a range of other benefits.

The Network for Engineering with Nature (N-EWN) is a community of educators, practitioners, and researchers actively working to research, develop, and promote NI. The US Army Corps of Engineers (USACE) Engineer Research and Development Center established N-EWN in 2019 with the University of Georgia and has expanded to include private, government, tribal, and university partners across the country. The efforts of N-EWN can support USACE in carrying out its missions by researching new and natural means of addressing old and worsening coastal defense issues. USACE has used coastal NI like dune replenishment and construction for decades, but new research has highlighted their social and environmental co-benefits alongside their success for coastal defense (Narayan et al. 2016; Polk and Eulie 2018; Powell et al. 2019). Additionally, well-planned NI have a higher potential for self-sustenance and resilience in the face of a changing climate than hard grey infrastructure projects do, as harnessing natural systems can build inherent reconstructive abilities into a project (Gittman et al. 2014; Chambers et al. 2021). These benefits are leading to an increasing demand for NI in both local governments and the federal government, and the bipartisan 2016 Water Infrastructure Improvements for the Nation (WIIN) Act and 2020 Water Resources Defense Act (WRDA) added the requirement that USACE include NI options in planning and project feasibility reports.

With increasing focus on NI, sediment is the currency of coastal resilience. Coastal projects like marsh thin layer placement, beach renourishment, and dune and sill construction and renourishment require large volumes of sediment that are contaminant-free and match project-specific color and grain size requirements. Matching sediment sources with project needs is an ongoing problem for coastal infrastructure, as it requires tracking numerous sediment sources and sinks at a relatively fine scale. The Savannah River Harbor undergoes regular dredging to maintain its use as a navigable channel for international commerce, and large quantities of sediment are stored in both upland and offshore disposal areas. In this study, N-EWN is working to develop a sediment budget for the Savannah Harbor that accounts for local sediment fluxes and project needs with a methodology that is adaptable to other localities.

Methodology. In order to create a sediment budget for the Savannah River Harbor, we started with a conceptual model of sources and sinks of sediment for the local area (**Figure 1**). Quantification of each sediment flux is described in greater detail below.

River Inputs. A total of 143 concurrent suspended sediment and discharge measurements taken from 1974 to 1994 at the USGS Savannah River gage near Clyo, GA (USGS-02198500) were used to calculate annual average loads from 1974 to 2022. Data from this gage was used because it has the largest, most current suspended sediment dataset on the Savannah River at the furthest downstream point (Windom and Palmer 2022). We analyzed the full set of suspended sediment data for trends with discharge. Suspended sediment concentrations did not significantly correlate with discharge but did have fewer high concentrations at discharges above 20,000 cfs (**Figure 2**). While such a relationship is contrary to traditional positive trends between discharge and suspended sediment, it is theoretically sound for the Savannah River. This is because three large man-made lakes are situated along the river, altering the flow of approximately 58% of the river's total basin area (Meade 1982). Dams are known to trap riverine sediment with efficiencies of up to 80%, and controlled releases further alter natural correlations between discharge and suspended sediment (Vörösmarty et al. 2003, Syvitski and Milliman 2007). This is expected to have a particularly high impact on the Savannah River's sediment load, as the lakes are situated just upstream of the Fall Line, a geographic feature that separate's Georgia's hillier physiographic regions from its lower-energy Coastal Plains.

As such, we used a two-bin method to calculate the daily loads for all available daily discharge data between 1974 and present day. Daily loads calculated from median sediment concentrations were summed to calculate annual loads, and the reported average annual load was calculated from the most recent 20 years of discharge data. Annual bedload was calculated as 10% of suspended sediment load (Milliman and Farnsworth 2011). Conversion of calculated sediment mass loads into volumes was done using a density of 0.90g/cc. To find this bulk density value, we took sediment grain size data available at the Georgia Coastal Hazards Portal (https://gchp.skio.usg.edu/) and classified each point as either "sandy" (Phi < 4) or "fine" (Phi > 4). Bulk densities of 1.48g/cc and 0.68g/cc were then assigned to each class, respectively, based on previously collected field data. The sediment volume of each grain size class was then calculated by applying the point data across the 10,000ft channel reach it was in. If more than one grain size class existed in a single reach, the percentage of points in each class was assumed to be the percentage of volume belonging to each class for that reach (ex, Points of Fines / Total Points * Volume). Details on volume calculations are provided in the *Dredging* section below. Finally, we used the volumes of each class across the channel to calculate a volume-weighted average bulk density of 0.90g/cc. This value matches well with those reported by Eulie, Corbett, and Walsh (2018) for clayey sands in the Tar-Pamlico Estuary.

Marine Fluxes. Offshore sediment movement is generally categorized into long-shore (parallel to shore) and cross-shore (perpendicular to shore) transport when estimating sediment fluxes near the shoreline. Estimation of their respective magnitudes is thus largely reliant on modeling and depends on wave energy, sediment concentration, and mean sediment grain size. Modeling work by our team is ongoing, and our current numbers for long-shore transport come from previous literature (Wang, Kraust, and Davis 1998; Olsen Associates 2002, van Gaalen, Tebbens, and Barton 2016).

Dredging. Ten years (2013 - 2022) of daily dredged volumes were aggregated by both the channel reach they were pulled from and the upland dredged material containment area (DMCA) they were placed in to yield annual average total volumes. For the purposes of this study, the channel was divided into 10,000-foot long reaches that are equally split along the main federal channel line. In cases where a day of dredging crossed the channel divisions we chose, the total volume of that day was added to the channel section that a greater length of dredging was conducted over. It should also be noted that while we report annual average disposal volumes to each DMCA, not all DMCA's are used in any given year. Total volumes of stored sediment for each DMCA were calculated by adding the 2020 and 2021 disposal volumes to the total stored volumes reported in a 2020 Taylor Engineering report (Taylor Engineering, Inc. 2020).

Dredge volume data for channel reaches beyond the harbor entrance (0 to 90B, **Figure 3**) were not available, but volumes dredged from there are placed in the offshore dredge material disposal site (ODMDS). An average annual volume of 1,000,000 cubic yards is disposed of to the ODMDS (USACE and USEPA 2013), and we applied that volume across the nine, 10,000ft channel reaches that contribute to it for the purposes of mapping.

Channel Volume Changes. Another component of the sediment budget is annual accumulations or losses of sediment in the lower Savannah River. To quantify sediment volume changes in Savannah Harbor, a time series analysis of bathymetric data was performed using a GIS-based workflow. The workflow involved differencing elevation values of the time-series digital elevation models (DEMs) (i.e., T2 - T1), and then dimensionally-integrating the resultant differential values by the two-dimensional area of the DEM grid cell. Annual channel volume changes for years 2014-2021 were calculated.

Shoreline Changes. To quantify sediment volume changes along beach-dune systems in coastal Georgia, a time series analysis of LiDAR-derived topobathymetric data was performed using a similar workflow as was used for the Savannah Harbor—i.e., differencing elevation values of a more recent DEM with those of an older DEM and then multiplying those differential elevation values by the two-dimensional area of the DEM grid cell. Annual shoreline sediment volume changes for years 1999, 2006, 2009, 2010, 2016, and 2017 were completed based on available LiDAR data.

Project Sediment Needs. Several beneficial use (BU) placement areas are currently being considered by USACE Savannah District, according to correspondence with their staff. Placement elevations for these projects are still being determined, and thus we only show planned areas for these projects. Volumes will be incorporated into the overall sediment budget once they are calculated. Additionally, our team is modeling local thin layer placement needs to help salt marshes keep pace with sea level rise.

Results. The Savannah River was found to provide an annual average sediment load of 133,000 cubic meters to the Savannah River Harbor, and estimates by Olsen Associates predict an additional 613,000 cubic meters of sediment influx from marine fluxes. An annual average of 3,840,000 cubic meters of sediment is dredged from the entire length of the Savannah River Harbor Channel, with 79% of that sediment going to DMCAs and the remaining 21% going to the ODMDS. Thus, there is a net annual deficit of 2,850,000 cubic meters of sediment which are either coming from channel storage or being deposited in the Savannah River Channel by an unaccounted-for mechanism (**Figure 3**). Larger differences between the sediment inputs and dredging volumes from 2019 – 2021 are due to additional dredging to deepen the channel during the Savannah Harbor Expansion Project (SHEP). Dredge records from 2022 are incomplete and end in August.

Bathymetry-based channel volume calculations show an average fluctuation of 1,928,000 cubic meters for the Savannah River Harbor channel, but there is a general pattern of gross volume change flipping from negative to positive in successive years. Applying the volume over the entire area of the channel yields an average depth change of 0.16m. Overall, little volume change occurs along the channel because dredging operations are intended to maintain a constant depth across the constant channel area. Greater fluctuation is found near Port Wentworth and beyond the harbor entrance (**Figure 4**; 0 – 70B on **Figure 5**). LiDAR-based shoreline volume change calculations show an average gain of 151,000 cubic meters of sediment along Tybee Island's shore but incorporating the annual average renourishment of 200,000 cubic meters of sand since 1975 yields a net natural loss of 50,000 cubic meters of sediment per year.

Discussion. Overall, the Savannah River Harbor appears to have a large volume of sediment available for beneficial use projects. Additionally, the DMCA's represent an even larger source for sediment to be used in BU projects.

Future work. The most obvious need for future work is to address the discrepancy between sediment sources and dredged volumes. One potential method is conducting DEM-based volume change analysis along the Savannah River shoreline to help quantify the amount of sediment that erodes along the riverbank. Our team also intends to create a new longshore transport model for the area, which may show current sediment influx from offshore is greater than what the 2002 Olsen Associates model predicted (Olsen Associates 2002).

The heightened channel volume fluctuation near Port Wentworth (**Figure 4**) may provide a means of quantifying bedload beyond our assumed 10% of suspended sediment calculation, and future work will attempt to separate out dredging operations from the channel depth changes. Work is also ongoing to automate the GIS workflow used to calculate shoreline volume changes for Tybee Island so that it can be readily applied to other areas around, and potentially beyond, the Savannah River Harbor.

Additional project goals include incorporating the sediment volume requirements of nearby nourishment projects, including modeling of salt marsh thin layer placement needs. From there, more specific tabulation of sediment grain size and quality in each DMCA and channel reach will yield a budget that is useful for matching sediment needs with sediment availability.

References:

Cazenave, Anny, and Gonéri Le Cozannet. 2014. "Sea Level Rise and Its Coastal Impacts." *Earth's Future* 2 (2): 15–34. https://doi.org/10.1002/2013EF000188.

Chambers, R.M., A.L. Gorsky, R.E. Isdell, M.M. Mitchell, and D.M. Bilkovic. 2021. "Comparison of Nutrient Accrual in Constructed Living Shoreline and Natural Fringing Marshes." *Ocean & Coastal Management* 199 (January): 105401. https://doi.org/10.1016/j.ocecoaman.2020.105401.

Dugan, J. E., K. A. Emery, M. Alber, C. R. Alexander, J. E. Byers, A. M. Gehman, N. McLenaghan, and S. E. Sojka. 2018. "Generalizing Ecological Effects of Shoreline Armoring Across Soft Sediment Environments." *Estuaries and Coasts* 41 (S1): 180–96. https://doi.org/10.1007/s12237-017-0254-x.

Eulie, Devon O., D. Reide Corbett, and J.P. Walsh. 2018. "Shoreline Erosion and Decadal Sediment Accumulation in the Tar-Pamlico Estuary, North Carolina, USA: A Source-to-Sink Analysis." *Estuarine, Coastal and Shelf Science* 202 (March): 246–58. https://doi.org/10.1016/j.ecss.2017.10.011.

Gaalen, Joseph F. van, Sarah F. Tebbens, and Christopher C. Barton. 2016. "Longshore Sediment Transport Directions and Rates from Northern Maine to Tampa Bay, Florida: Literature Compilation and Interpretation." *Journal of Coastal Research* 322 (November): 1277–1301. https://doi.org/10.2112/JCOASTRES-D-15-00002.1.

Gittman, Rachel K., Alyssa M. Popowich, John F. Bruno, and Charles H. Peterson. 2014. "Marshes with and without Sills Protect Estuarine Shorelines from Erosion Better than Bulkheads during a Category 1 Hurricane." *Ocean & Coastal Management* 102 (December): 94–102. https://doi.org/10.1016/j.ocecoaman.2014.09.016.

Meade, Robert H. 1982. "Sources, Sinks, and Storage of River Sediment in the Atlantic Drainage of the United States." *The Journal of Geology* 90 (3): 235–52. https://doi.org/10.1086/628677.

Milliman, John D., and Katherine L. Farnsworth. 2011. *River Discharge to the Coastal Ocean : A Global Synthesis*. Cambridge: Cambridge University Press. https://search.ebscohost.com/login.aspx?direct=true&AuthType=ip,shib&db=nlebk&AN=337656&site=eds-live&custid=uga1.

Narayan, Siddharth, Michael W. Beck, Borja G. Reguero, Iñigo J. Losada, Bregje van Wesenbeeck, Nigel Pontee, James N. Sanchirico, Jane Carter Ingram, Glenn-Marie Lange, and Kelly A. Burks-Copes. 2016. "The Effectiveness, Costs and Coastal Protection Benefits of Natural and Nature-Based Defences." Edited by Maura (Gee) Geraldine Chapman. *PLOS ONE* 11 (5): e0154735. https://doi.org/10.1371/journal.pone.0154735.

Nicholls, Robert J., and Stephen P. Leatherman. 1996. "Adapting to Sea-level Rise: Relative Sea-level Trends to 2100 for the United States." *Coastal Management* 24 (4): 301–24. https://doi.org/10.1080/08920759609362298.

Olsen Associates. 2002. "Review Comments Regarding 'Draft - Savannah Harbor Beach Erosion Study (October 2001)' Applied Technology & Management (ATM)."

Pilkey, Orrin H, and Howard L Wright. 1998. "Seawalls Versus Beaches." *Journal of Coastal Research*, no. 4: 41–64.

Polk, Mariko A., and Devon O. Eulie. 2018. "Effectiveness of Living Shorelines as an Erosion Control Method in North Carolina." *Estuaries and Coasts* 41 (8): 2212–22. https://doi.org/10.1007/s12237-018-0439-y.

Powell, Emily J., Megan C. Tyrrell, Andrew Milliken, John M. Tirpak, and Michelle D. Staudinger. 2019. "A Review of Coastal Management Approaches to Support the Integration of Ecological and Human Community Planning for Climate Change." *Journal of Coastal Conservation* 23 (1): 1–18. https://doi.org/10.1007/s11852-018-0632-y.

Syvitski, James P. M., and John D. Milliman. 2007. "Geology, Geography, and Humans Battle for Dominance over the Delivery of Fluvial Sediment to the Coastal Ocean." *The Journal of Geology* 115 (1): 1–19. https://doi.org/10.1086/509246.

Taylor Engineering, Inc. 2020. "SAD SAND DMMA Offloading and Sediment Exchange Study."

Temmerman, Stijn, Patrick Meire, Tjeerd J. Bouma, Peter M. J. Herman, Tom Ysebaert, and Huib J. De Vriend. 2013. "Ecosystem-Based Coastal Defence in the Face of Global Change." *Nature* 504 (7478): 79–83. https://doi.org/10.1038/nature12859.

USACE, and USEPA. 2013. "Savannah Ocean Dredged Material Disposal Site Site Amanagement and Monitoring Plan."

Vörösmarty, Charles J, Michel Meybeck, Balázs Fekete, Keshav Sharma, Pamela Green, and James P.M Syvitski. 2003. "Anthropogenic Sediment Retention: Major Global Impact from Registered River Impoundments." *Global and Planetary Change* 39 (1–2): 169–90. https://doi.org/10.1016/S0921-8181(03)00023-7.

Wang, Ping, Nicholas C Kraust, and Richard A Davis. 1998. "Total Longshore Sediment Transport Rate in the Surf Zone: Field Measurements and Empirical Predictions," 15.

Windom, Herbert L, and Jonathan D Palmer. 2021. "Changing River Discharge and Suspended Sediment Transport to the Georgia Bight: Implications to Saltmarsh Sustainability." *Journal of Coastal Research* 00 (0): 11.

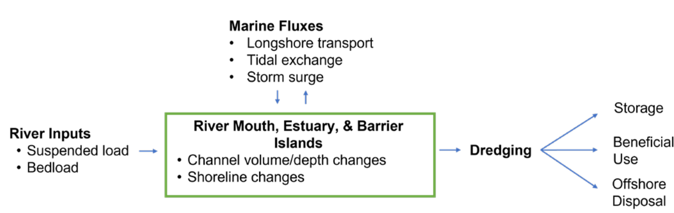

Figure 1. The basic conceptualization of this sediment budget treats shorelines, the Savannah River channel and estuary system, and dredge material disposal sites as storage cells with dredging activities, marine fluxes, and river inputs as the main drivers of volume change.

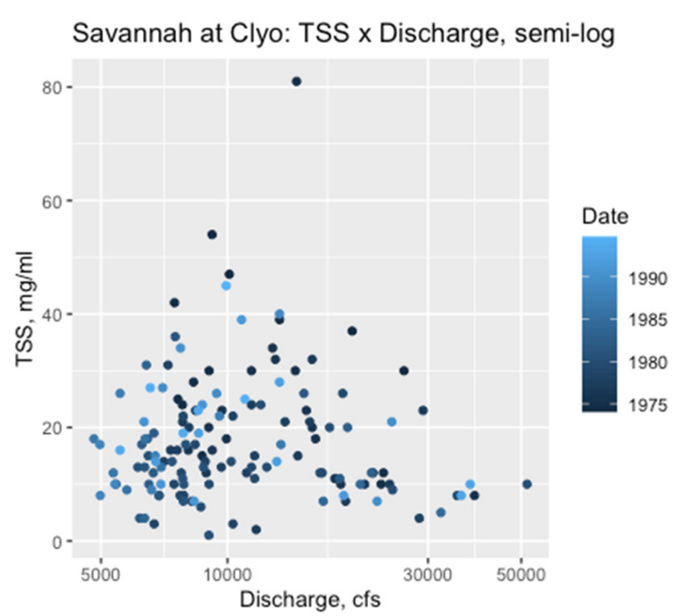

Figure 2. Total suspended sediment (TSS, mg/ml) plotted against discharge (cfs) on a semilog plot shows no clear correlation. TSS values decrease around the 20,000cfs point.

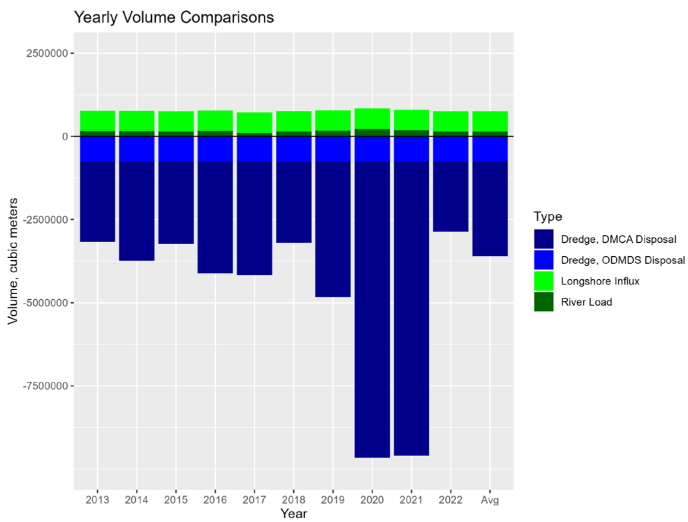

Figure 3. Yearly and average sediment flux balance for the Savannah River Channel shows a large volume of dredged material comes from an unknown source. Because the Savannah Harbor Expansion Project (SHEP) occurs between 2019 and 2022, the DMCA Disposal dredge average is based on years 2013 – 2018.

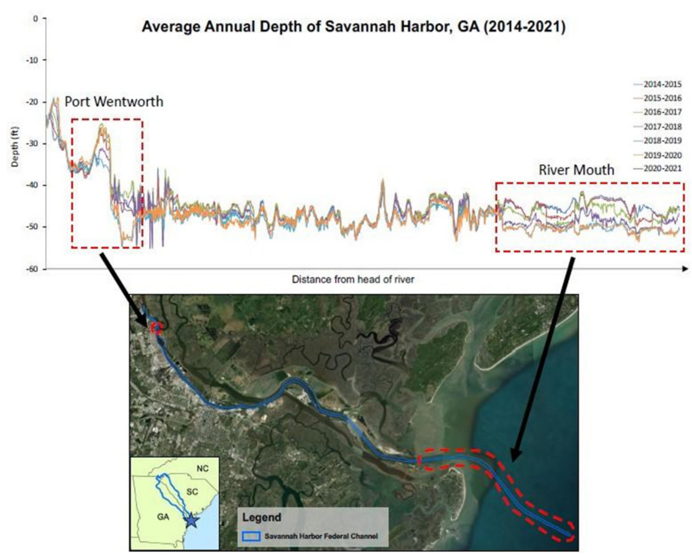

Figure 4. Analysis of channel depth along the entire Savannah River federal channel shows variability at the top and bottom but little change along the center.

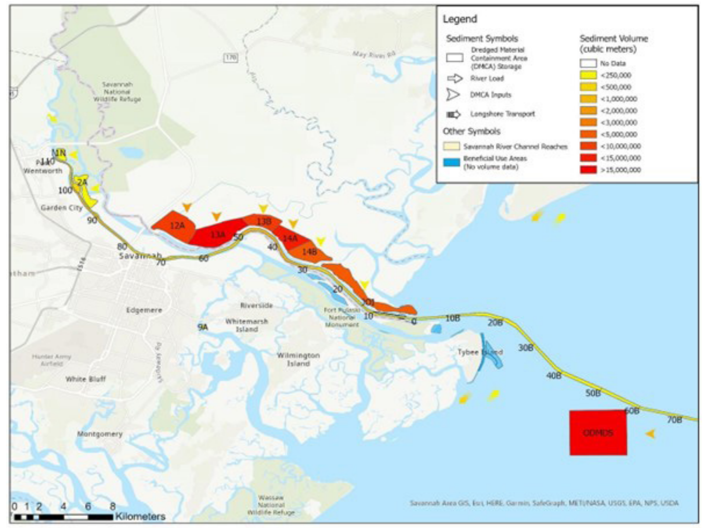

Figure 5. Statistical Map of the Savannah River Harbor showing channel volume fluxes and storage.

PREVALENCE OF WELL WATER CONTAMINANTS IN GEORGIA FROM 2010-2022

Angelique B. Willis, MPH[1,2], Suhasini Ramisetty-Mikler, Ph.D.[1], Uttam K. Saha, Ph.D.[3], Christine E. Stauber, Ph.D.[1]

[1]School of Public Health, Georgia State University, [2]Department of Geosciences, Georgia State University, [3]Agricultural and Environmental Services Laboratories, University of Georgia

REFERENCE: *Proceedings of the 2023 Georgia Water Resources Conference*, held March 30–31, 2023, at the University of Georgia.

Abstract. Safe, reliable, and clean drinking water sources are a basic necessity; however, many of those relying on private wells as their drinking water source are confronted with water quality challenges stemming from chemical contamination. More than 1.7 million individuals rely on private wells for drinking water in Georgia; nonetheless, wells are not under mandated regulations as municipal water supplies. In Georgia, previous studies suggested that the variation of soil and rock in a physiographic province (region) plays an essential role in the quality of private well water. There is a need to understand the distribution of these chemical contaminants above the federal Maximum Contaminant Level (MCL) and how different geologies in each physiographic province might influence such concentrations. Therefore, this study aimed to examine the distribution of arsenic, uranium, radon, nitrate-nitrogen, and lead concentrations above the federal MCL in private well water and examine an association of contamination with physiographic provinces in Georgia by utilizing private well water data collected by the University of Georgia's Agricultural and Environmental Services Laboratories (AESL). Over 26,000 well water samples were collected and tested for a least one chemical contaminant from 2010 through 2022. Cross-tabulation indicated associations between physiographic provinces and the proportion of private well water samples containing arsenic concentrations exceeding the federal MCL in the Coastal Plain, $\chi^2(3) = 95.53$, p = <.001, and the proportion of private well water samples containing nitrate-nitrogen concentrations exceeding the federal MCL in the Coastal Plain, $\chi^2(4) = 11.56$, p = .021. The adverse health impacts of arsenic, uranium, radon, nitrate-nitrogen, and lead are well established, including chronic toxicity, liver and kidney damage, anemia, and cancer, stemming from the chemical contamination of wells. Gaining insight into the geological factors responsible for the suboptimal quality of well water can facilitate the development of public health initiatives that raise public awareness and create opportunities to preserve and maintain healthy well water quality in Georgia.

Introduction. Access to dependable, uncontaminated, and safe drinking water is crucial for maintaining good human health (World Health Organization, 2022). In the United States, to ensure drinking water sources are safe and clean for human consumption, the Safe Drinking Water Act (SDWA) was established to protect the quality of drinking water in Community Water Systems (CWS) (United States Environmental Protection Agency, 2022). In conjunction with these laws, the Environmental Protection Agency (EPA) set federal Maximum Contaminant Limits (MCLs) for specific chemical contaminants in drinking water that pose the most severe risk to human health such as arsenic, uranium, radon, nitrate-nitrogen, and lead. The MCL for arsenic is 0.01 milligrams per liter (mg/L), uranium is 0.03 mg/L, nitrate-nitrogen is 10 mg/L, lead is 15 micrograms per liter (µg/L), and the recommended limit for radon is 4,000 picocuries per liter of air (pCi/L) (United States Environmental Protection Agency, 2021). However, these laws and standards are not applicable to private wells (United States Environmental Protection Agency, 2022). Private drinking water wells may be vulnerable to chemical contamination if they are located close to contamination sources, improperly constructed, or draw water from shallow, unconfined aquifers susceptible to contamination from naturally occurring sources or anthropogenic activities. Georgia's geology consists of different regions containing unique minerals, rock types, and landforms that can influence private well water quality (Clarke & Pierce, 1986; **Figure 1**). There is a need for a better understanding of the association between the physiographic provinces and concentrations of arsenic, uranium, radon, nitrate-nitrogen, and lead above the federal MCL in private well water. This study aimed to examine the distribution of arsenic, uranium, radon, nitrate-nitrogen, and lead concentrations above the federal MCL in private well water and to examine an association of contamination with physiographic provinces in Georgia by utilizing private well water data collected by the University of Georgia's Agricultural and Environmental Services Laboratories (AESL).

Methods. The data used in this study were obtained from the University of Georgia's AESL and the United States Geological Survey. Data from the University of Georgia's AESL were collected from samples of private well water provided by residents of Georgia who requested to have their samples tested for chemical contaminants between January 2010 and March 2022. Data from the United States Geological Survey were collected from Fenneman's "Physical Divisions of the United States," which is based on eight major divisions, 25 provinces, and 86 sections representing distinctive areas having common topography, rock types and structure, and geologic and geomorphic history originally published on January 1, 1946 (United States Geological Survey, 2004). Univariate analyses included descriptive statistics to study the distribution of arsenic, uranium, radon, nitrate-nitrogen, and lead concentrations above the federal MCL in Georgia. To test for bivariate associations between the physiographic provinces and the proportion of arsenic, uranium, radon, nitrate-nitrogen, and lead concentrations detected in private well water samples above the federal MCL, cross-tabulation with the chi-squared (χ^2) option was conducted. Phi (φ) was used to measure the strength of association between the two categorical variables with statistically significant results, with Alpha set at $p < .05$.

Results. Out of 26,686 private well water samples, 2,671 samples were tested for arsenic, 7,562 samples were tested for lead, 14,384 samples were tested for nitrate-nitrogen, 589 samples were tested for radon, and 1,480 samples were tested for uranium.

As seen in **Figure 2**, Coastal Plain (10.8% of private well water samples with arsenic concentrations exceeding the MCL) had more private well water samples with arsenic concentrations exceeding the federal MCL compared to the other physiographic provinces (between 0% and 1.33%). There was a statistically significant, though weak association between the physiographic province and the proportion of private well water samples containing arsenic concentrations exceeding the federal MCL, $\chi^2(3) = 95.53$, $p = <.001$, $\varphi = 0.189$.

As seen in **Figure 3**, Blue Ridge, Piedmont, Valley and Ridge, and Coastal Plain had private well water samples with lead concentrations exceeding the federal MCL. However, Blue Ridge had more samples exceeding the federal MCL than all physiographic provinces, but there was no statistically significant association between the physiographic province and the lead concentrations exceeding the federal MCL, $\chi^2(4) = 2.731$, $p = .604$. discharge.

As seen in **Figure 4**, Coastal Plain (1.8% of private well water samples with nitrate-nitrogen concentrations exceeding the MCL) had more private well water samples with nitrate-nitrogen concentrations exceeding the federal MCL compared to the other physiographic provinces (between 0% and 1.4%). There was a statistically significant but weak association between the physiographic province and the proportion of private well water samples containing nitrate-nitrogen concentrations exceeding the federal MCL in the Coastal Plain, $\chi^2(4) = 11.56$, $p = .021$, $\varphi = 0.028$.

As seen in **Figure 5**, Piedmont and Blue Ridge had more private well water samples with radon concentrations exceeding the federal MCL compared to the other physiographic provinces, but the relationship between exceedance and physiographic province was not statistically significant ($\chi^2(3) = 4.395$, $p = .222$).

As seen in **Figure 6**, Piedmont had more private well water samples with uranium concentrations exceeding the federal standard compared to the other physiographic provinces (between 0% and 3.9%), but differences among physiographic provinces were not statistically significant ($\chi^2(3) = 2.583$, $p = .461$).

Discussion. This study is the first to explore the association between private well water containing concentrations of arsenic, uranium, radon, nitrate-nitrogen, and lead above the federal MCL and the physiographic province from which the sample was obtained. The proportion of private well water samples containing arsenic concentrations exceeding the federal MCL was highest in the Coastal Plain physiographic province. This result is consistent with previous studies that have identified a higher prevalence of arsenic in groundwater in the Coastal Plain region due to the aquifers containing limestone and dolomite, which naturally contain arsenic (Ayotte et al., 2017; Clarke & McConnell, 1986). The proportion of private well water samples containing nitrate-nitrogen concentrations exceeding the federal MCL was also statistically significant in the Coastal Plain physiographic province, which could be attributable to agricultural practices, particularly the use of nitrogen fertilizers.

The findings of this study have significant implications for public health initiatives in Georgia. Enhancing public awareness and education regarding the potential adverse health outcomes associated with private well water contamination is imperative for improving testing habits and promoting safe drinking water practices. Raising public awareness can help mitigate the potential health risks of chemical contamination of private well water and improve health outcomes for individuals and communities in Georgia. Policymakers and health professionals can use these results to inform targeted interventions and policies to address the issue of chemical contamination in private well water, ultimately leading to improved public health outcomes.

Conclusion. The findings of this research provide compelling evidence of the widespread presence of chemical contaminants in private well water in Georgia, with the Coastal Plain physiographic province showing notable concentrations of arsenic and nitrate-nitrogen. These results strongly suggest that geological factors play a significant role in determining the quality of private well water in the state. Such findings underscore the urgent need to increase public awareness, education, and intervention to minimize the potential health risks associated with chemical contamination in private well water, as the negative health impacts of arsenic, uranium, radon, nitrate-nitrogen, and lead are well established and can cause chronic toxicity, liver and kidney damage, anemia, and cancer. Gaining insight into the geological factors responsible for the suboptimal quality of well water can facilitate the development of public health initiatives that raise public awareness and create opportunities to preserve and maintain healthy well water quality in Georgia.

References:

Ayotte, J. D., Medalie, L., Qi, S. L., Backer, L. C., & Nolan, B. T. (2017). Estimating the High-Arsenic Domestic-Well Population in the Conterminous United States. *Environmental Science and Technology*, 51(21), 12443–12454. https://doi.org/10.1021/ACS.EST.7B02881/ASSET/IMAGES/LARGE/ES-2017-02881W_0002.JPEG

Clarke, J. S., & McConnell, J. B. (1986). Georgia ground-water quality. In *US Geological Survey Open-File Report* (Vol. 0720).

Clarke, J. S., and Pierce, R. R., 1985, Georgia groundwater resources, in U.S. Geological Survey, National Water Summary, 1984: U.S. Geological Survey Water-Supply Paper 2275, p. 179–184, https://pubs.er.usgs.gov/publication/wsp2275

United States Environmental Protection Agency. (2021, November 24). *Drinking Water Requirements for States and Public Water Systems: Chemical Contaminant Rules*. https://www.epa.gov/dwreginfo/chemical-contaminant-rules

United States Environmental Protection Agency. (2022, May 26). *Private Drinking Water Wells*. https://www.epa.gov/privatewells

United States Geological Survey. (2004). *Physiographic Divisions of the Conterminous U.S.* https://water.usgs.gov/GIS/metadata/usgswrd/XML/physio.xml

World Health Organization. (2022, March 21). *Drinking-water*. https://www.who.int/news-room/fact-sheets/detail/drinking-water

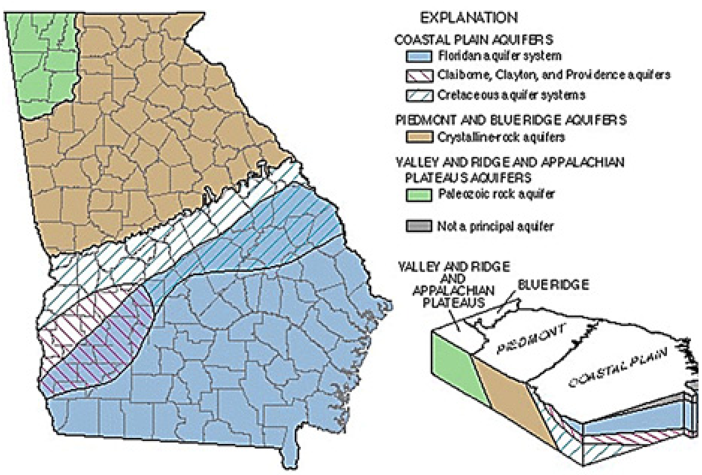

Figure 1. Map Area of use of principal aquifers and generalized diagram showing aquifers and physiographic provinces in Georgia.

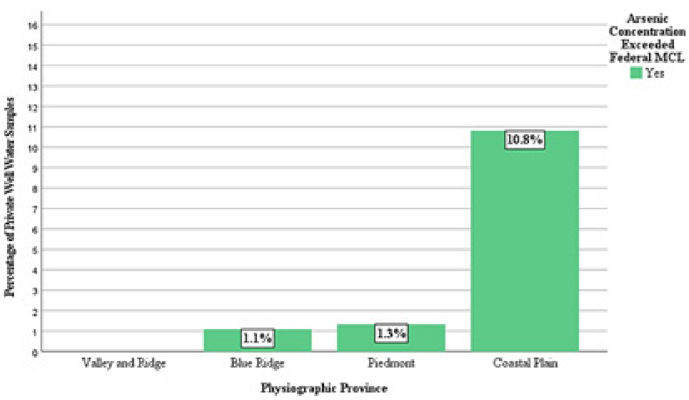

Figure 2. The percentage of private well water samples containing arsenic concentrations exceeding the federal MCL in each physiographic province.

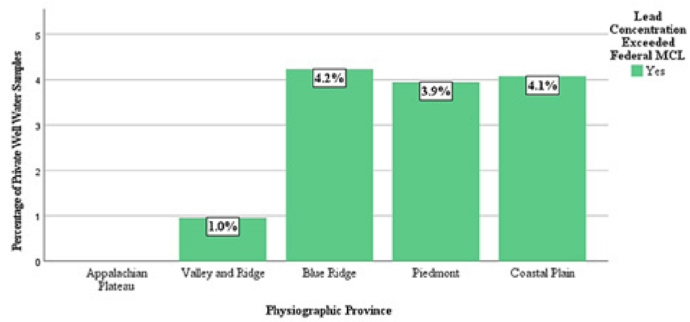

Figure 3. The percentage of private well water samples containing lead concentrations exceeding the federal MCL in each physiographic province.

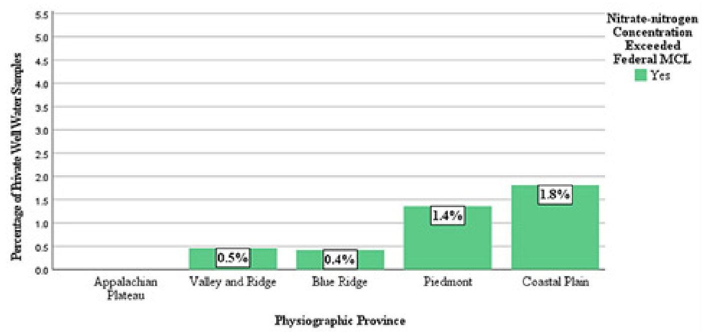

Figure 4. The percentage of private well water samples containing nitrate-nitrogen concentrations exceeding the federal MCL in each physiographic province.

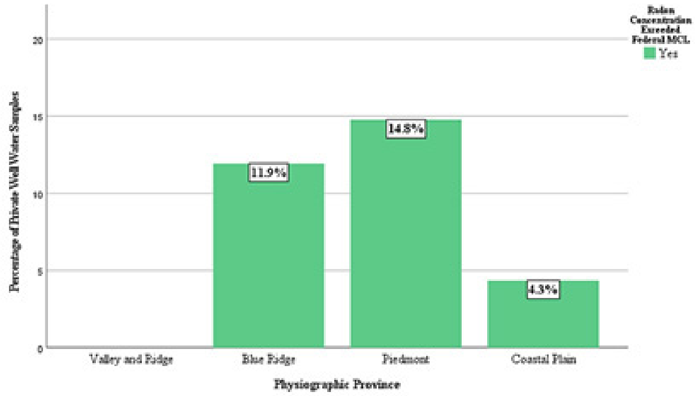

Figure 5. The percentage of private well water samples containing radon concentrations exceeding the federal MCL in each physiographic province.

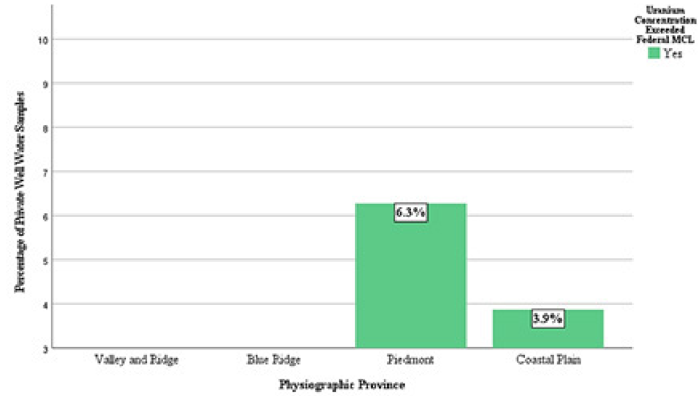

Figure 6. The percentage of private well water samples containing uranium concentrations exceeding the federal MCL in each physiographic province.

NEW CAPABILITIES PROVIDED BY ARCGIS PRO IN THE AQUATIC VEGETATION MANAGEMENT CONTEXT: POINT CLOUD ANALYSIS FROM LAKE SEMINOLE, GEORGIA, USA

Philip Ashford[1], Can Vatandaslar[2,3], Steve Golladay[4], and Marguerite Madden[5]

[1]School of Environmental, Civil, Agricultural and Mechnical Engineering, University of Georgia (philip13@uga.edu), [2]Visiting scholar at Warnell School of Forestry and Natural Resources, University of Georgia, [3]Affiliated with Faculty of Forestry, Artvin Coruh University, Artvin, Turkey (canvatandaslar@artvin.edu.tr), [4]UGA adjunct faculty, Aquatic Ecologist at Jones Center at Ichauway, Newton Georgia, [5]Geography Department, University of Georgia

REFERENCE: *Proceedings of the 2023 Georgia Water Resources Conference*, held March 30–31, 2023, at the University of Georgia.

Aquatic resource managers need practical tools and techniques for mapping actual shorelines, detecting invasive plants, monitoring nuisance vegetation, and determining the effectiveness of management decisions. Spatially explicit data collected by consumer-grade drones can provide timely information to guide decision-makers in a cost-effective way. However, 2-D data (optical images) creation and analysis are challenged by limitations in photogrammetric processing and they fail to completely characterize complex aquatic systems. By contrast, 3-D data (point clouds) offer a more realistic representation of the environment but the file size and configuration means that they can hardly be analyzed with traditional GIS software.

Therefore, the present study aims to differentiate between land and aquatic vegetation classes in Lake Seminole, GA, as well as delineate the lake's shoreline based on dense point clouds created by a DJI Phantom 3 drone. Unlike other image analysis studies, we conducted all data analysis steps in one workplace, ArcGIS Pro, which allowed us to segment, classify, edit, and visualize point clouds within a 3-D scene. As such, the high-resolution height data were employed as a discriminator between land and aquatic vegetation. For model validation, the outputs were compared against the US Census Bureau's shapefile data for land use land covers and ArcGIS Pro basemaps. Initial findings showed that Lake Seminole's shoreline and its small islets could be successfully delineated based on digital surface model (DSM) alone. Accordingly, the area coverage of the mapped lake was 1,083,105 m^2 which was <1% larger than the reference data. The difference between the islets areas and the reference was more remarkable. For example, the area coverage of the largest island (12,124 m^2) was underestimated by 20%. The average error in delineations ranged from 1.5 m to 6.8 m. Maximum error was as much as 60 m in the lake's shoreline which could be attributed to the seasonal changes in water level.

Regarding vegetation, DSM did not adequately classify terrestrial and aquatic plants because different vegetation types co-occurred on the same level. Thus, we segmented the ultra-high-resolution (≤ 10 cm) ortho-mosaic based on the similarity of image features using the Segment Mean Shift tool of ArcGIS Pro. Through trial and error, the best classification result was achieved by the parameter values of 20, 15, and 5000 for the image's spectral, spatial, and minimum pixel size features, respectively. Then, we compared the classification map against the ArcGIS Pro's basemap imagery with randomly distributed accuracy assessment points. According to the confusion matrix, the highest and the lowest accuracies were observed in water (91%) and barren land classes (20%), respectively. The overall accuracy and kappa coefficient for the produced map were 70% and 0.63. These results suggested that terrestrial and aquatic vegetation, as well as other land use land cover classes, could be separated from each other with satisfying accuracy rates. Thus, we conclude that aquatic resource managers might benefit more from drone-based solutions when coupled with the 3-D data analyzing capabilities of ArcGIS Pro.

Keywords: Lake and Reservoir Management, Environmental Monitoring and Assessment, Geographical Information Systems (GIS), Unmanned Aerial Systems (UAS), Image Segmentation, Accuracy Assessment, 3-D Spatial Analysis, Drone Mapping.